Microseismic Monitoring Work in the Vicinity of Asfordby Colliery Including the Seismic Mapping Of the Location of Mechanical Failures in Overburden

Research Contract No: 2069/3

Period of Investigation : 1 October 1994 to 31 March 1996

FINAL REPORT

Prepared for:

International Mining Consultants Limited

by P. Styles , S. Toon & A. Bryan-Jones
Microseismological Research Group
Department of Earth Sciences
University of Liverpool
Brownlow Street
Liverpool
L69 3BX

Contents

1. Executive Summary

The objectives of this investigation were as follows:

i *To use microseismic energy generated by rock fracturing to map the caving height and fracture architecture above a Longwall coalface.*

ii *To determine the spatial and temporal relationships between the fractures delineated by the microearthquake hypocentres and mining activity and roof control, particularly weightings on the face.*

iii *To investigate geological controls on the location of seismicity.*

iv *To attempt to determine the nature of the fractures forming above the extracted panel and assess their significance for roof control and water percolation from overlying aquifers.*

The site chosen for this investigation was Asfordby Colliery, panel 101 because of the lack of previous mining, complex geology and the overlying Sherwood Sandstone aquifer.
The main findings and conclusions are as follows:

i. *Equipment, technical expertise and software have been developed which can detect record and locate and analyse induced microseismic activity generated by the extraction of coal from a longwall panel.*

ii. *The microseismic activity clearly delineated zones of failure in the Sherwood Sandstone bounding a major block which was responsible for periodic weightings on the face and eventual water ingress associated with the propagation of the fracture network down to the seam level. Periods of enhanced activity were associated with major roof control problems.*

iii *There were strong geological controls on the location of seismicity which were associated with the presence of the overlying strong sill and strong sandstones and*

while there was some relationship between face position and seismic activity this was superimposed upon a primary fracture architecture controlled by the geomechanical properties of the overburden.

iv *Source mechanism studies were limited to some extent by data coverage but clearly showed that the orientation of the individual microcracks were strongly controlled by the maximum regional compressive stress.*

2 INTRODUCTION AND OBJECTIVES

The location of fracturing associated with caving around a longwall face is of great importance as it is fundamental to roof control that fracturing is principally confined to the region behind the face and in close proximity to it. This is particularly important where the overlying strata contain aquifers which if breached might lead to water inflow to the colliery as happened at Wistow Mine in the Selby Complex in 1983. Here , weightings on the face and water inflow stopped production on Face A. Similar incidents have occurred in the Durham Coalfield and internationally , notably in India (Singareni Coalfield) and Australia (Illawarra Coalfield) . The principal objective of this investigation is to determine whether microseismic monitoring can detect and map fracturing associated with longwall extraction of coal and the nature of the interaction with geological features. The site chosen for this investigation is Panel 101 in the Deep Main seam at Asfordby Colliery , near Melton Mowbray, Leicestershire which is a new face in a new mine in a previously unexploited coalfield. The presence of sills of variable thickness in the Coal measures above the working seams and the close proximity (100 to 200 metres) to the Sherwood Sandstone aquifer were thought to be potentially problematic. The microseismic monitoring at Asfordby was part of an overall project aimed at mapping caving behaviour by means of seismic monitoring plus observation of water pressure in the aquifer, surveying for subsidence effects at the surface, and monitoring for breaks in optical and electrical cables cemented into the project boreholes.

2.1 Fracture Delineation and prediction using currently available technology.

The direct detection of the location and extent of fracturing around a longwall face or extracted pillar can only be carried out with considerable difficulty and usually in only a very limited area accessible from the workings by the installation of extensometers in long boreholes in the face or gate roads. This can give information over a limited geographical extent and can not be easily moved to

monitor other problem areas which may develop. The determination of the extent of fracture zones around total extraction panels has been attempted using extensometers, Peng and Chiang (1984). However this is difficult, time consuming and expensive and as a result cannot be routinely conducted. The fracturing in the roof can also be assessed to a limited extent from the monitoring of support leg pressures.

A number of theoretical relationships have been postulated in order to predict the extent and nature of fracture zones around total extraction panels. The majority of these link the seam thickness to the extent of rock mass failure. Much of this work is based upon physical and numerical modelling studies that have largely not been completely validated from measurements. Currently the extent of caving and fracturing above the seam is considered to be in the region of 50 times the seam thickness for a 200 m wide longwall panel, with an approximately linear decrease with decreasing panel width; a figure of 10 times seam thickness has been suggested for a 40 m wide panel for example (Choi and McCain, 1982, Bieniawski, 1987, Peng and Chiang, 1984, Follington, 1988). Little information exists with respect to the fracturing around pillar extraction panels.
There is no general consensus as to the depth of fracturing in the floor, other than it is significantly less than for the roof. It is generally perceived that the seam thickness also influences this. Although seam thickness will undoubtedly influence the extent of fracturing, the complex interaction between seam thickness, depth, magnitude and direction of in-situ stresses, panel width and geomechanical properties of the strata will be controlling factors. Although numerical models have increased in sophistication and accuracy, they are not as yet a reliable guide in this complex geomechanical environment. More direct measurements of the extent of fracturing are needed.

2.2 Basic Principles of Microseismic Monitoring

When a solid fails mechanically, vibrations travel away from the point of failure in all directions, as illustrated in figure 2.1. In the case of rocks within the Earth, these vibrations are referred to as seismic waves. There are many types of seismic wave generated depending on the exact nature of the surroundings . The principal types are P-waves which are compressional waves travelling through the body of the material and S-waves which are shear or transverse waves which again travel through the body of the rock. Waves which travel as trapped modes or guided waves are also important, particularly where monitoring is taking place from detectors placed within a coal-seam which acts as a wave-guide.

The study of such seismic activity is referred to as Microseismic Monitoring.

If it is possible to record, at a number of different locations, the seismic waves resulting from rock failure, then the true geographical position of the point of failure can be estimated. This is achieved either by study of the time of arrival of the seismic wave at each detector, or alternatively the direction of particle motion or polarisation.

The main aim of a programme of microseismic monitoring in the context of coal mining is to map the pattern of caving behaviour created by extraction, or to detect overloading symptoms in support pillars. In addition, seismic events resulting from fracture development contain evidence of the fracture mechanism (eg failure in shear, tension or compression, and orientation of the resultant fracture) and this can further contribute to the understanding of caving behaviour.

2.3 Equipment Requirements.

The basic necessities for a programme of microseismic monitoring are:-

- At least three geophone assemblies, each containing three vibration sensors, spaced around the volume in which rock failure is anticipated.

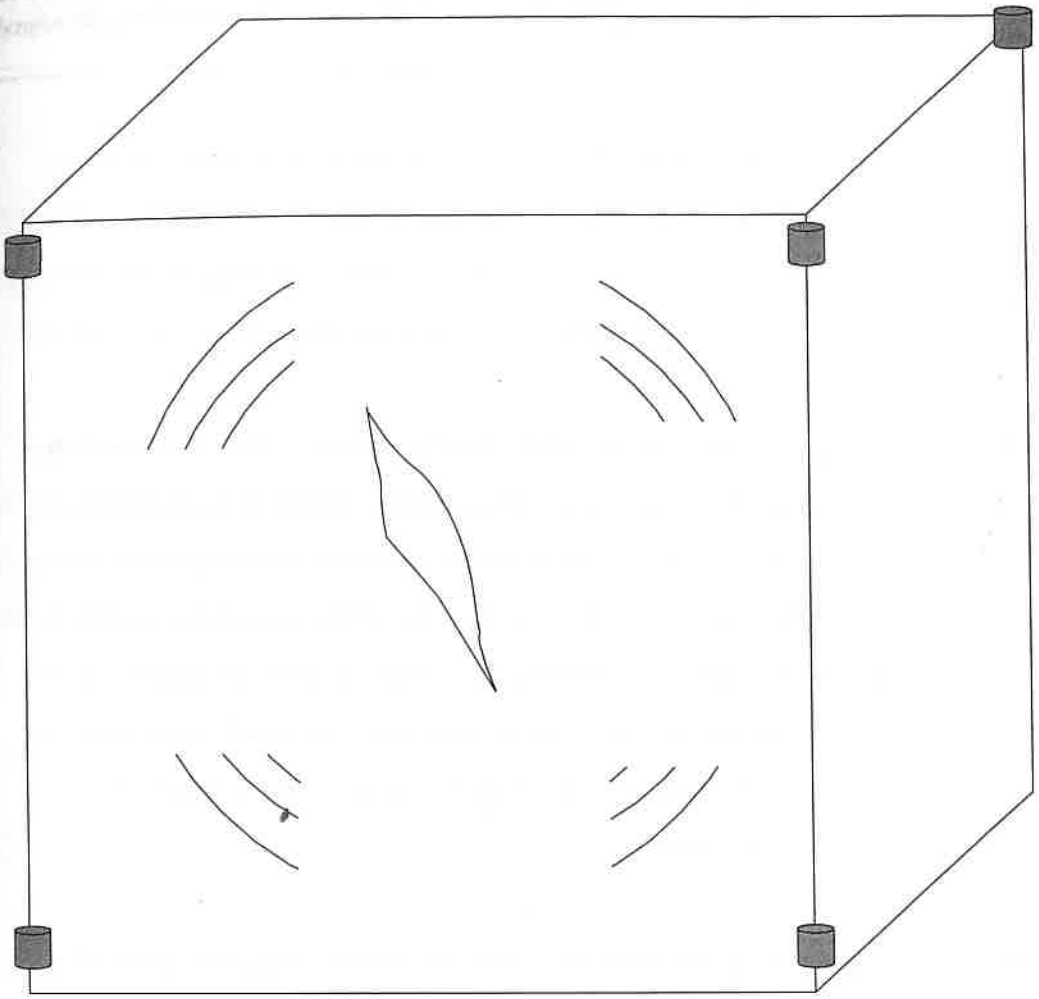

Figure 2.1 Seismic waves generated from rock fracture process.

The greater the number of geophones installed, the more accurate the mapping operation. Each geophone assembly needs to be firmly cemented into the strata at a point remote from any marked geological boundary or fault, and away from disturbed ground associated with a mine opening.

- Self-triggering seismic recording devices for each vibration monitoring sensor installed. These devices permanently "listen" to each geophone, but are triggered to actually record seismic data only when a pre-set threshold level of vibration is exceeded. In the case of the equipment used here, the Magus Vibrosound SP1, seismic records are written to memory cards which are periodically removed for data analysis. Each instrument can handle 6 vibration monitoring channels, which is sufficient for two geophone assemblies.

- Data processing hardware and software for converting the recorded seismic data into maps of caving behaviour, and for interpretation of failure mechanisms.

2.4 Three-dimensional, dynamic fracture imaging from borehole in-seam microseismology

Every fracture which develops around a zone of coal extraction will radiate energy as micro-earthquakes and sometimes as larger seismic events. These events provide a very clear insight into the state of stress present around the area of extraction. They can be used to monitor roof stability and the development of fractures around the extracted zone and the nature of interactions with previously extracted areas, aquifers and major faults.

The seismic events can be detected and imaged to delineate the locus of fracturing anywhere from several hundred metres beneath the seam up to the surface. The location of the fracture , however, is only the first (although very

important) part of the information which can be extracted from the microseismicity. The following parameters can also be obtained with the appropriate processing of the full waveform:

i the orientation of the fracture causing the micro-seismic event

ii energy released during that particular failure

iii source radius and hence an estimate of fracture dimension,

iv the nature of the fracture process, ie propagating fracture, bed separation, gas-driven dilatant microfracture can be derived from analysis of the whole waveform and the extraction of the moment tensor for the event.

All of these parameters can contribute information which is relevant to our understanding of the geomechanical behaviour of the rock-mass above and surrounding a longwall coal-face. The objectives of this investigation are to determine these parameters and hence map the **fracture architecture** for the zone around Asfordby Panel 101 and relate this information to mining activity and roof behaviour.

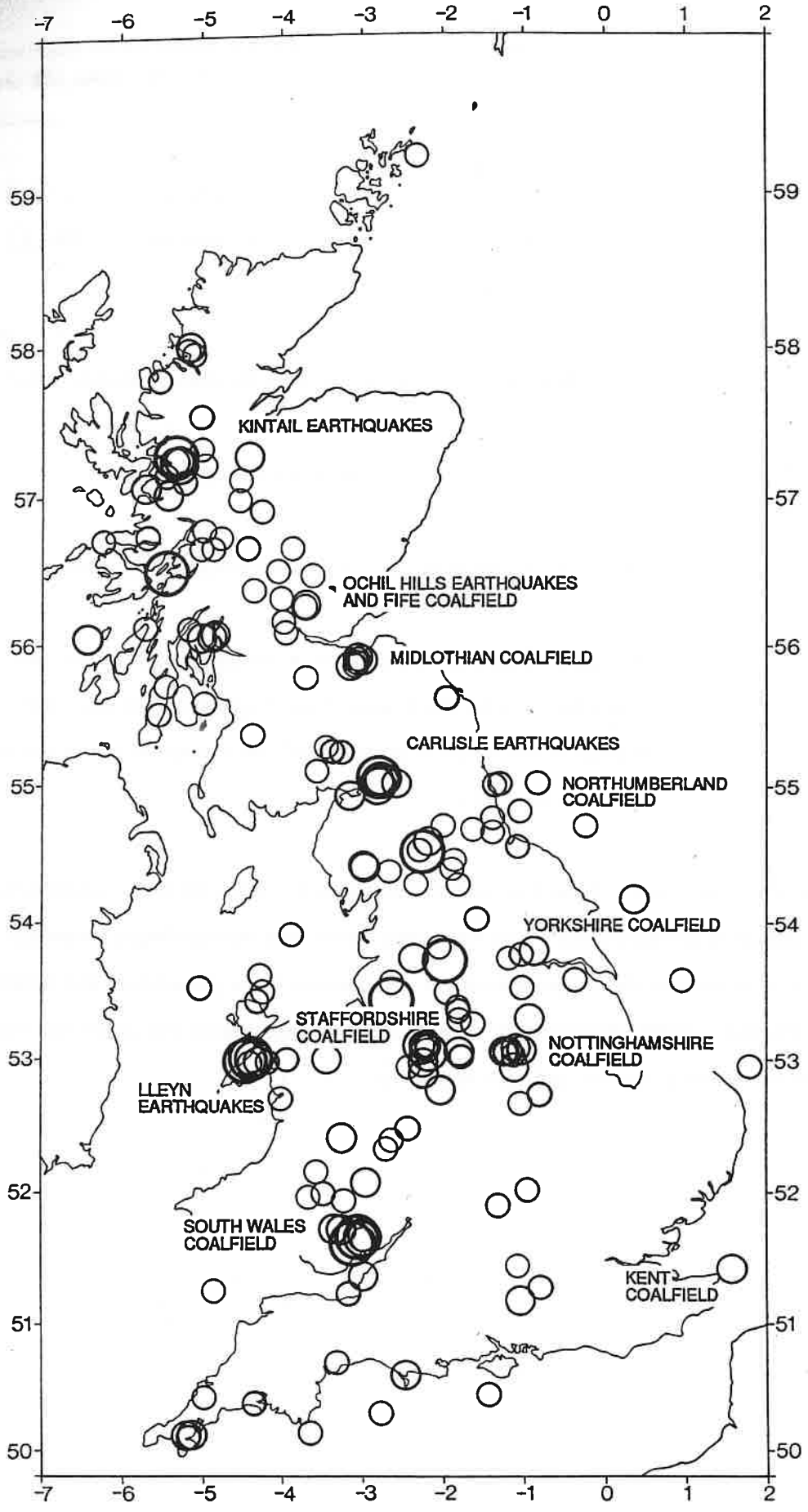

Figure 3.1 UK seismicity showing close association with the principal coal fields.

3. PREVIOUS MICROSEISMIC MONITORING OF COAL MINING ACTIVITIES IN THE UNITED KINGDOM

An extensive review of global microseismic monitoring in mining and other applications is found in Appendix 2. This Chapter is confined to UK monitoring and other specific experiments of direct relevance to this project.

3.1 UK Mining Induced Seismicity

Microseismic activity, ie the occurrence of minor, generally unfelt, but with occasional felt, earthquakes, associated with the extraction of deep-mined coal by long-wall methods has been reported in UK coal mining areas since at least the turn of the century. The association with coal production from deep mines has often been assumed but rarely proven, Davison (1905), Davison (1919), Dollar (1951), Neilson *et. al.*, (1984). The coalfields can clearly be seen on a map of the British earthquakes (Figure 3. 1) as concentrations of activity along with the normal background of tectonic seismicity such as the Carlisle (1979) and Lleyn (1984) earthquakes and aftershocks and events from Kintail and the Ochil Hills in Scotland. The coalfields of Midlothian, Staffordshire, Nottinghamshire and South Wales are clearly shown but Northumberland, Fife, Yorkshire have fewer events. The British Geological Survey report that about 25 per cent of small to moderate earthquakes (less than $M_L = 3$) recorded by the UK regional seismometer network occur in the coalfields (Redmayne, 1988).

Following public concern over mining induced seismicity in the Midlands, the British Geological Survey installed 4 seismometers (Browitt 1979), augmented by mobile networks that could be used to examine small areas in greater detail. After a damaging earthquake in the Stoke-on-Trent area (body wave magnitude, m_b=3.4, modified Mercalli scale, MM=VI) and several smaller tremors on the 15th of July, 1975, a network of seismometers (aperture of about 10 km) was deployed to monitor the spatial and temporal pattern of activity which continued over the

next five years. Westbrook *et. al.*, (1980) concluded that the earth tremors were caused by longwall coal mining at a depth of 1000 metres, that the event rate correlated with coal production in both space and time and that previous mining played an important part in the size of the tremors.

3.2 Mining-Induced Seismicity in Staffordshire and Nottinghamshire

Westbrook *et. al.*. (1980), Kusznir *et. al.*. (1980, 1984) and Kusznir & Farmer (1983), carried out a considerable period of monitoring of mining–induced seismicity associated with coal extraction in the North Staffordshire Coal Field, U.K. They recorded events as large as magnitude 3.5, using standard global seismological Willmore Seismometers at the surface and identified events associated with the collapse of the waste with implosive mechanisms and also pillar collapse, which was the origin of the largest events with shear mechanisms.

Using a small aperture array (1.5 km) to concentrate on two adjacent working panels, Kusznir *et. al.*, (1984) identified two separate mechanisms responsible for generating the seismicity. The smaller events (M_L<2.5) with an implosional source mechanism were thought to be generated by waste collapse. The larger events (M_L>2.5), with shear source mechanisms, occurred in pillars of old workings in adjacent seams and were caused by the superposition of the pillar stress-field and the front abutment pressure of the advancing face, when the face passed above or below the pillar.

Investigations by Isaacs and Follington (1988) during mining of the H65 seam at Cotgrave Colliery, Nottinghamshire, have shown that high loading levels on the powered supports were caused by failure of the Deep Soft Seam and the roof immediately above the Deep Hard Seam which was being mined. These beds were unable to transmit support resistance to the bridging siltstones above, which resulted in the generation of brittle failures which propagated into the overlying strata. This type of roof failure will certainly give rise to energetic microseismic activity which will be detected at considerable distances and will couple strongly

into the seam as guided waves. Floor failures also generate microseismic activity which is detectable in the same way. The fewer remaining, generally larger events were shown to be associated with pillar failure in workings above or below the active seam caused by the superposition of the pillar stress field and the front abutment pressure. This type of event is also likely to be generated when faults are re-activated by mining activity. It is apparent that the microseismic activity associated with the development of fractures associated with caving of the roof can be monitored using surface seismic networks although with limited precision in the final position.

3.3 Mining-Induced Seismicity and Outbursts of Coal-Dust and Methane

Cynheidre Colliery, Dyfed, in the South Wales Coalfield, where anthracite of very high quality is mined had been the site of 114 serious outbursts since it opened in 1960. Cynheidre Colliery was monitored microseismically from a surface network of 8 seismometers for 7 years from 1982 to 1989. One of the principal objectives was to study the activity associated with active longwall mining in a situation where there was no interaction with other mine workings. Styles *et. al.* (1991) distinguished two types of microseismic activity. The first type showed clear correlations between underground working practices and microseismic activity with as many as 800 (unfelt) microseismic events detected during an eight-hour shift. They concluded that the activity was localised in front of the advancing face and suggested that it was generated by the brittle failure of the sandstone roof and floor and was directly correlated with the rate of extraction of coal. Kusznir *et. al.*, (1985), found seismicity clustering around the active faces with magnitudes in the range M_L = 1 to -1.

Data recorded using an underground accelerometer and a portable tape recorder showed conclusively that there was in–seam microseismic activity and that this increased at about the time of roof collapse, as the powered supports were

advanced. Spectral analysis of these events suggested they had a frequency spectrum ranging from 400Hz to 1250Hz (Hughes, 1973).

An underground microseismic monitoring system was developed by the University College of Cardiff (Brown and McDonald, 1984, Rigby and Wardle, 1984, Rigby and Bolt, 1989). The system comprised a four–channel set of geophones grouted into boreholes in the coal seam with FM telemetry to the surface for on–line detection and processing. The system appeared to work reliably and well, picking up three main types of seismic event with dispersive characteristics showing them to be propagating within the seam. They show excellent correlations with methane emission from the face, however, no outbursts occurred during the period of full–time deployment and it is not clear whether this type of seismic activity, while clearly correlated with mining extractive processes, has any bearing on the mechanism or prediction of outbursts.

Using a surface network of five vertical component Willmore seismometers deployed in a 6 km by 6 km cross array, Styles *et. al.* (1987a) showed that it was possible to detect, identify and locate microseismic activity associated with normal mining activity, i.e. extraction of coal, and the subsequent collapse of the waste, and to make preliminary correlations with the rate of advance and hence the volume of coal won.

3.3.1 *Normal* Microseismicity

The `**Normal**' activity consists of impulsive seismic events which show the usual sequence of arrival of seismic phases expected for brittle failure of a rock mass, ie P and S waves propagating at normal velocities (V_p = 3500 m/s and V_s = 2000 m/s) and can easily be located using normal seismological hypocentral location algorithms.

3.3.1 Outburst Microseismicity

A new type of seismic activity was recognised which appeared to be associated with the microfracturing of the coal and the emission of methane during periods of abnormal face conditions. `**Outburst**' activity appears to be associated with emergent, monochromatic events with a dominant frequency of 32 Hz with very slow and variable apparent velocities of propagation across the colliery.

This type of `**Outburst**' activity is rarely seen when face conditions are normal but can rise to levels in excess of 100 events/hour immediately prior to an outburst. A real–time, on–line microprocessor based monitoring system was developed to monitor the levels of activity on each individual channel and to issue audible alarms to the Colliery Control Room operator. This was used successfully in conjunction with the stress dissipation technique of pulsed infusion firing (Davies *et. al.*. 1983) to successfully control a serious gas emission incident on 19 February 1986 when more than 8,500 m^3 of methane were released in a controlled manner (Styles *et. al.*., 1987a, 1987b, 1990).

At Cynheidre, the microseismic network was deployed in order to monitor and discriminate microseismic activity associated with mining. In particular to investigate whether there are precursors to outbursts and, if so, whether these could be used as a predictive tool, or an aid to management, for the safe working of the colliery. As a consequence of the many outbursts that had occurred within Cynheidre, mining proceeded in a very restricted manner, governed by a Code of Practice. The microseismic network was therefore linked to a micro–processor that monitored the incoming data in real time and issued warnings to the Colliery management at times of potential outburst risk. The integrated monitoring system allowed the mine to obtain exemptions from some of the Regulations and to mine more productively, thus making the operation

profitable. It was considered that the monitoring method, combined with a specialised destressing technique, pulsed–infusion firing, resulted in the mine being worked for more than four years without an outburst occurring.

3.4 Surface Microseismic Monitoring in the North Nottinghamshire Coalfield

Between July 1989 and August 1990, over 130 separate earth tremors were reported to the Thoresby Estate Offices, Thoresby Park, Nottinghamshire. Following the increasing concern from the general public in the Thoresby/Edwinstowe area of Nottinghamshire and in order to determine whether the tremors were caused by mining activity, British Coal commissioned the University of Liverpool to deploy a network of surface seismometers around the take of Thoresby Colliery, whose workings lie beneath Thoresby Park and Edwinstowe. This provided an opportunity to carry out a detailed study of the temporal and spatial changes in seismicity for an area where large amounts of energy are being released seismically. Around Thoresby Colliery, the surface rocks are Permo-Trias (Sherwood Sandstone). These rocks conceal part of the East Pennine or Nottinghamshire coalfield and dip gently towards the east. Production began in 1982 with coal from the 2 metre thick Top Hard coal seam in the Middle Coal Measures, 650 metres below datum. This seam was effectively worked out by 1986 and has been removed from above the Parkgate Seam over most of the area. Thoresby's current production came solely from the Parkgate Seam in the Lower Coal Measures which was being worked between 700 and 820 metres below datum, from workings in two areas; the South West where the seam section is about 2.4 metres and the East where the section is between 1.9 and 2.0 metres. During the period of this work, several panels started and finished their production lives.

Figure 3.2 shows the location of all the seismometer stations, the villages around the Thoresby take and the areas where coal from the Parkgate Seam had been worked in the past or was being worked (labelled) during the period of the

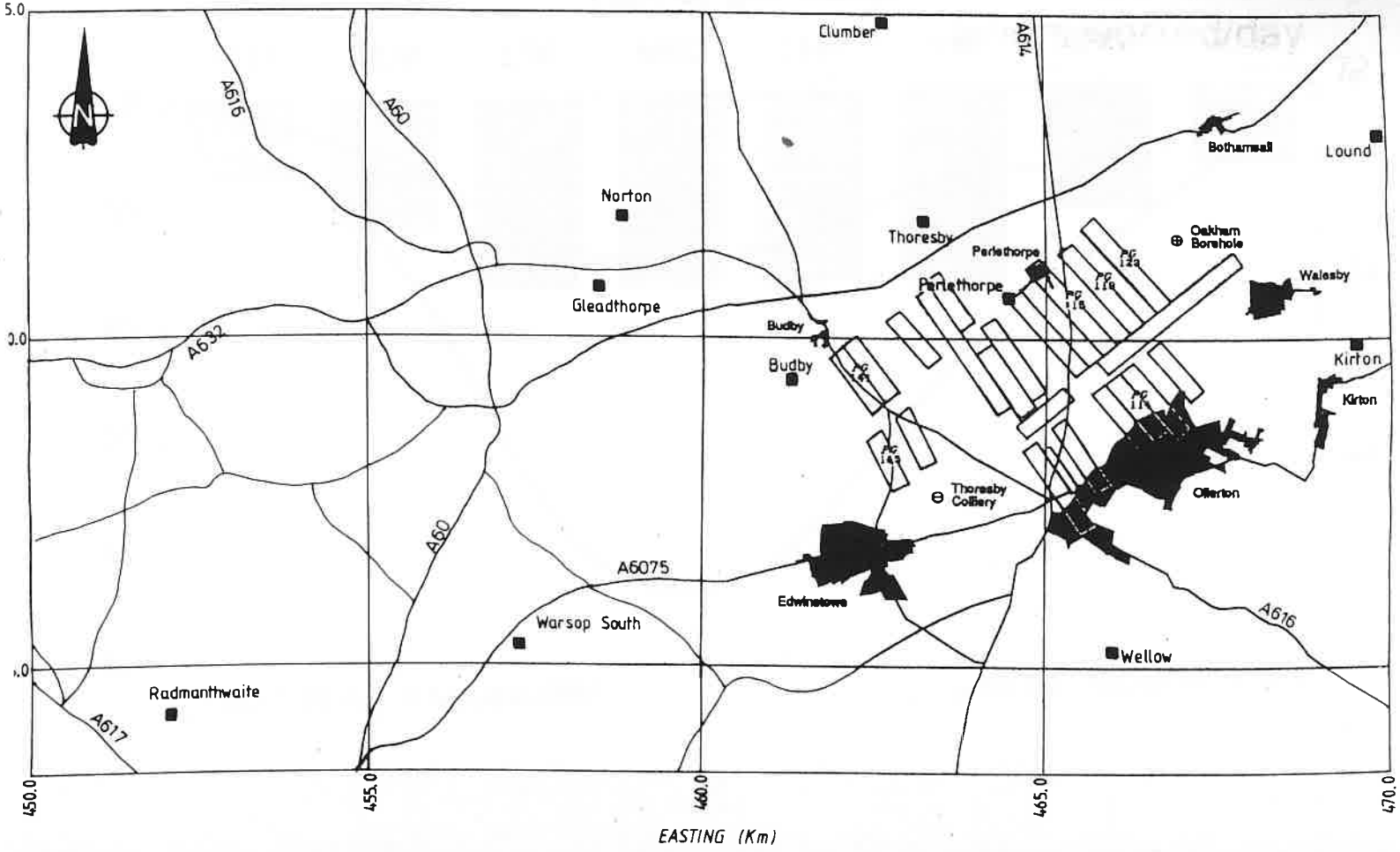

Figure 3.2 Seismometer stations and principal faces, Thoresby area, N. Notts.

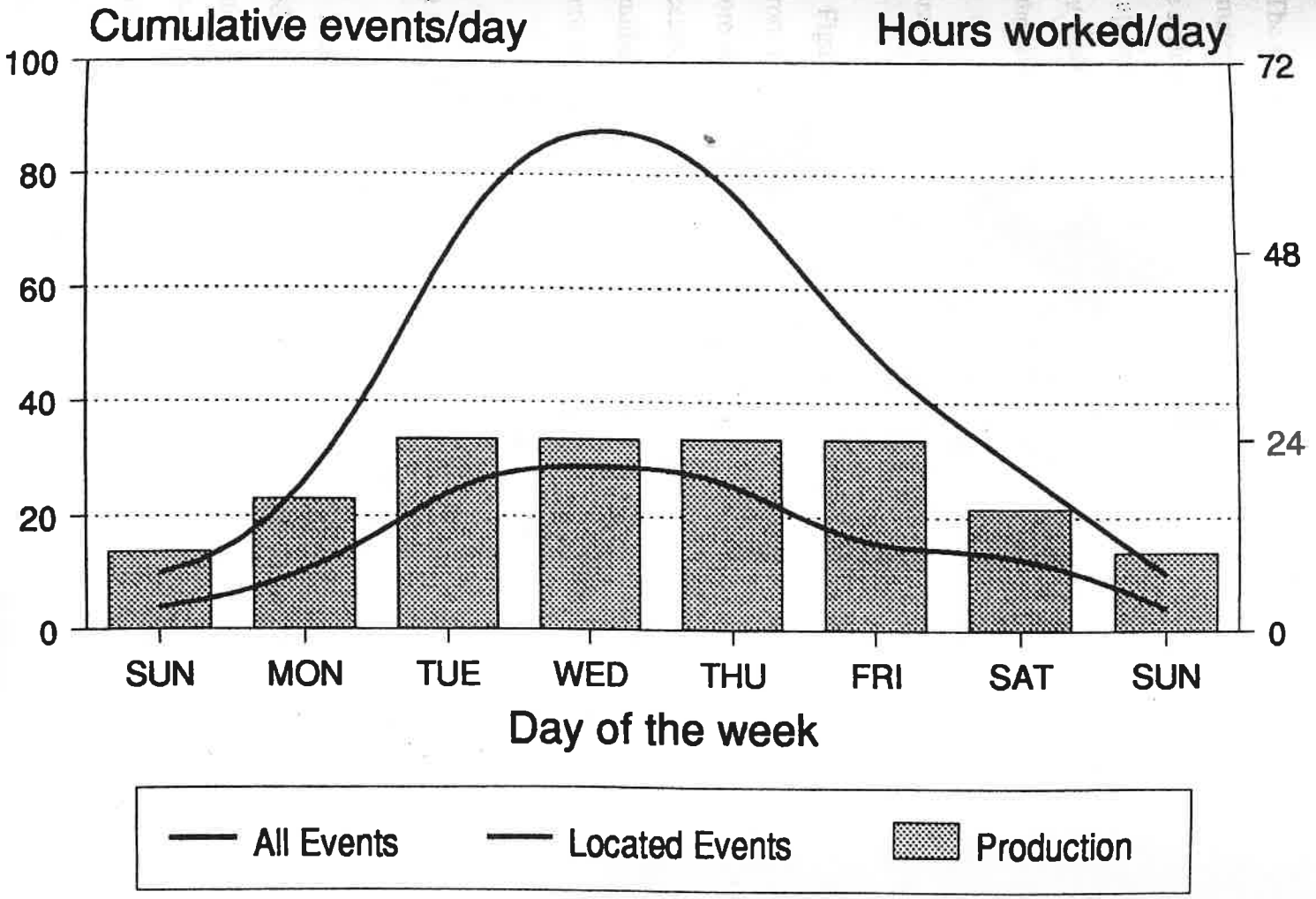

Figure 3.3 Cumulative event rate for events from the Thoresby take.

study. The stations are equipped with 1 second period Willmore Mk. IIIA seismometers and transmitted and recorded on an EARTHDATA 9690 digital seismic system. Mining-induced events were located between the surface and depths up to about one km and in the takes of either Thoresby Colliery or one the adjacent working collieries i.e. Manton, Bevercotes, Ollerton, Bilsthorpe, Clipstone and Welbeck .

3.4.1 Temporal variations of seismicity in the Edwinstowe area

Figure 3.3 shows the cumulative daily event rates for those events known to be from within the Thoresby take indicating that there is more seismicity and also more of the large magnitude events in the middle of the week. The event rate then decays, reaching a minimum on Sunday. Also shown in Figure 3.3 are the total number of hours worked each day over this time period. This demonstrates that there is good correlation between event rate and production.

3.4.2 Spatial Variation of Seismicity from Thoresby Colliery

From the 22nd of August 1990 to the end of July 1991, some 785 mining-induced events were detected on two or more seismometers of the network, with estimated magnitudes from -2 to approximately 2.4. Of this data set 23 events were felt and reported from the Edwinstowe region. Only one of the events was felt within the colliery. Of the 23 events, 14 originated from within the Thoresby take.

At the beginning of the period, panels PG114 and PG115 in the north eastern area and PG141 in the south western area were in full production. These faces were replaced by PG119 and PG145. At the end of the monitoring period (July 1st 1991) PG145 had finished leaving PG119 nearing the end of it's production life.

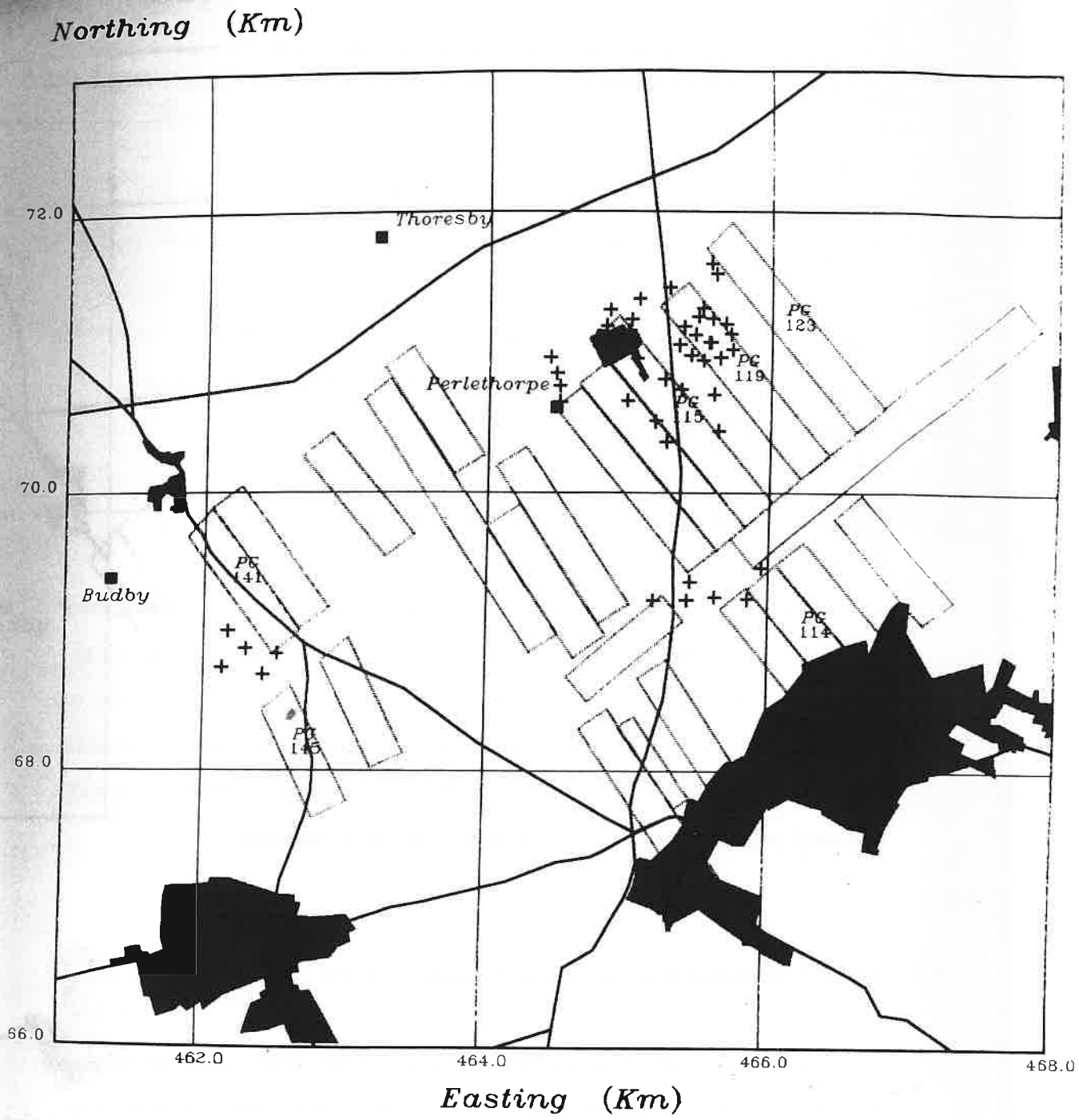

Figure 3.4 Seismicity from Thoresby take from 22/8/90 to 4/2/91.

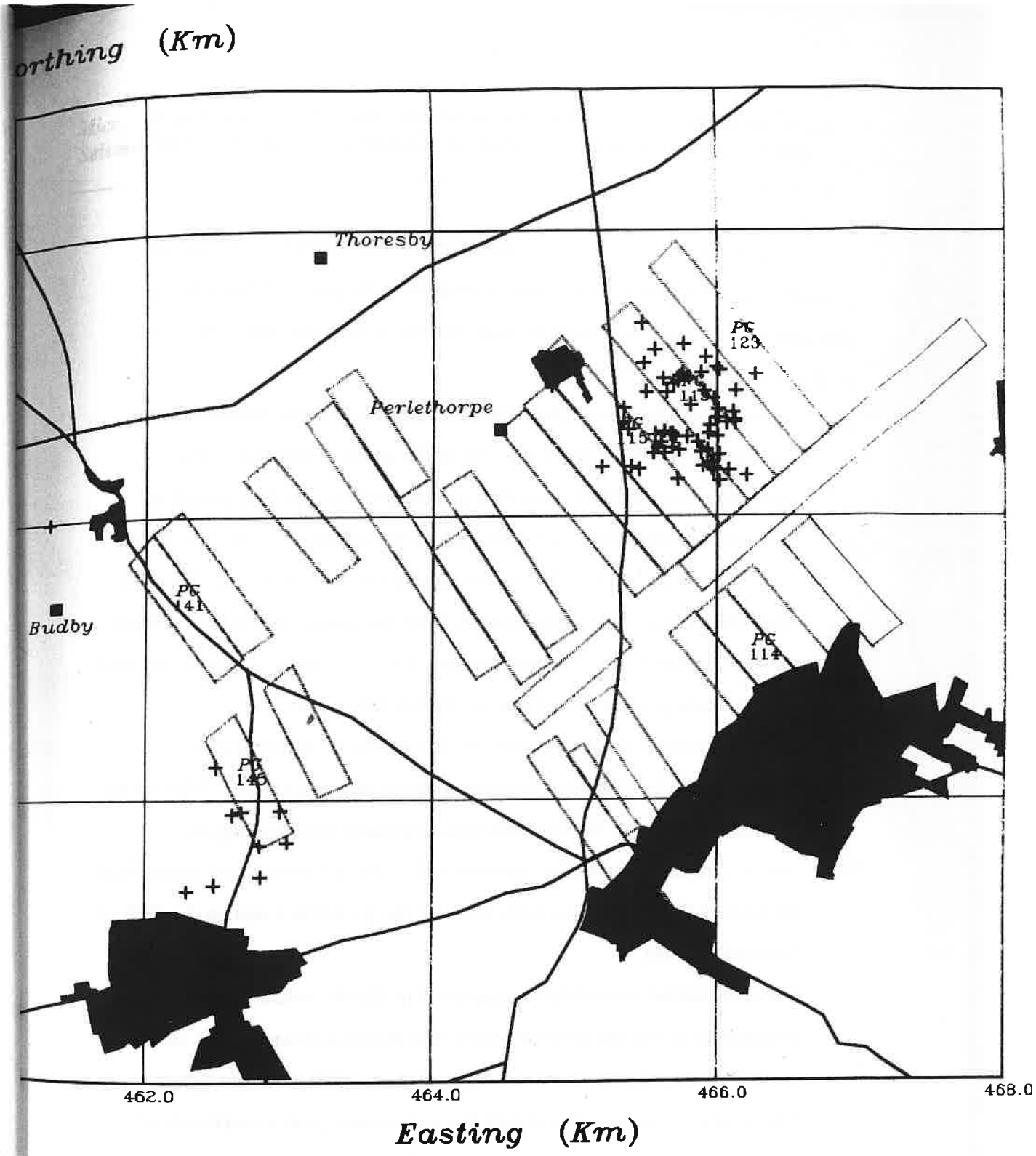

Figure 3.5 Seismicity from Thoresby take from 2/5/91 to 30/6/91.

Figures 3.4 and 3.5 show the epicentres of seismicity from within the Thoresby take. The figures cover two periods from August the 22nd 1990 to February the 4th, 1991 and from February the 5th to June the 30th 1991. The principal observations are:

i) events clustered around the northern end of PG115 which finished production in November at that end of the panel. There was some seismicity from PG115, even after production from the face ceased in November 1990. This is probably due to the proximity of PG119, which altered the local stress field and the presence of a pillar of coal, left in the Top Hard Seam which runs roughly down the centre of PG115 at a depth of approximately 530 m. below datum. There is a range of depths for these events, from ground level down to 1020 m. below datum.

ii) events clustered around the northern end of PG119 which started production in late October from the northern end of the panel. Most of the seismicity from the Thoresby take has originated from this region.

iii) events clustered around the northern end of PG114, production from which finished at the end of December with the last locatable event on the 28th of November 1990.

iv) events clustered around the southern end of PG141 which finished production on the 4th February 1991. The events although few in number, were located at depths from near the surface to 1000 m. below datum. The largest event recorded during this experiment, with a magnitude of 2.25 and a depth of 610 m., came from this area and was reported from Thoresby Colliery and the village of Budby .

Figure 3.5 shows the seismicity from the 5th of February, 1991 onwards;

i) a few events clustered around the northern end of PG115 which finished production in November 1990.

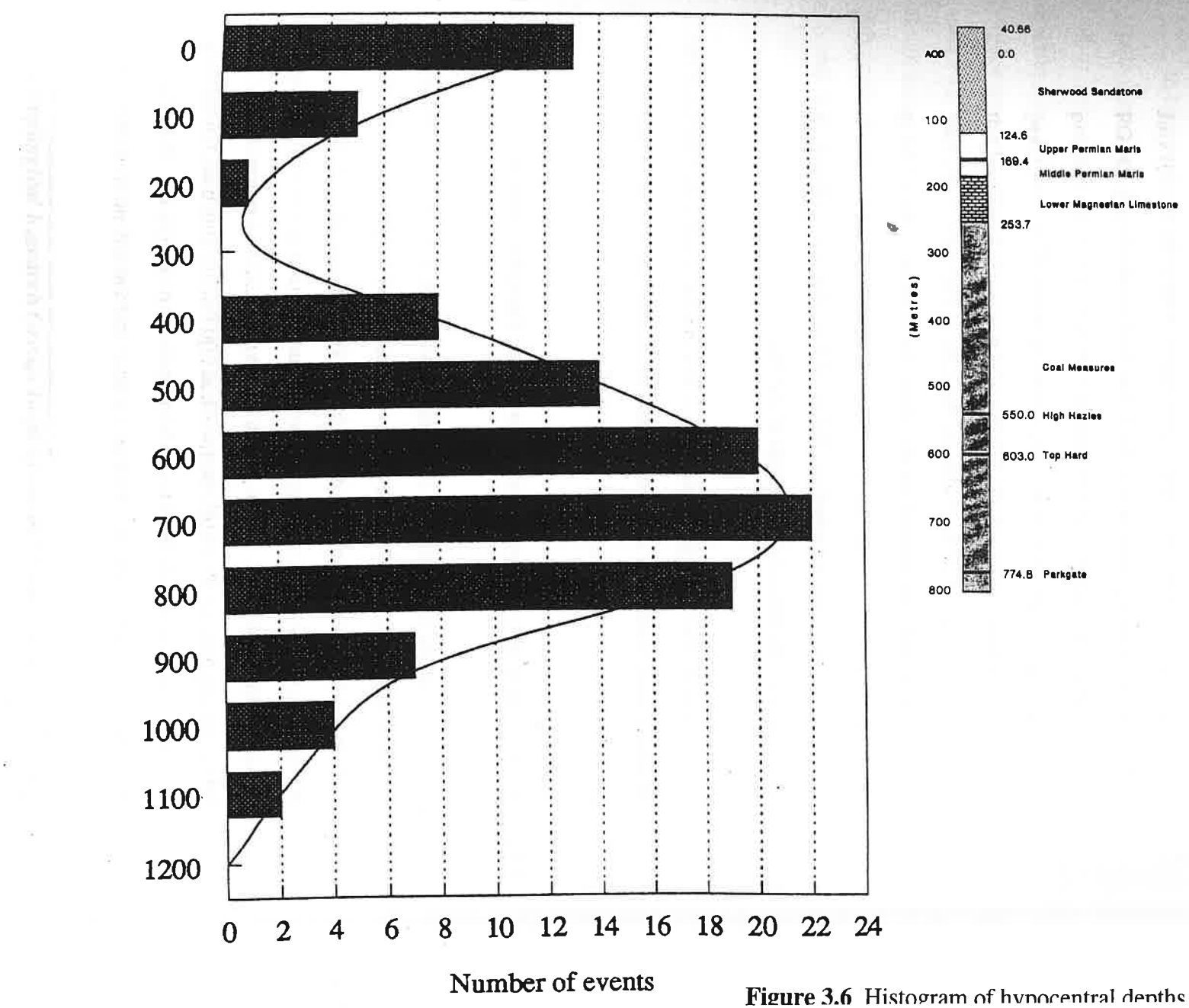

Figure 3.6 Histogram of hypocentral depths for events from Thoresby take

ii) events clustered around the northern end of PG119 with the epicentres migrating down the panel towards the southern end as production continued.

iii) Events originated from PG145 which commenced production at the southern end on the 4th of February and finished at the northern end on July the 3rd 1991. Four felt events locate around the southern end of PG145 where production started. The first occurred only three days after production started and was located 190 m. to the south of the edge of the panel at a depth of 680 m.. The event lies about 40 m. away from a pillar in the Top Hard seam (depth 470 m.) which was left because the coal was faulted. Two of these events on the 13th of February, 1991 nine days after production commenced, locate above the southern edge of the panel (depth 460 and 10 m.). The last few located events occur about 280 m. along the face. The face had retreated 330 m. at this time and it appears that the seismicity followed the retreat of the face.

Overall, the data appear to show a clear spatial relationship between the seismicity and production status of a panel indicating that the seismicity is generated and controlled by the extraction of coal.

3.4.3 Hypocentral depths for events within the take of Thoresby Colliery

Figure 3.6 is a histogram showing the variation in hypocentral depths for events located within the Thoresby take, placed in 100 m. bins from 0.0 m. to 1200 m together with a simplified well log of the geology. Most of the hypocentres fall into two regions, one at or near the surface, the other at depths of between 400 and 900 m.. In this area, the Parkgate seam is approximately 700 to 800 m. below datum. The Top Hard seam at 600 m. has also been completely extracted in this area with the exception of some remnant pillars. The depth distribution of the hypocentres implies a causal relationship between the seismic

activity and active retreat mining and its associated roof collapse for the Parkgate seam and the older workings above. If the distribution of the hypocentres is compared with the log, it shows that the brittle failure appears to be associated with two parts of the stratigraphic section:

(i) the Sherwood sandstone and that it is presumably associated with the fissuring seen at the surface in the village of Perlethorpe. Figure 3.4 shows a linear feature consisting of a series or burst of felt events, located at or near the surface. Within a few minutes, this burst was followed by another earthquake swarm whose epicentres all appear to lie along a NW/SE line just to the west of Perlethorpe coinciding with a series of major fissures seen in nearby fields exposed during remedial works carried out during September 1990. Small cracks were observed and later repaired in the tarmac of the B6034, which runs north out of Edwinstowe and directly over PG145.

(ii) at depths greater than 400 m. and less than 1000 m., which is in the productive or Middle Coal Measures, with a peak at the level of the Parkgate workings which lies almost completely within the 700 m. bin (i.e. 700 to 800 m.).

Felt events experienced in the Edwinstowe area of Nottingham have been caused by longwall mining in the surrounding collieries and the majority of the other events detected appear to be mining-induced for the following reasons:

1) The daily event rates show excellent correlation with current mining production
2) The epicentres fall on the active longwalls in the Parkgate Seam between 700 and 800 m. depth.

3) Activity closely follows production with little or no seismicity from the region of a longwall before or after extraction. The seismicity starts from the same end of the longwall as production and follows the face retreat.

4) Hypocentres are shallow (less than 1 km) and concentrate in two areas:

i) peaking around the Parkgate workings (700 to 800 m. and also including the worked out Top Hard seam (600 m.).

ii) in the Sherwood sandstone, from the surface down to about 200 m.. The surface expression of the shallowest events must be related to the mechanism causing the extensive, near vertical fissuring seen around the village of Perlethorpe where cracks over a metre wide, several hundred metres. long and of unknown depth were observed.

3.5 Borehole Microseismology

An enormous increase in precision in the location of events can be achieved by the incorporation into the network of detectors located in boreholes. One example of the advantages gained from borehole detectors is demonstrated by the Hot Dry Rock project operated at Rosemanowes Quarry, Cornwall by Camborne School of Mines where, using hydrophones in shallow boreholes (200 metres) they have location accuracies of c 20 metres (Baria *et. al.* 1989) for fractures generated by hydraulic stimulation of granite for the extraction of geothermal energy down to depths of c 2.5 km.

A further very significant increase in the accuracy of hypocentral position determination is made possible in coal mining aresa because of the particular seismic attributes of the floor-coal-roof 'rock sandwich'. The low seismic velocity and low density of coal means that the acoustic impedance contrast between coal and the roof and floor is often a factor of four. This physical situation means that

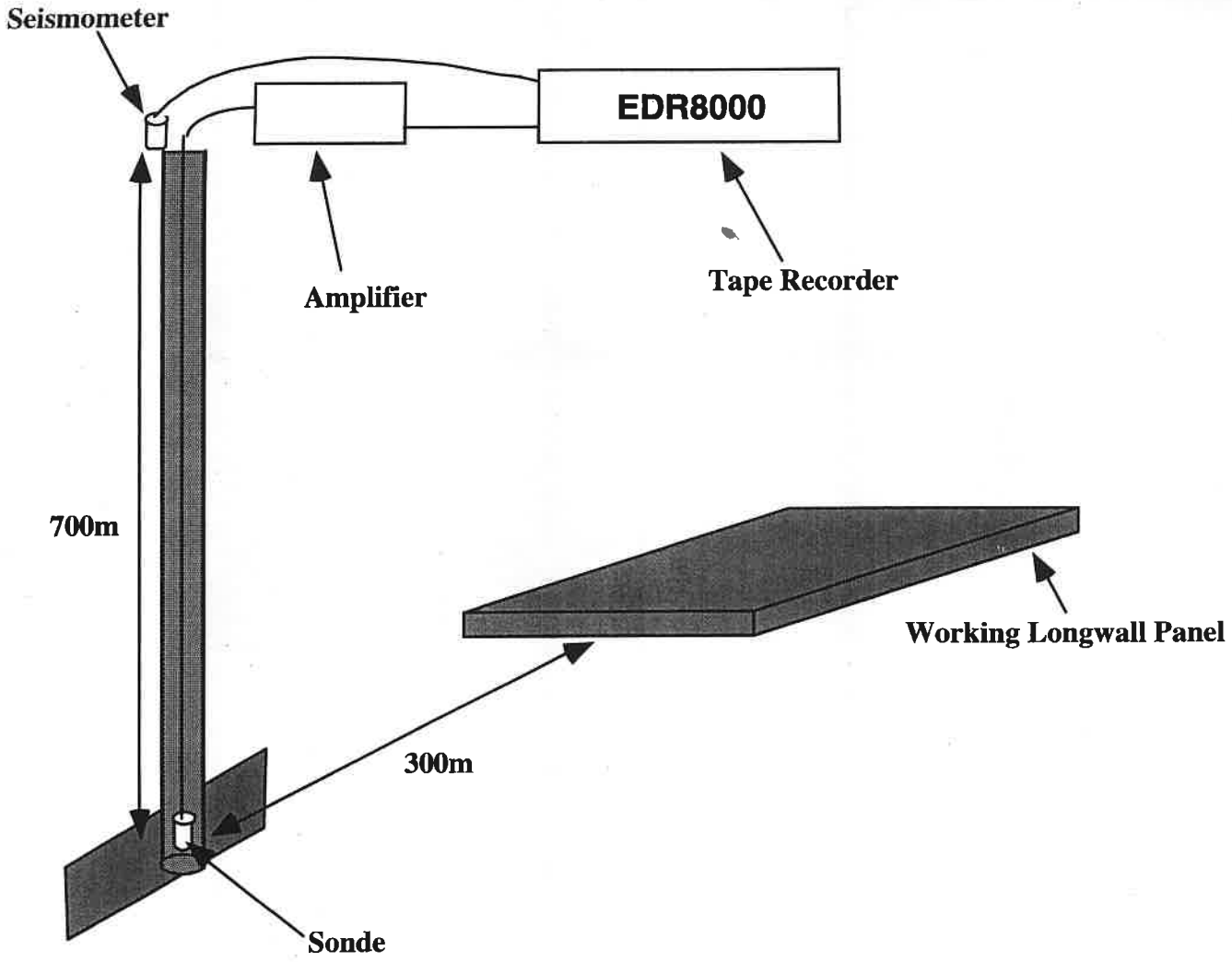

Figure 3.7 In-seam borehole geophone configuration at Coventry colliery.

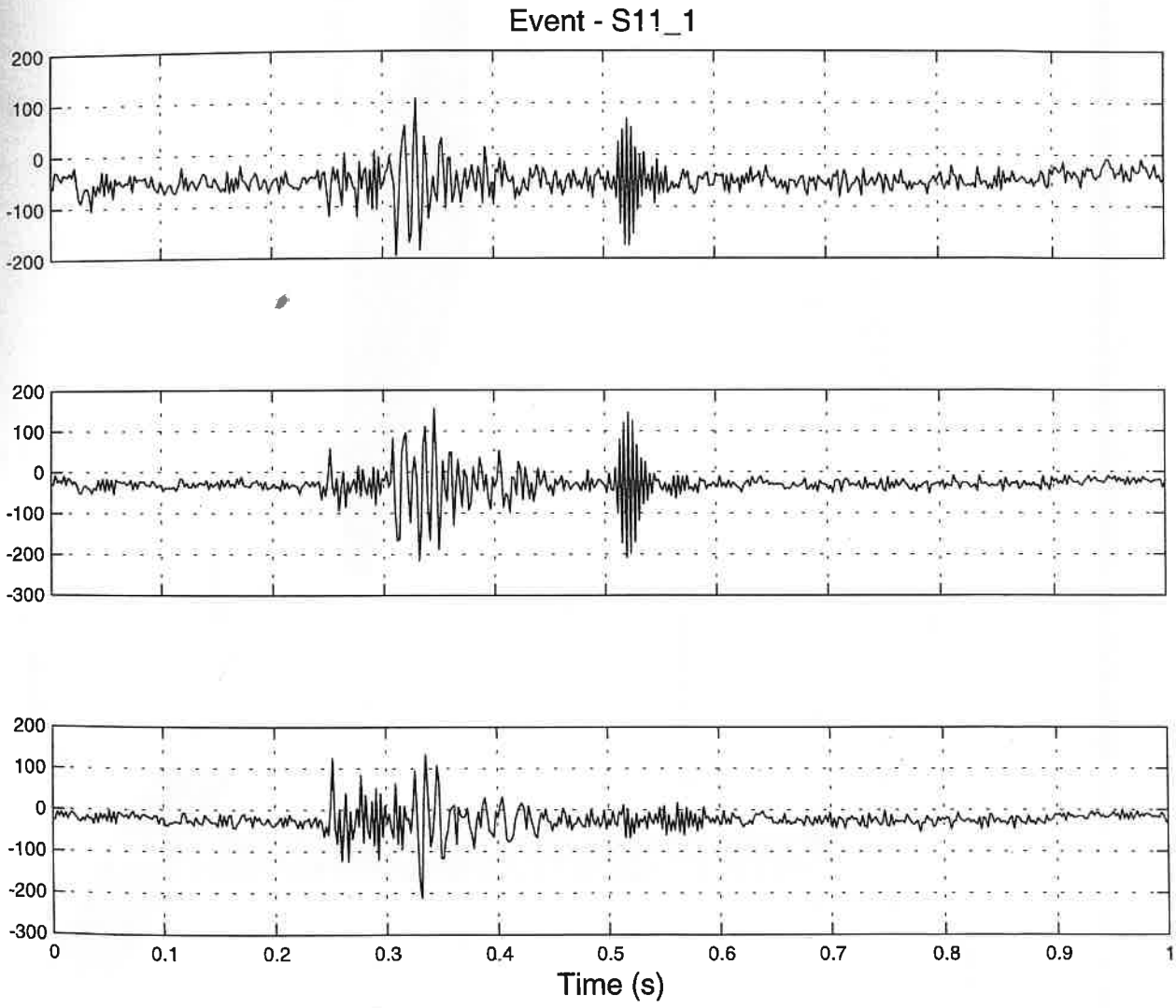

Figure 3.8 Seam waves generated by a mining-induced microseismic event.

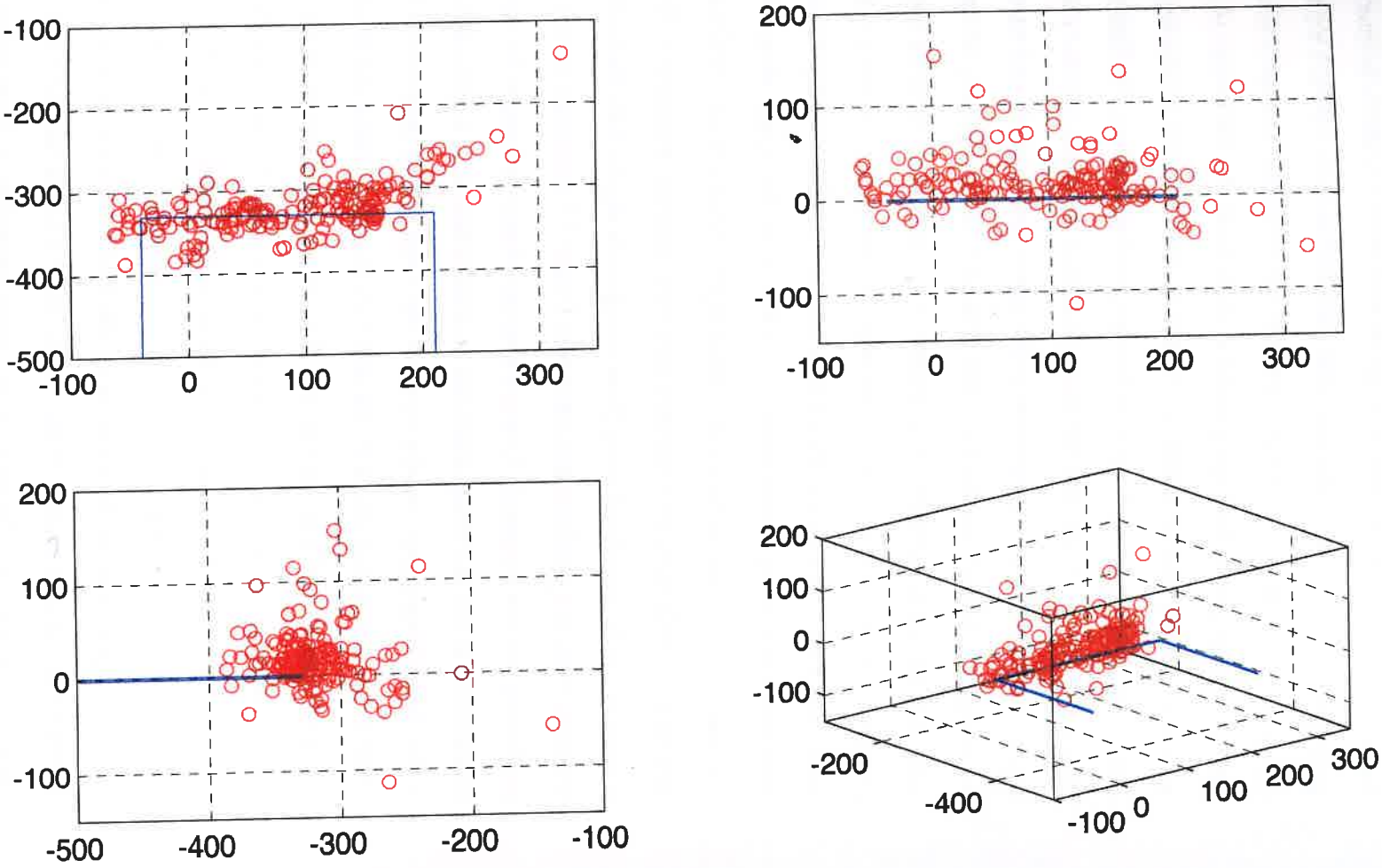

Figure 3.9 Seismicity detected during a 24 hour period at Coventry Colliery

the coal acts as a very efficient waveguide with waves trapped in the seam propagating for very large distance with little attenuation. Using a borehole 6-component (two three-component sets with the horizontal components spaced at 45 degrees) geophone package grouted at seam-level the University of Liverpool have successfully detected naturally occurring microseismic events some 500 metres ahead of an active long-wall face at Littleton Colliery, Staffordshire and Coventry Colliery, Warwickshire using geophone packages grouted into the seam together with a surface seismometer in the top of the borehole and monitored at the surface on digital cassette recorders (Figure 3.7) . The quality of these data was very high and clear guided waves (Figure 3.8) can be seen with the dispersive characteristics readily associated with seam waves. In the Coventry experiment more than 2000 events were detected in only two days of monitoring even in a relatively noisy surface environment (c 1 Km from the Jaguar Motor Works as compared to c 0.8 km to the seam). Toon (1990),Styles *et. al.* (1992) and Toon and Styles (1992) have demonstrated how very accurate locations (c 10 metre accuracy) can be generated using three-component digital data from only one borehole using the configuration shown in Figure 3.7 (although two or more are preferable, but not essential). Using a Spectral Matrix technique the azimuth of propagation of the incoming wave can be determined from a cross-power analysis of the three-components and the range of the event can be determined from the relative times of arrival of the P, SH and Airy phase assuming the dispersion characteristics of the seam are known. The surface seismometer and the borehole P-wave onset give extra precision in the calculation of the height of the event relative to the seam. Effectively a 3-D location problem is reduced to two 2-D problems which are much easier to solve. Knowing the direction and distance, a hypocentral position can therefore be established from a single borehole. Examples of the distribution of the events relative to the face for Coventry are shown in Figures 3.9 . The bulk of the events lie within 50 metres above and below the seam but there is activity up to 2-300 metres above the seam presumably associated with bed separation. In section the events appear to

delineate inclined surfaces hading away from the long-wall corners in accord with numerical predictions of the mode of failure for this type of mine opening. The events are generated above and below seam-level but because of the spatial spread of the Green's function (the displacement response of the ground to a point impulse situated at the event location) seam waves will be stimulated even when the source is some considerable distance above the seam itself with the decay of the amplitudes of the Airy phase in particular being very sensitive to vertical distance above the seam. We believe that it is possible to use the ratio of the amplitudes of the various phases to establish the vertical location of events occurring above the seam as collapse progresses with considerable precision , probably to better than 5 metres, particularly for those events within 50 metres or so of the seam. Additionally, we have found that naturally occurring events are much more efficient stimulators of guided waves than are explosive shots in the seam probably because of the inherent asymmetry of natural events and the broad spectrum of frequencies they generate.

3.6 Relevant Microseismic Monitoring of Longwall Mining at Gordonstone Mine, Bowen basin, Queensland, Australia

An experiment with very similar objectives to this monitoring programme was carried out by CSIRO and Central Queensland University (Hatherley *et. al.* 1995) at Gordonstone Colliery, in the Bowen Basin, Queensland which is operated by ARCO. Their objective was to determine caving height from working in the Permian German Creek Seam which lies at a depth of 230 metres. In some adjacent areas , this seam is overlain in close proximity by Tertiary sands and volcanics which act as aquifers. Although this was not an issue at Gordonstone, this was a new mine and investigations could be carried out without too much interaction from older workings. Three boreholes were drilled and seven triaxial geophone strings were deployed at 30 metre intervals in each hole, together with some shallow holes to give a total of 27 tri-axial stations. SENSOR SM15B 14 Hz

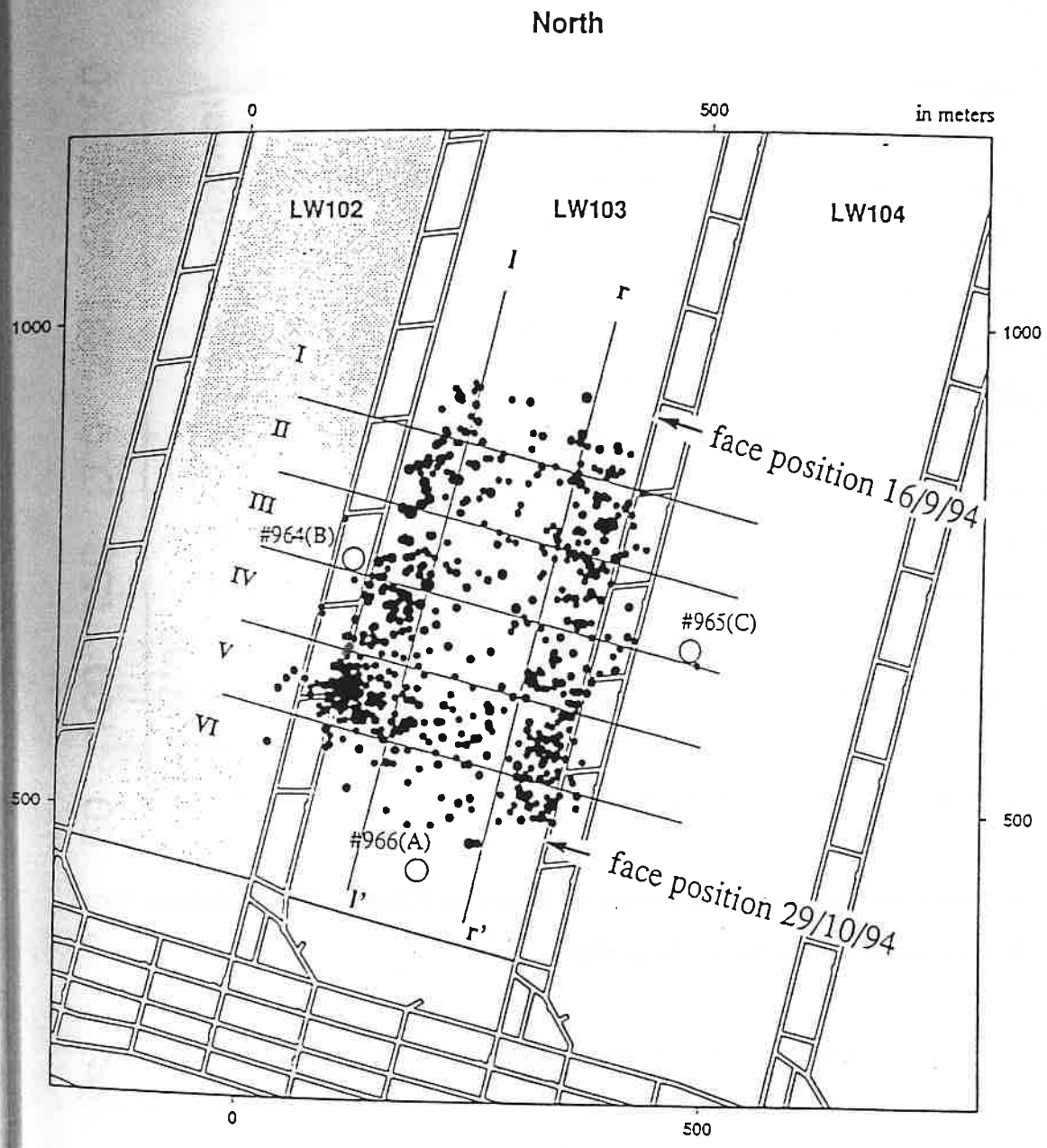

Figure 3.10 Plan view of the location of the 629 seismic events at Gordonstone colliery.

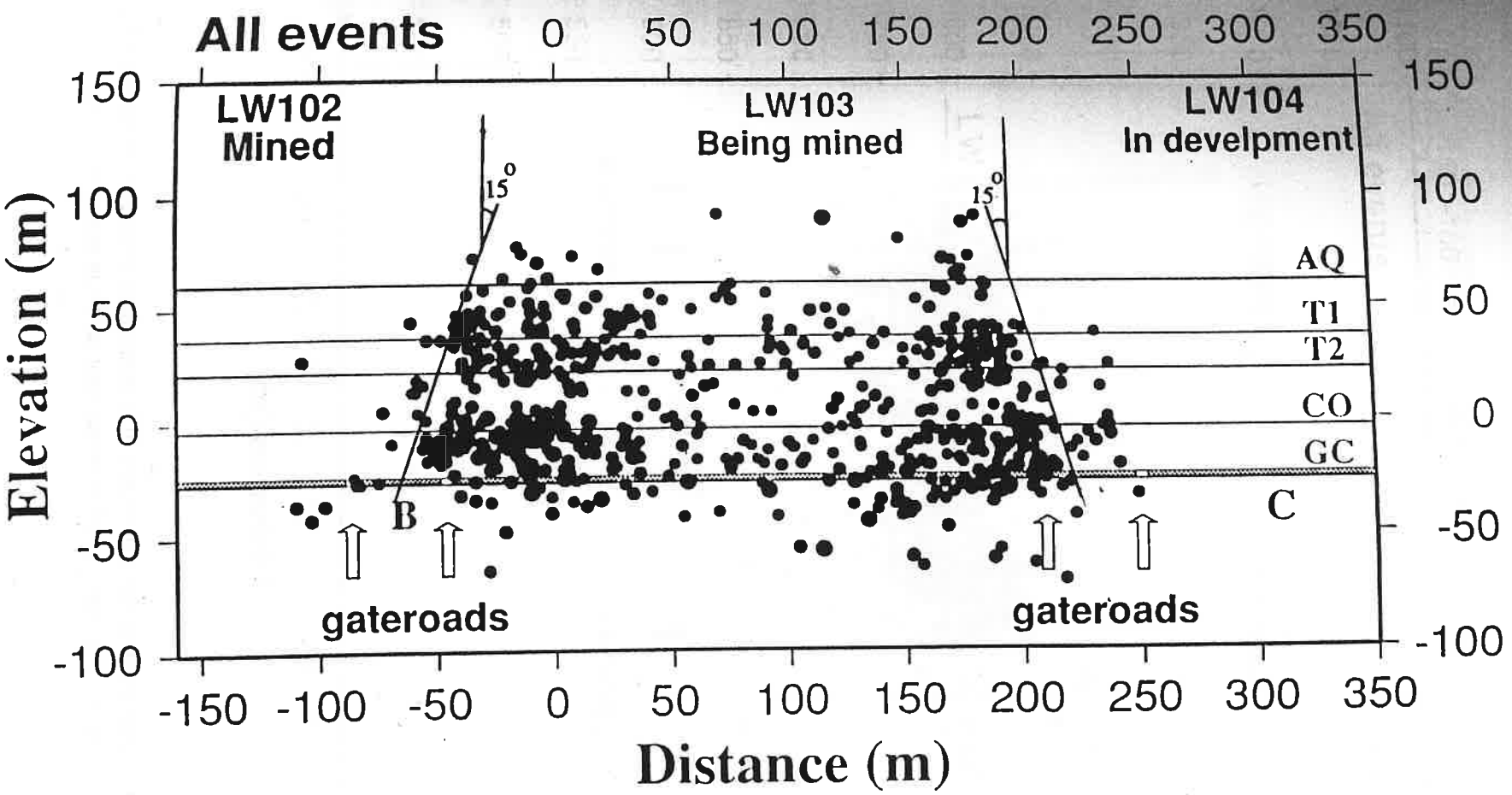

Figure 3.11 All events at Gordonstone colliery for the cross-section looking northwards along LW103.

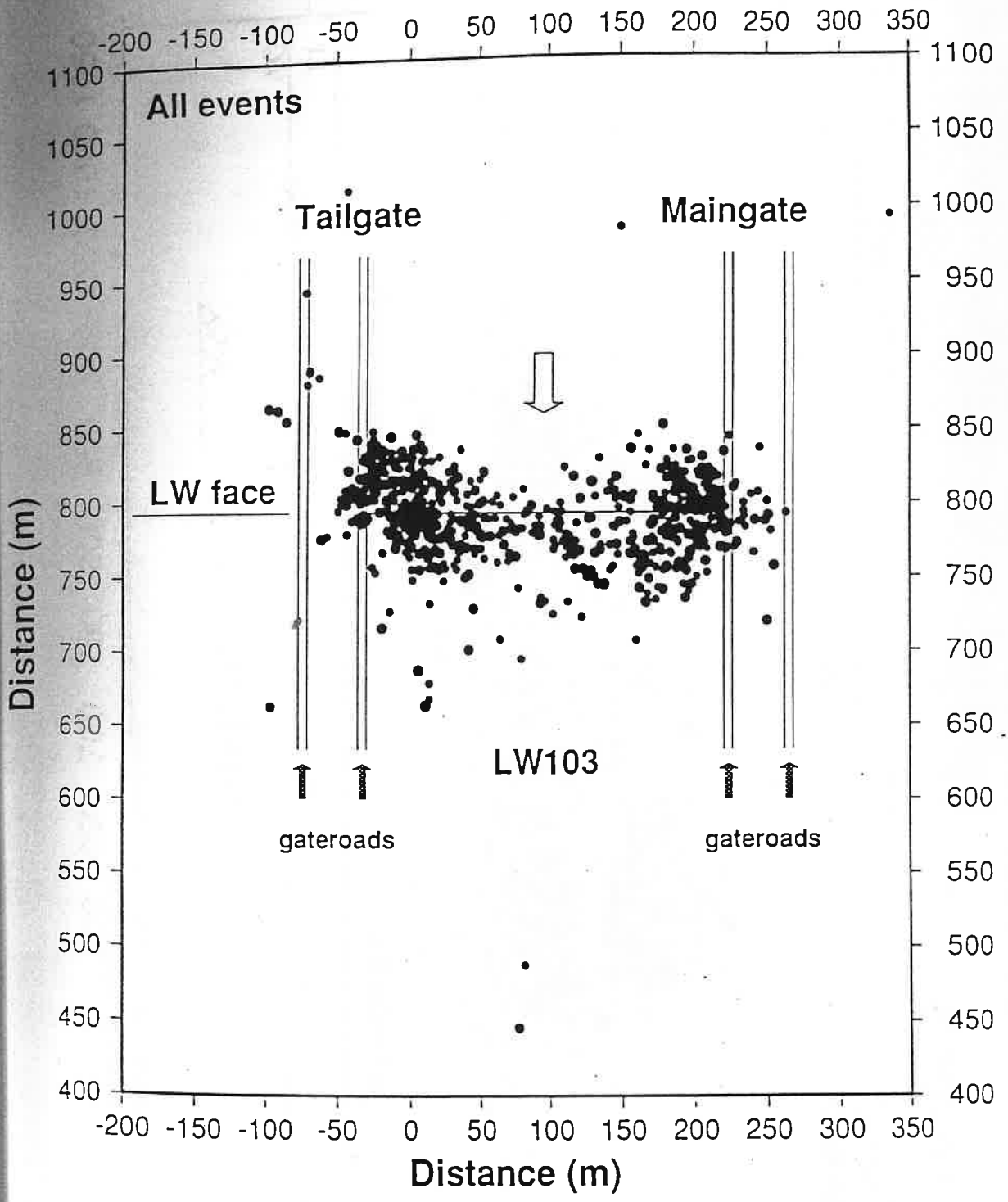

Figure 3.12 The plan view of the 629 events at Gordonstone colliery normalised to a fixed longwall position. The open arrow indicates the advance direction of the longwall face.

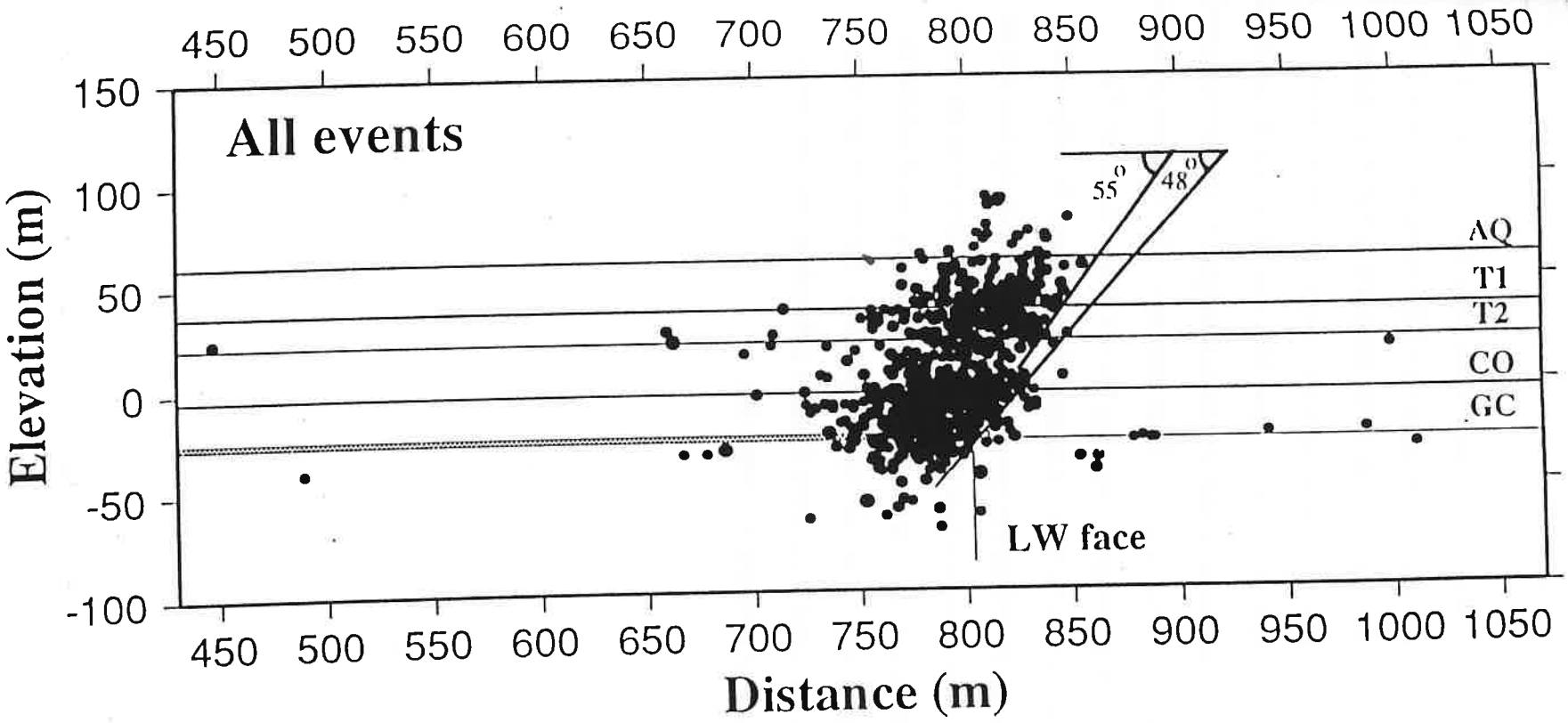

Figure 3.13 Distribution of the 629 events normalised to a fixed longwall position. The elevation of the ground surface is approximately 204m and the base of the Tertiary is at about 150m.

geophone inserts were assembled into sondes. Data acquisition was carried out on a PC-based system designed and built in-house by CSIRO using Microstar A-D boards. The data were then passed to a SILICON GRAPHICS INDY workstation running the ISS xmts seismic processing software. Some 1200 events were recorded during a two-month period and of these 629 were of sufficient quality for further analysis. The locations of the 629 events with respect to the working panel are shown in Figure 3.10 (Plan) and 3.11 (Face Section) . The locations plotted in a frame of reference with respect to a moving face are shown in Figure 3.12 (Plan) and Figure 3.13 (Gate Section). It is clear that the events lie within about 30 metres below to about 100 metres above and behind the working face and are constrained by an inclined surface hading at 55 degrees forwards from the face. It is very clear that there is a very important control on the location of seismicity exerted by the stresses induced around the face position. The results are very similar to those we recorded at Coventry Colliery although in that case some hundreds of events were detected in a single day.

4 GEOLOGICAL AND GEOMECHANICAL BACKGROUND FOR ASFORDBY MINE

4.1 General Geological Setting

This geological description is based on Whitworth *et. al.* (1994)

4.1.1 Structure

Asfordby mine forms an extension of the larger Carboniferous basin of South East Nottinghamshire. The Coal Measures dip into the basin at a very shallow angle towards the north and north east. The dips increase to the east and south where the Coal Measures overlap on to basement rocks. The position is further complicated in the area of Asfordby Shafts by extrusive volcanics of late Namurian or Westphalian A age which comprise mainly basalt lava flows. Over the rest of the Asfordby basin the Coal Measures are conformable on the Namurian Millstone Grit series.

4.1.2 Faulting

The faulting is generally east to west approximately parallel to the southern edge of the basement complex with throws up to 100 metres. Most of the faults were active in post Triassic times. A secondary fault trend running north west to south east has also been identified (see Figure 4.1) which seismic evidence suggests is Pre-Permian.

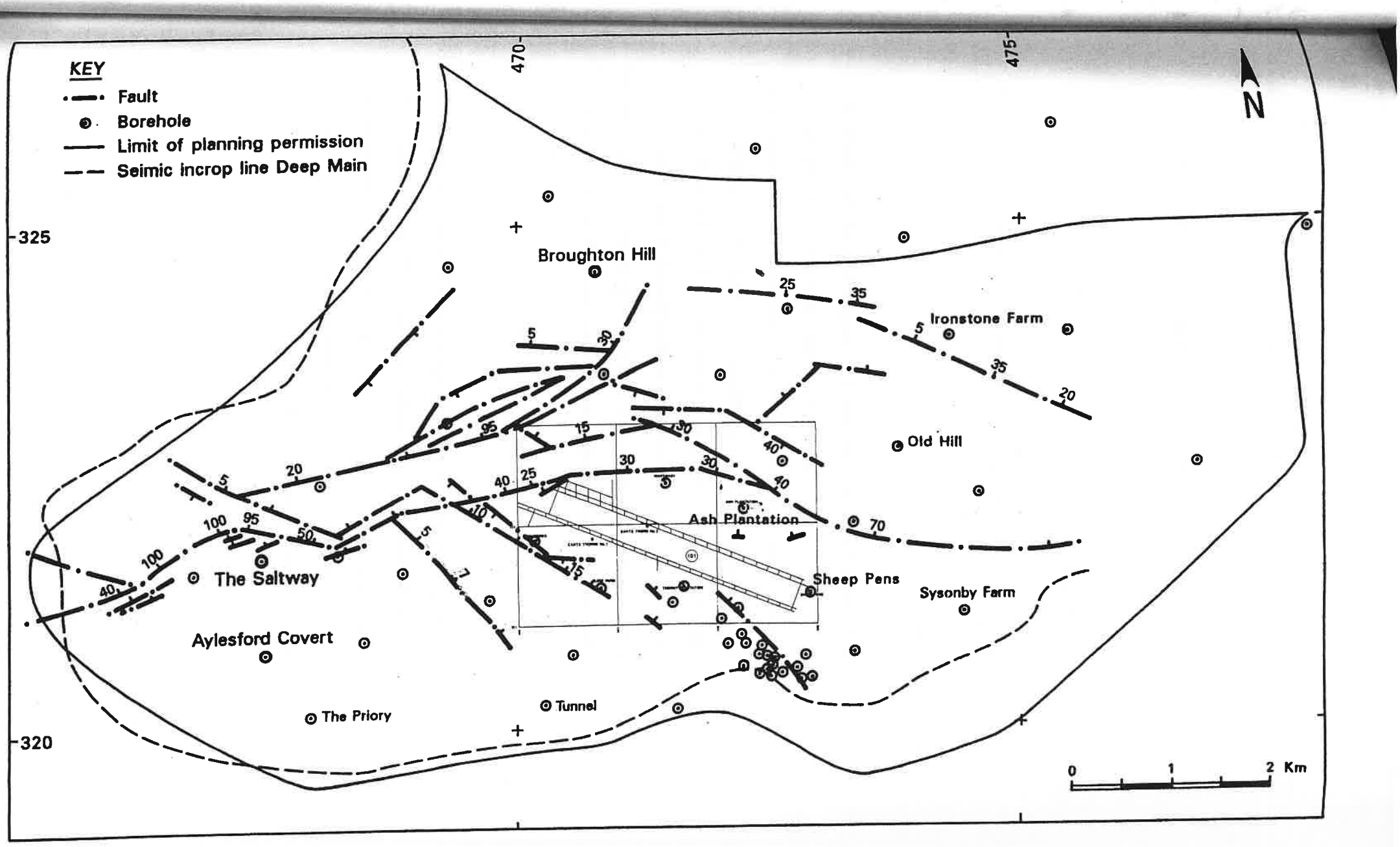

Figure 4.1 Plan of Asfordby Mine showing Faulting and Exploration Boreholes

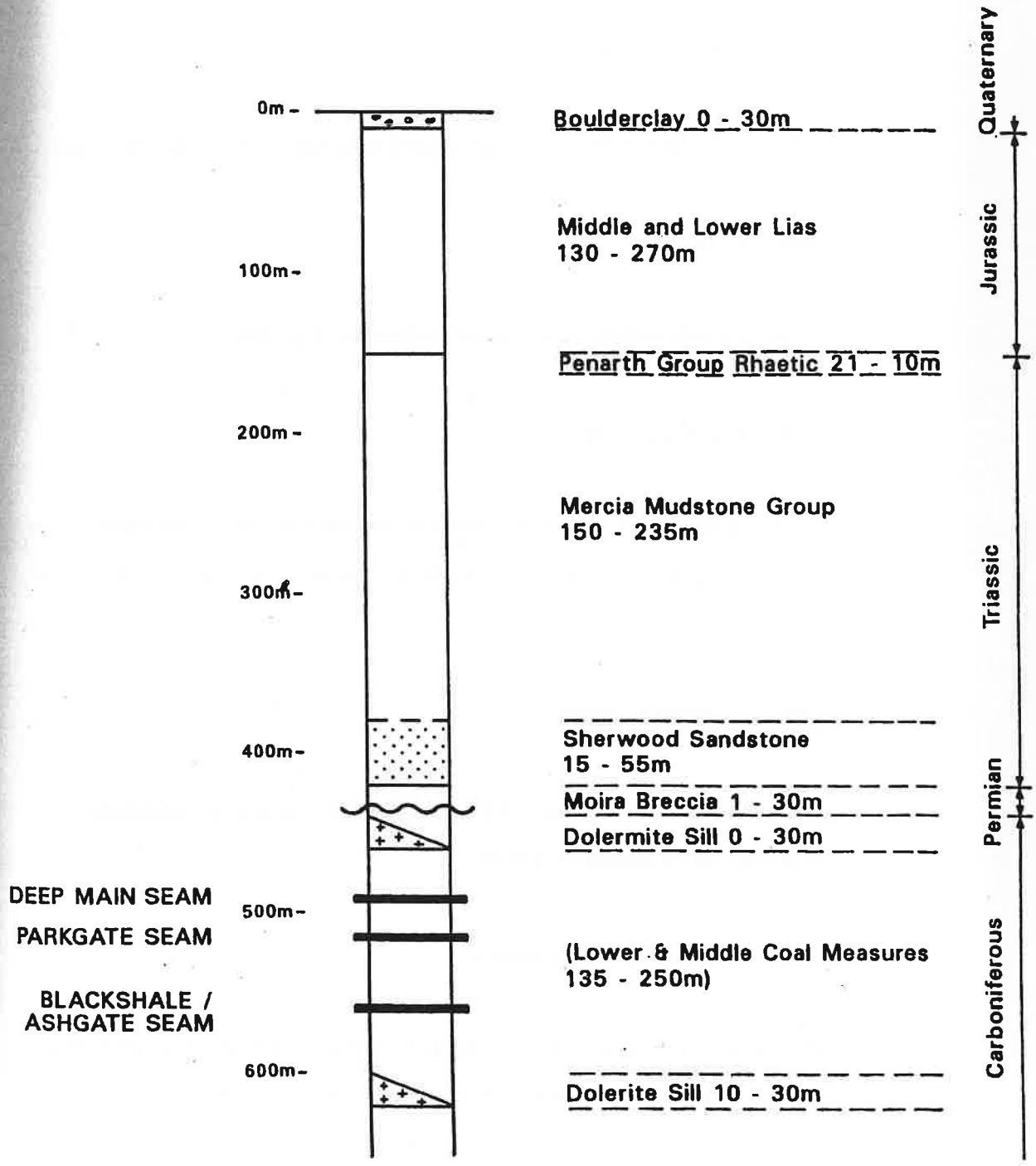

Figure 4.2 Generalised Geological Section at Asfordby Mine

4.1.3 Geological Succession

Figure 4.2 shows the general geological sequence in the Asfordby area.

Boulder Clay

Blue grey clay with brown patches and scattered pebbles.

Lower and Middle Lias

Mainly grey to dark grey mudstone with subordinate limestone bands. The basal 3 to 5 metres comprises fine grained muddy limestones known as the Hydraulic Limestones.

Triassic - Penarth Group

This consists of a thin bed (2-10 metres) of grey calcareous mudstones with thin sandy limestone bands.

Triassic Mercia Mudstone Group

The upper part of this group, the Keuper, consists of red brown siltstones and mudstones with numerous gypsum and anhydride bands and veins. Several flaggy sandstones known as skerries occur in this sequence.

The lower part of the Mercia Mudstone Group is known as the Waterstones and comprises fine grained sandstones and siltstones with occasional mudstone bands.

Triassic - Sherwood Sandstone Group

This is mainly a medium to course grained sandstone, often weakly cemented, inter-bedded with conglomeratic beds and thin silty mudstone and bands. The horizon is a major aquifer with generally high permeability and porosity.

Permian - Moira Breccia

This formation, which lies immediately above the Permo - Trias unconformity, is a breccia-conglomerate of sub-rounded to sub-angular pebbles in medium grained argillaceous sandstone.

Carboniferous - Lower and Middle Coal Measures
(Westphalian A and B)

This strata consists of a cyclic sequence of mudstones, siltstones and sandstones with coal seams and seatearths. At the Asfordby Mine three main coals are developed, the Deep Main, Parkgate and the Blackshale/Ashgate.

Two zones where dolerite sills commonly develop in the Coal Measures have been noted. The lower is below the Blackshale/Ashgate Coal most commonly either above or below the Kilburn Coal. This sill appears to be present over the whole of the Asfordby area and is up to 30 metres thick.

The second sill or group of sills occurs above the Deep Main usually between the Clay cross Marine Band and the 2nd Ell. coal. This sill often forms the boundary between the Carboniferous and the Permian unconformity. The dolerite is fine to medium grained and fresh. The

SECTION OF STRATA ABOVE DEEP MAIN
101's FACE START TO CANT'S THORN No.2
(DATUM = DEEP MAIN ROOF)

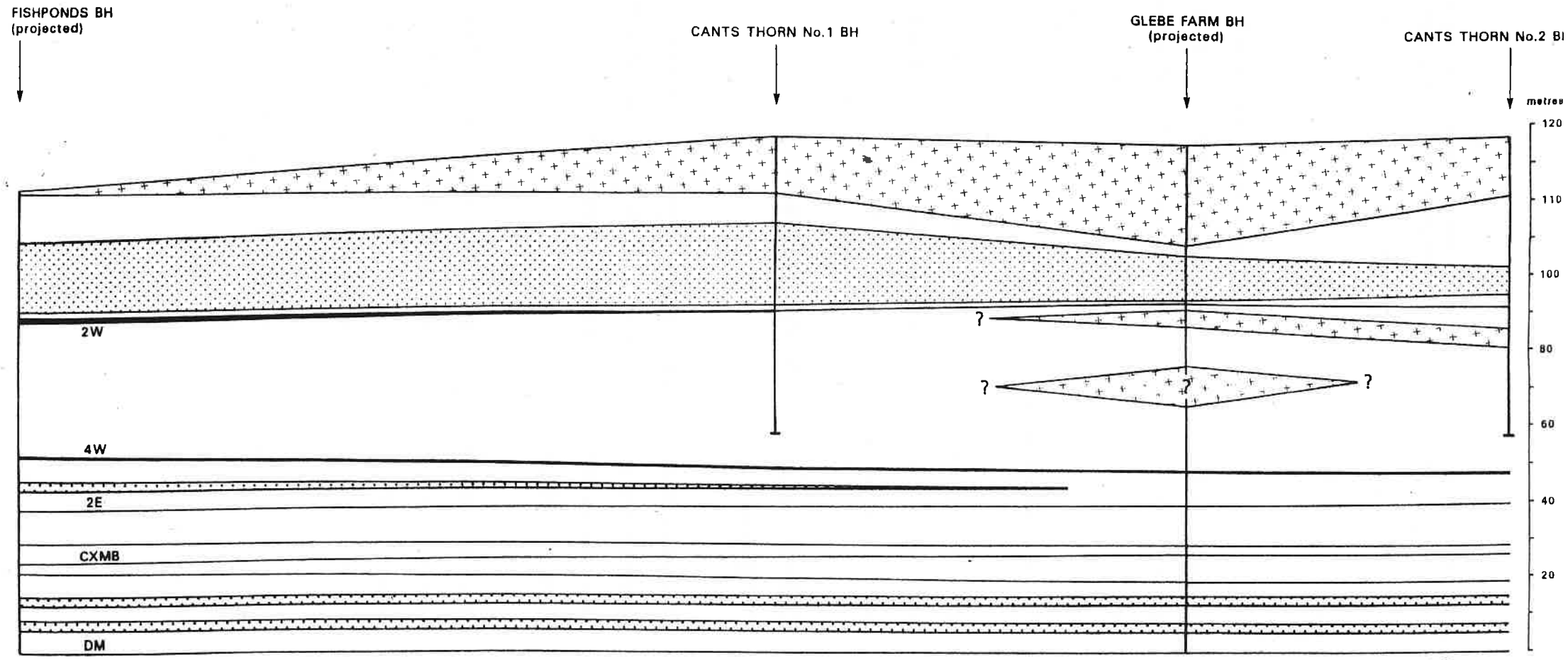

2W = Second Waterloo Seam
4W = Fourth Waterloo Seam
2E = Second Ell Seam
CXMB = Clay Cross (Vanderbeckei) Marine Band
DM = Deep Main Seam Roof

Horizontal Scale 1:2500

KEY

Sandstone

Igneous

Figure 4.3

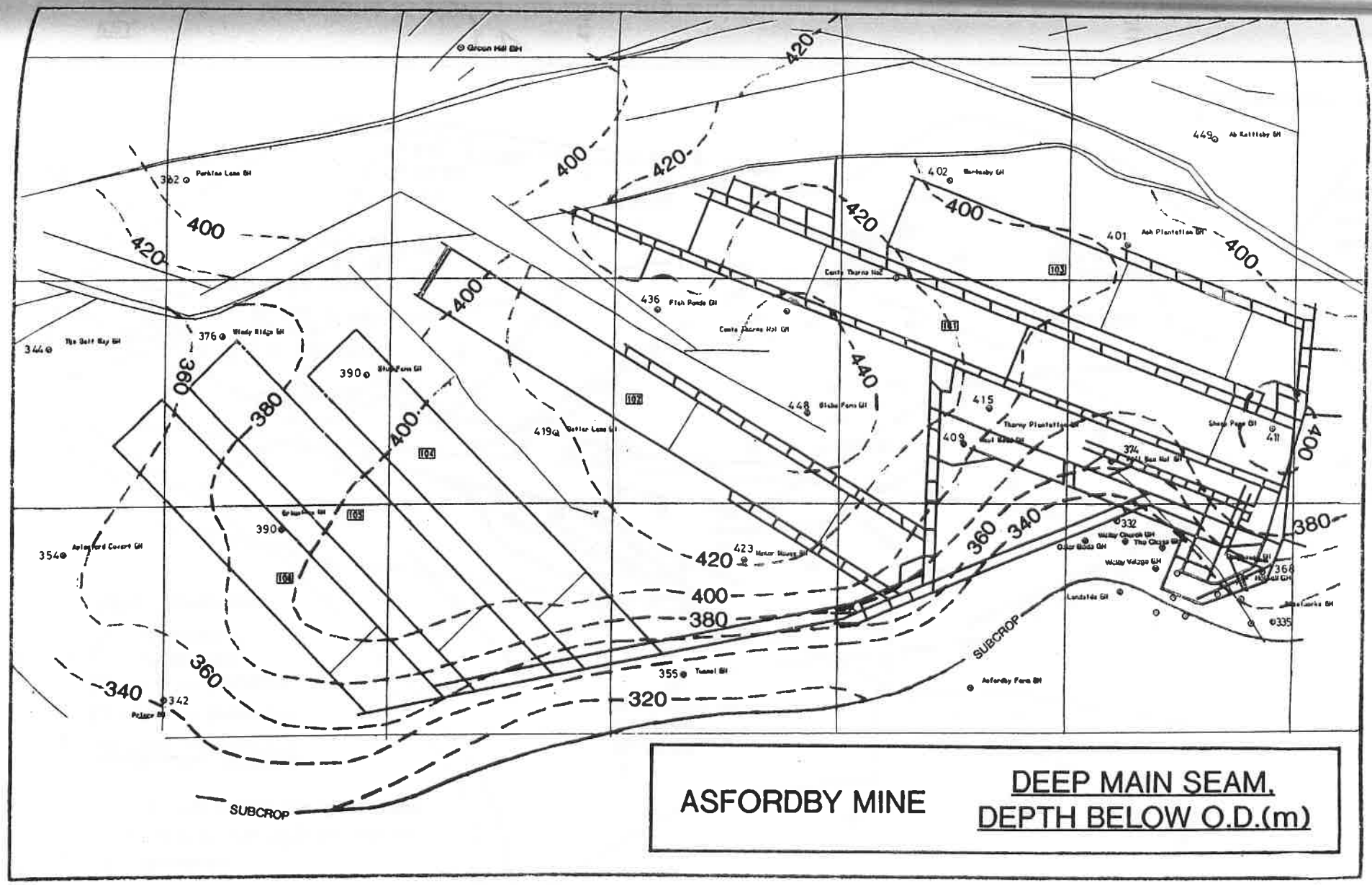
ASFORDBY MINE
DEEP MAIN SEAM.
DEPTH BELOW O.D.(m)
SUBCROP
SUBCROP
420
400
380
360
340
320
440
101
102
103
104
105
Green Hill BH
Parklea Lane BH
Windy Ridge BH
Tunnel BH
Asfordby Farm BH
Ash Plantation BH
Fish Ponds BH
Thorny Plantation
Valley Village BH
Landside BH

Figure 4.4

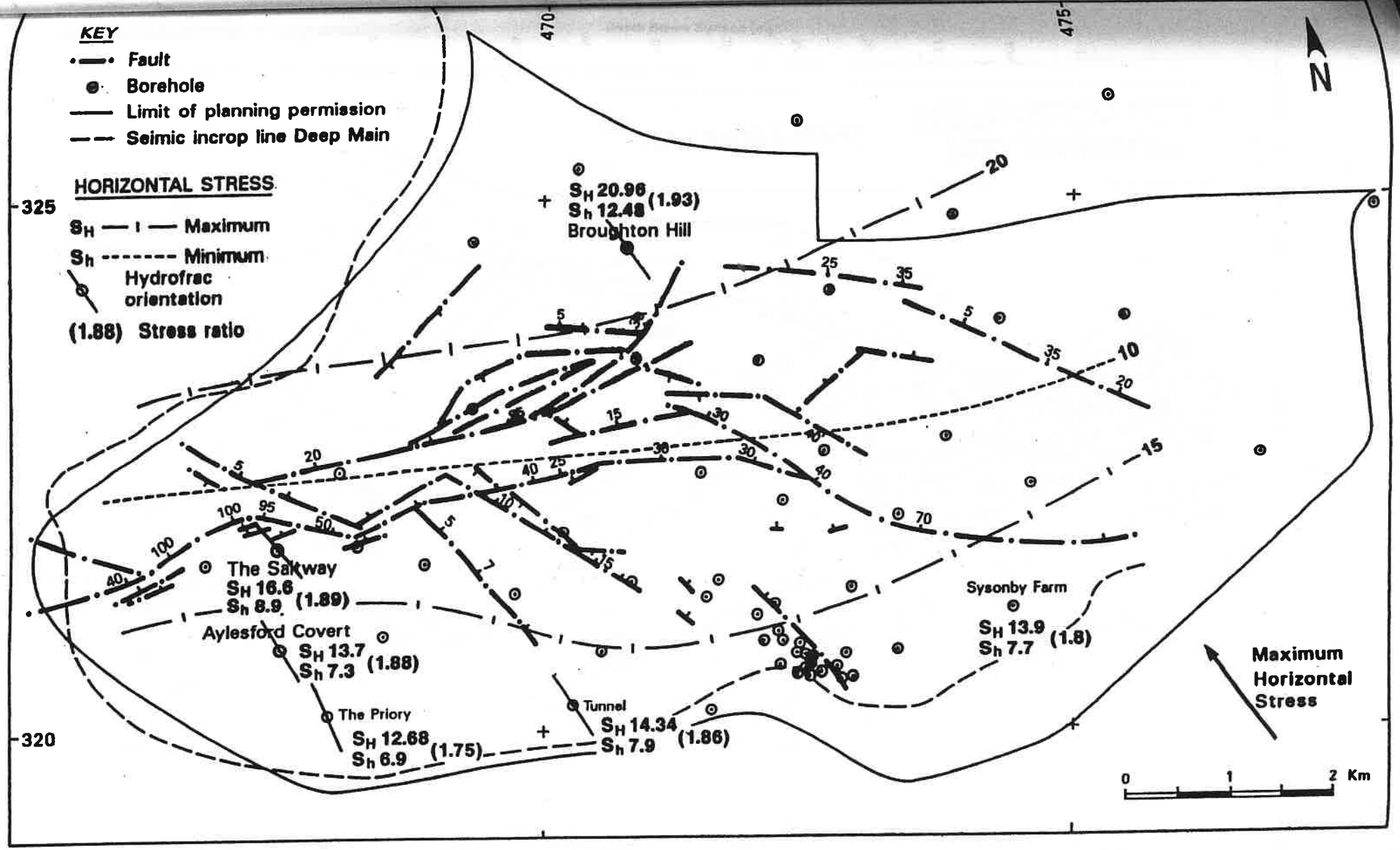

Figure 4.5 Variations in Horizontal Stresses and Stress Ratio over the Asfordby Mine

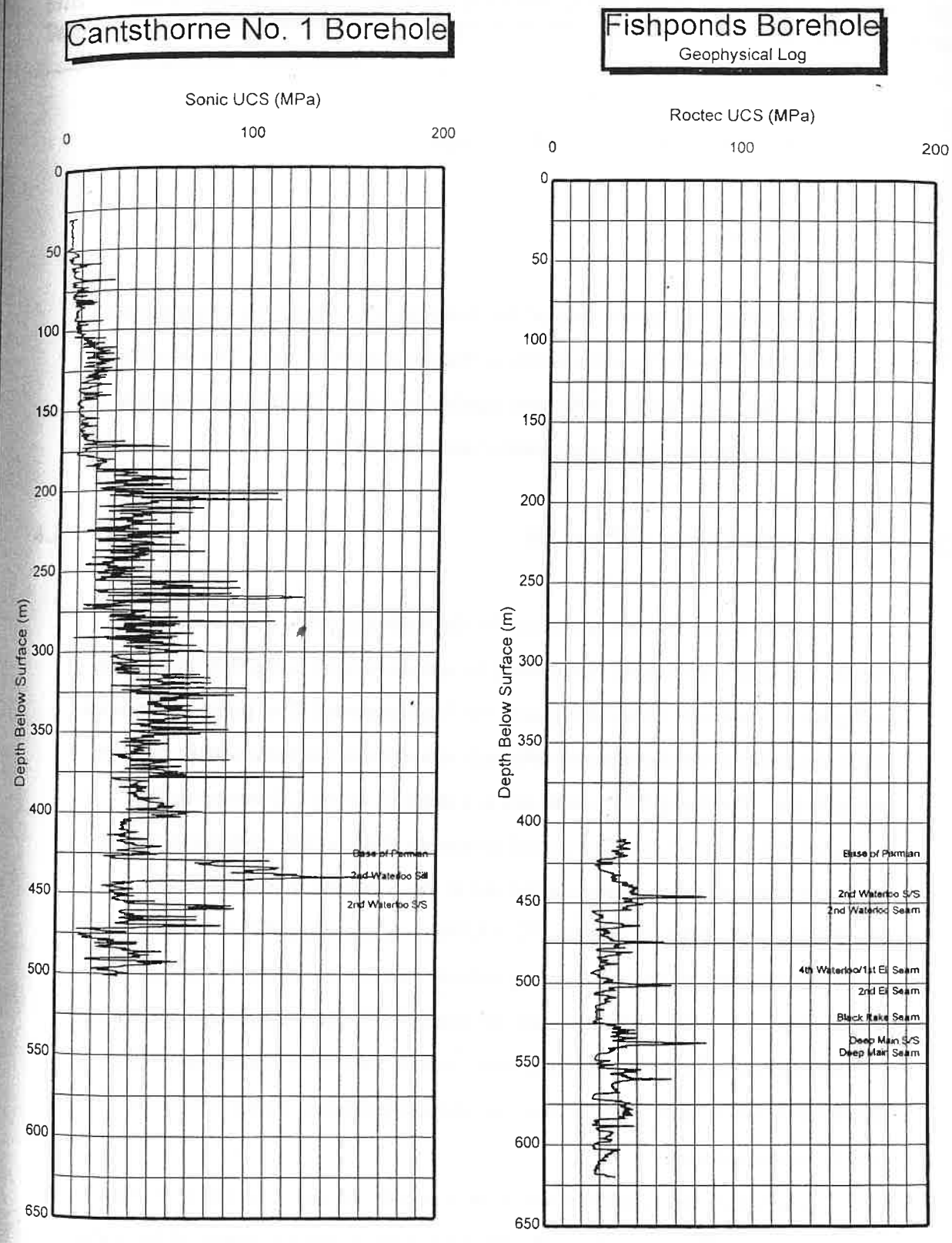

Figure 4.6 GEOPHYSICALLY DERIVED UCS LOGS OF FISHPONDS AND CANTSTHORNE No.1.BOREHOLES

joints in the sills are believed to be tight.

Volcanics

In the southern central area of the Asfordby Mine there is a volcanic pile believed to be of late Namurian or Westphalian A in age . The lava flows are dark grey basalt, rubbly and highly vesicular. The flows are jointed with occasional large open joints containing water.

4.2 Geology in the vicinity of Panel 101

A simplified geological section for the Asfordby Mine area is shown in Figure 4.3. The major faults determined by surface seismic reflection are shown in Figure 4.1 with the location of panel 101 superimposed. This panel was chosen to lie in a relatively unfaulted area although sub-seismic resolution faults can not be excluded. The Deep Main seam lies at a depth of about 430 metres in the region of Panel 101 and shallows in all directions (Figure 4.4) Extensive in-situ stress measurements have been carried out in the Asfordby region (Whitworth *et. al.* 1994) as part of ECSC project 7720-AF/854. A summary of the results of borehole breakout and hydrofracturing derived values is given in Figure 4.5. The principal stress has an azimuth of approximately 325^0 and values varying between 14 MPa and 21 MPa increasing from south-west across the Asfordby take. This is interpreted to be related to strike-slip faulting along the east-west Fault Zone which crosses the area.

The Sherwood Sandstone which is an aquifer for much of the Midlands lies only about 100 metres above the Deep Main Seam and has potential for water ingress if mining-induced fracturing propagates to that level or to water filled bed separartions. Figure 4.6 shows the geophysically-derived rock strength for Cant's Thorns #1 and Fishponds boreholes; of particular note is the very high value of

160 MPa at a level of 440 metres associated with the Second Waterloo Sill in Cant's Thorns #1

5 MICROSEISMIC RECORDING EQUIPMENT

5.1 Vibrosound SP1 Seismic Recorder

A capability was required for the monitoring and recording of borehole microseismic data from downhole geophones grouted in-seam. In order to meet this need a triggered 24-bit seismic event recorder with flash-card storage was commissioned from Magus Electronics Ltd, Wheelock, Crewe, Cheshire. This equipment was delivered to the Microseismology Research Group, University of Liverpool for laboratory and field evaluation together with hardware and software for reading PCMCIA cards. Software was subsequently written on SUN workstations and PC's by the Department of Earth Sciences and also by MAGUS. After initial tests at Daw Mill Colliery and in the laboratory it was deployed for the period 2 September to 9 September 1994 at Roughs Borehole in close proximity to Daw Mill Colliery workings. This section summarises the operational findings , evaluates the equipment performance and gives preliminary results of the seismic monitoring over this short period.

5.2 Description of the instrument

The Vibrosound SP1 seismic monitor is a development of a Vibrosound blast vibration monitoring system. It has the capability to record 6 vibration channels and one sound-pressure channel. In order to achieve the dynamic range necessary for recording naturally-occurring mining-induced microseismicity it was essential to have 24-bit digitisation. Additionally, in order to have a long-term recording capability the events were to be stored on 20 Mbyte Flash- EPROM cards. Both of these modifications led to some implementation difficulties initially.

The equipment is contained within a large weatherproof case carrying handle and lockable clips sealed to IP65.

Inside the casing is an alphanumeric keyboard with 4 by 20 character display and a 4 colour pen graphics printer . The on/off switch is also on the inside of the case. This is operated by a key in order that the equipment can be enabled and so can be left running without the fear of being accidentally switched off. The equipment can be powered from mains power, internal rechargeable batteries or an external 12 Volt supply. On the inside of the lid there are storage clips for a microphone stand and small wallet for a sheet containing a summary of the operating commands.

On the outside of the casing there are plugs to receive incoming seismic data on six channels, sound signals from a microphone, and the external 12V power supply. There are also plugs to output data straight onto a PC. The details of operation are contained in the Vibrosound operation manual although it is clear that this is very much an ad-hoc document generated by editing of the previous manual with many omissions and some material included which does not apply to this instrument.

Gains can be set at 1 and 10, and thresholds can be set in microvolt steps from 1 microvolt upwards. Geophone sensitivities can be set and sampling rates of 250, 500 and 1000 Hz are available. A total data length per event of up to 2499 samples can be set giving almost 10 seconds of continuous data at 250 Hz or c 2.5 secs at 1000 Hz.

5.3. Testing the Vibrosound Recorder

5.3.1 Laboratory Evaluation

The equipment was tested in the laboratory using a SENSONICS SM14 geophone as a source and appeared to trigger satisfactorily and to store recorded events on to the Flash Card. The duration of the recording process which is of the order of a minute per event may be problematical as the repetition rate of natural seismicity may be of this order. Real seismic data recorded during a previous

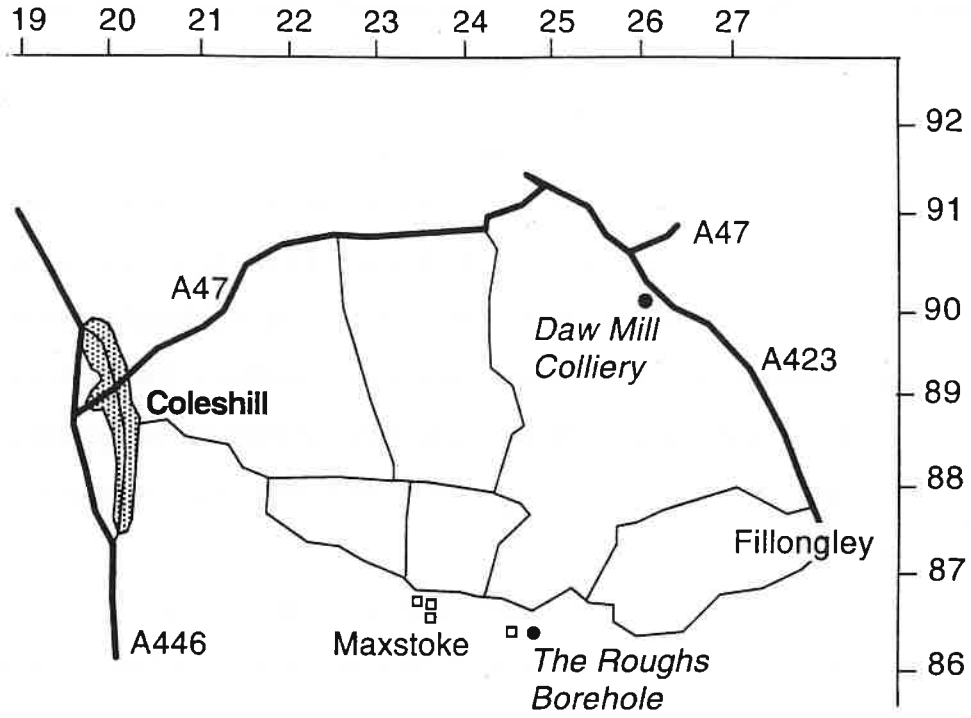

Figure 5.1 Map to show the location of Daw Mill Colliery and The Roughs borehole. The coordinated system is taken from O.S. 1:50,000 sheet 131.

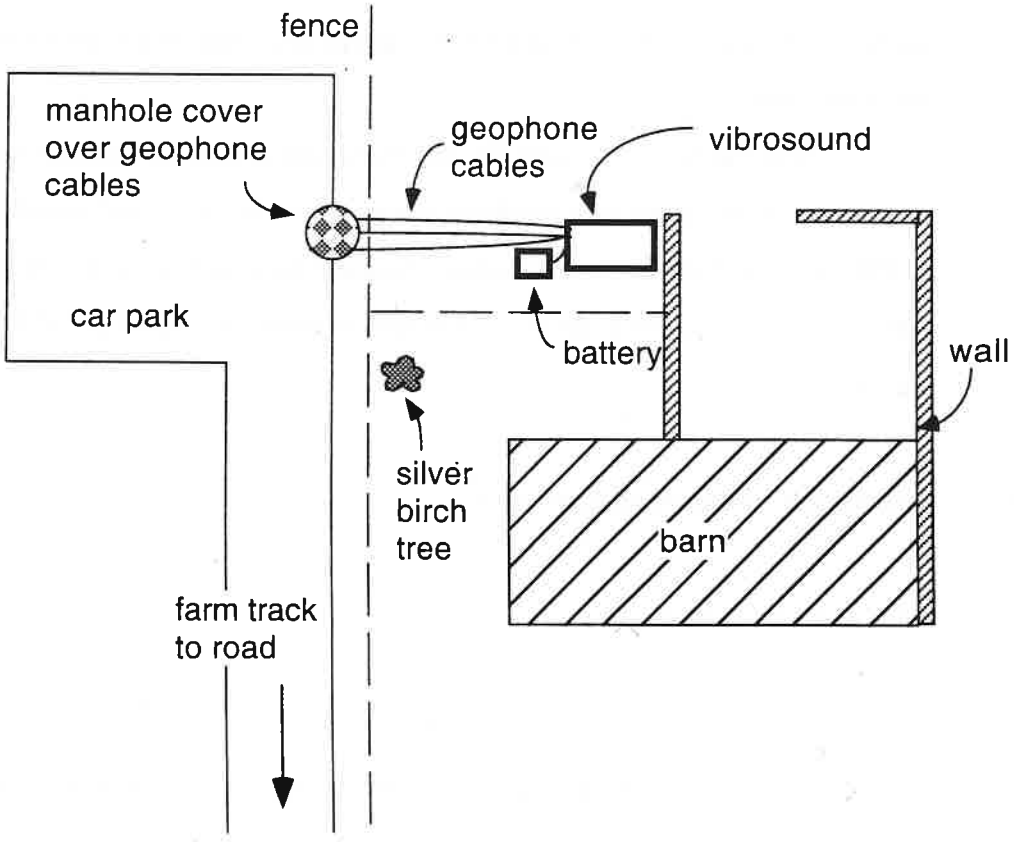

Figure 5.2 Location of the Vibrosound at the Roughs borehole site.

monitoring experiment was then input to all six channels of the recorder and after some difficulty in setting the trigger thresholds events were captured from digital cassette tapes.

5.3.2 Field Evaluation

The Vibrosound recorder was taken to Rough's Borehole, Maxstoke, (O.S. 1:50,000 sheet 131 grid ref. E245,N866) in order to evaluate its performance by monitoring mining-induced seismicity generated by mining operations from Daw Mill Colliery (Figure 5.1). Current mining operations are approximately 1 km away from the borehole where extraction is proceeding from the Warwickshire Thick Seam which is approximately 6 metres thick. The current 91's face and the 92's face development lie approximately ENE of the borehole with older workings immediately to the north of the borehole.

The Rough's borehole is located in a field owned by Mr M. Gold. With his permission we set the Vibrosound up to monitor earthquakes during the period 2nd to 9th September 1994. The Vibrosound was stationed in the adjacent field (Figure 5.2). About 10m of multicore cable was run from the top of the borehole to the Vibrosound. IMCL borehole geophone packages contain a six-component instrument with orientations and colour coded as described in table 1. All of the six channels were connected up, 2 vertical geophones, one horizontal orthogonal pair oriented S-N and W-E and another orthogonal pair SE-NW and SW-NE.

To ensure the safety of the equipment, all the apparatus was covered by wooden pallets that the farmer had discarded and were lying around the field. . The cables were buried in a shallow slit cut into the turf. The Vibrosound was powered by one 12V car battery which was changed daily although power consumption appeared to be very low. The flash card was also changed every day. With the trigger level set sufficiently far above the background noise level not to trigger on ambient noise, the maximum number of events recorded in a 24 hour period, was 289. With a sample rate of 1000 samples per second and a 1000 ms

event length, this meant that 38% of the storage space on the FLASH card had been used. This would give a recording period of c 2.5 days if this is a typical microseismicity rate. Our experience, however, is that much higher rates can be generated by some faces with up to 2000 events per day and if rates such as this were experienced the storage capacity would probably be determined by the writing rate to the FLASH card.

5.4 Data Analysis

5.4.1 PCMCIA software, (JC-CARD)

The JC_CARD card software supplied by Magus Electronics enables the data to be read off the FLASH card and onto a PC. The hardware was installed in a DELL XP 466V desktop computer. The software allows the user to read, erase and check various makes and models of FLASH cards. The data are then stored in a hexadecimal format as shown in Appendix B. At the start of each file there are markers to indicate such things as how many events have been recorded followed by the data for each event. It was necessary to alter the binary code for this software using the hex editor to enable it to read data from the PCMCIA slot of a VIGLEN DOSSIER notebook computer for field use.

5.4.2 CONVERT

A program, CONVERT, written in compiled BASIC supplied by Magus Electronics, was one of the programs used to convert the hex files into decimal files. This took the hex file and split it into separate event files with the filename in the format:- name event number and a .vib extension. It automatically increments the filename for every event detected until the end of the hex file is reached.

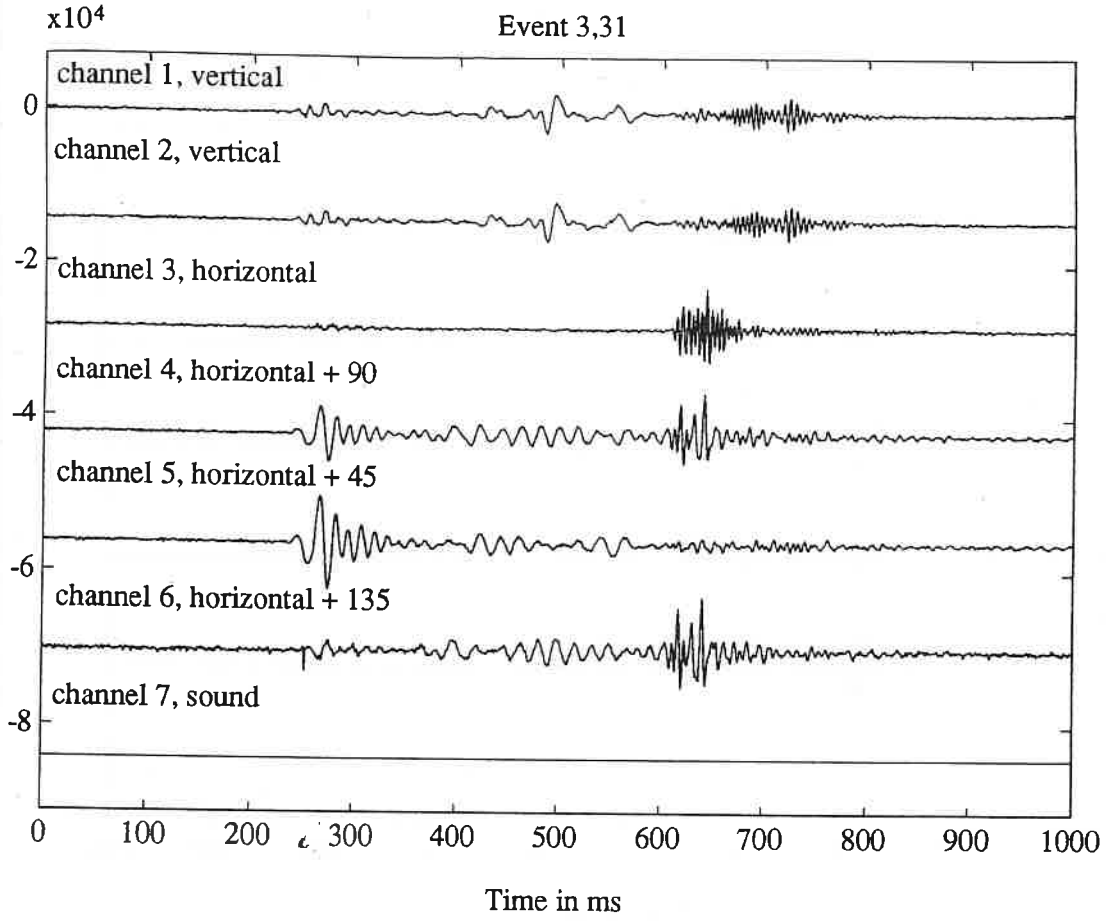

Figure 5.3 A plot of event 3,31 displaying each channel separately. Note that channel 7 does not have any signal as there was no sound input.

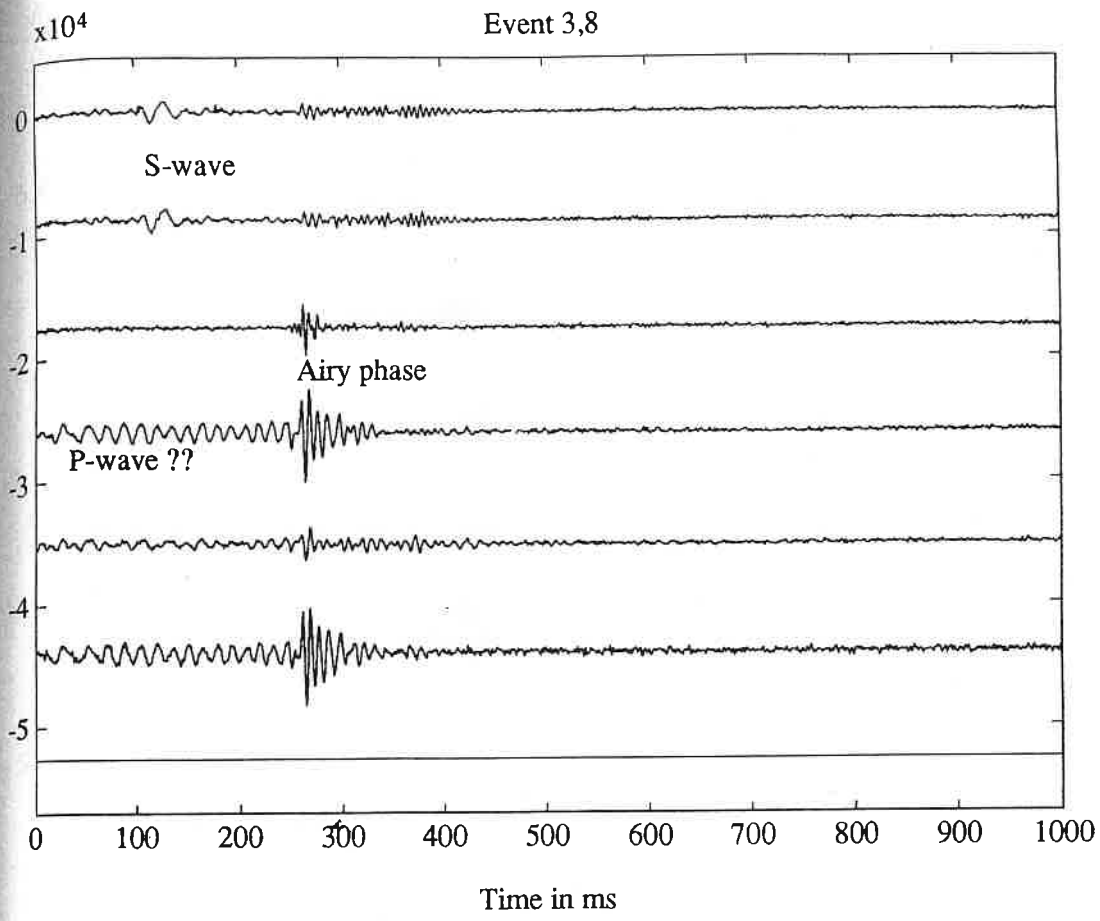

Figure 5.4 A plot of event 3,8 showing the problem with the trigger position. The S-wave and Airy phases are clearly seen, but there is not enough space to clearly see the P-wave onset.

5.4.3 RDFLASH

This program was written in house at the University of Liverpool in C. It is available on both SUN workstations and for PC's . It may also be used to convert hex files into separate ASCII event files. The advantage of this program is that it also writes a report file which contained the total number of events on the card and for each file it writes the name of the input and output files, the time and date of the event and the length of the file. Both RDFLASH and CONVERT give identical numerical output .

5.4.4 MATLAB Data Processing

The events were read into Matlab and displayed as seven individual traces using utilities developed at University of Liverpool (Figure 5.3). It became clear during this analysis that the maximum pre-trigger interval available on the Vibrasound of 250 samples was not sufficient as there were many events which had triggered on the S-wave and the P-wave was not detected at all or incompletely. Figure 5.4 shows an example of this for event 3,8. It was also clear that Channel 3 of this sonde was not operating well at lower frequencies for this sonde.

5.5 Analysis of data acquired over the period 2nd - 9th September 1994

5.5.1 Statistics

After initial testing data acquisition and analysis on 2 -4 September 1994, the Vibrosound was set running on Monday 5th Sept evening at 17.30. The FLASH cards were changed at 09.20 Tuesday 6th after recording 31 events. The recording parameters used were:-

Parameter	Value
Geophone sensitivity	28.8 V/m/s
Event length	2000 ms
Sampling rate	1000 samples per second
Pre-trigger length	250 ms
Trigger value	15 µm/s
Instrument gain	10

It was decided to lower the trigger level to 12 µm/s for the next recording period, to see if this would result in more events being recorded. In anticipation of this happening, we reduced the event length to 1000 ms. The Vibrosound then ran until 12.15 Wednesday 7th recording 241 events. The trigger level was raised to 13 µm/s and the machine ran until 11.15 Thursday 8th recording a further 289 events. The final period, from 11.30 Thursday until 11.30 Friday 9th, was run with a trigger of 14 µm/s and recorded another 82 events.

After each card was removed from the Vibrosound, each event was inspected in MATLAB. It was found that only about 1 in 10 events actually contained an earthquake, the rest of the declared events being either electrical spikes or large amplitude noise. The final number of earthquakes recorded was 93.

5.5.2 Discussion of the types of events

The true seismic events fell into two broad categories, those with an Airy phase and those without (Figure 5.5a & 5.5b). Those without an Airy phase were generally of much lower frequency and came from further away. It was noted that channel 3 appeared not to be recording in the low frequency ranges. The spectra of both of these event types are shown in Figure 5.6a and 5.6b. The low frequency events do not have any energy above 60Hz while the high frequency events contain energy up to 250 Hz. The low frequency portions of both are clearly similar. It seems likely that the low -frequency events have propagated through an

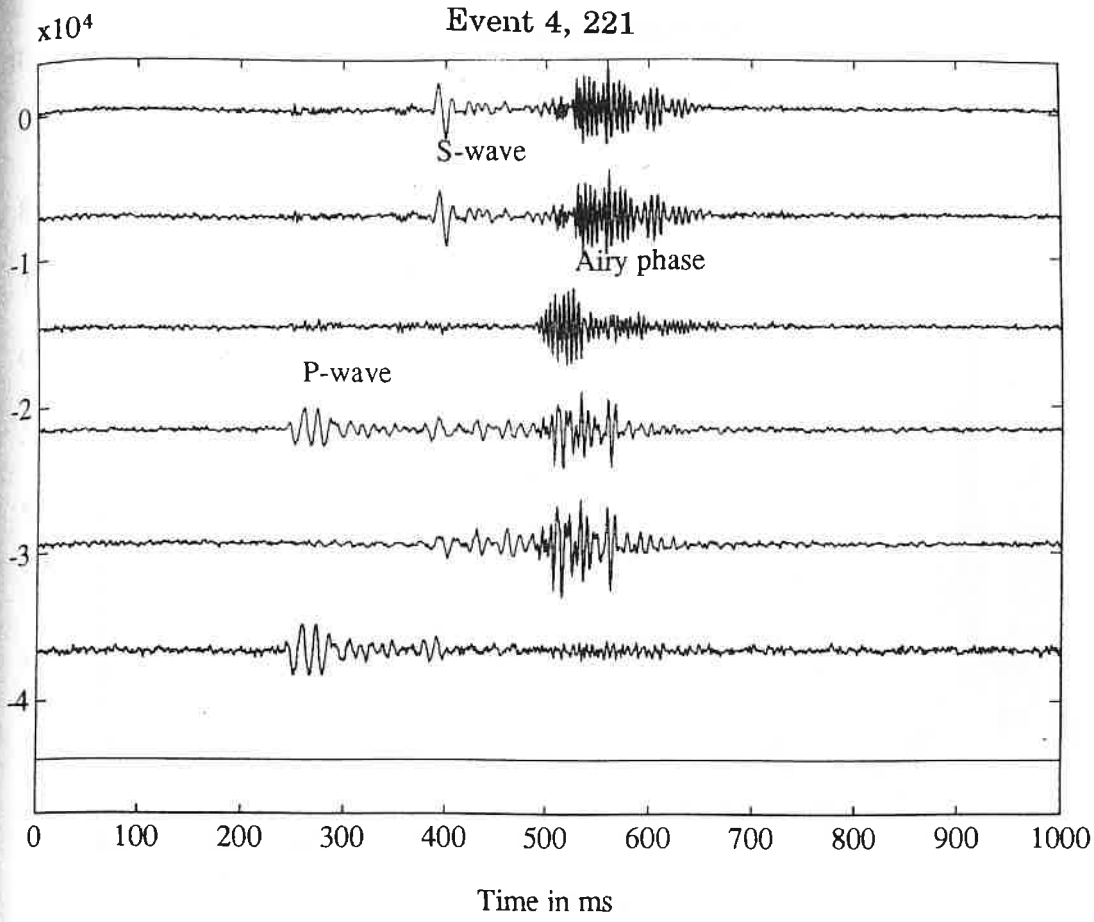

Figure 5.5a A plot of Event 4,221 showing the high frequency late arrival of the Airy phase.

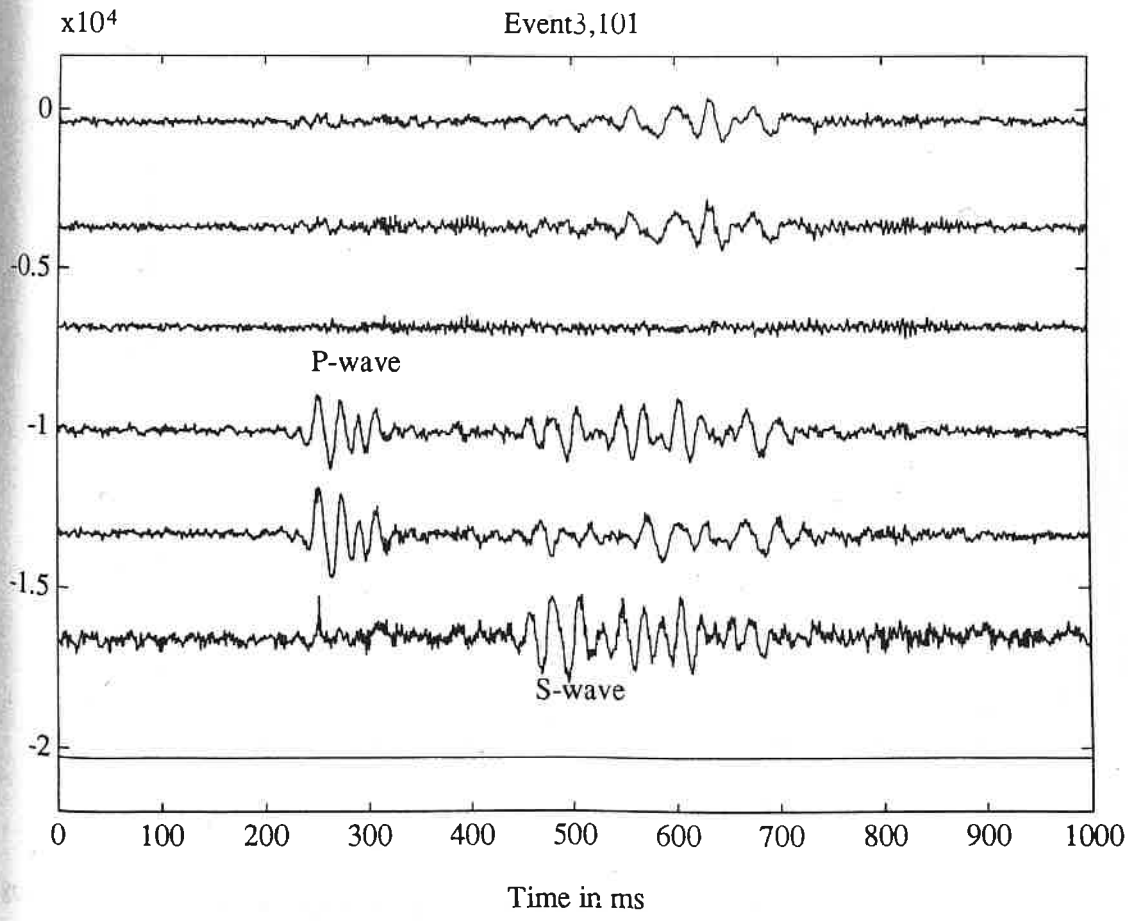

Figure 5.5b An example of the lower frequency, more distant earthquakes.

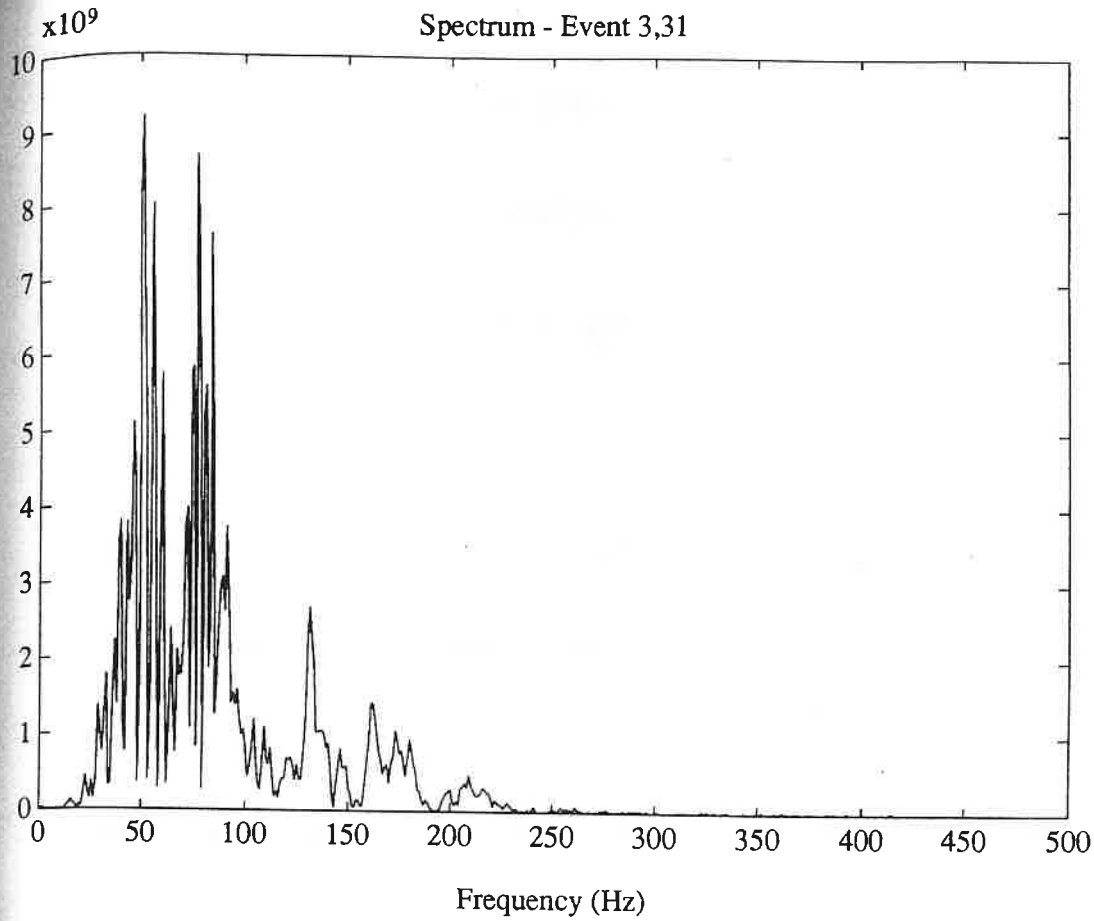

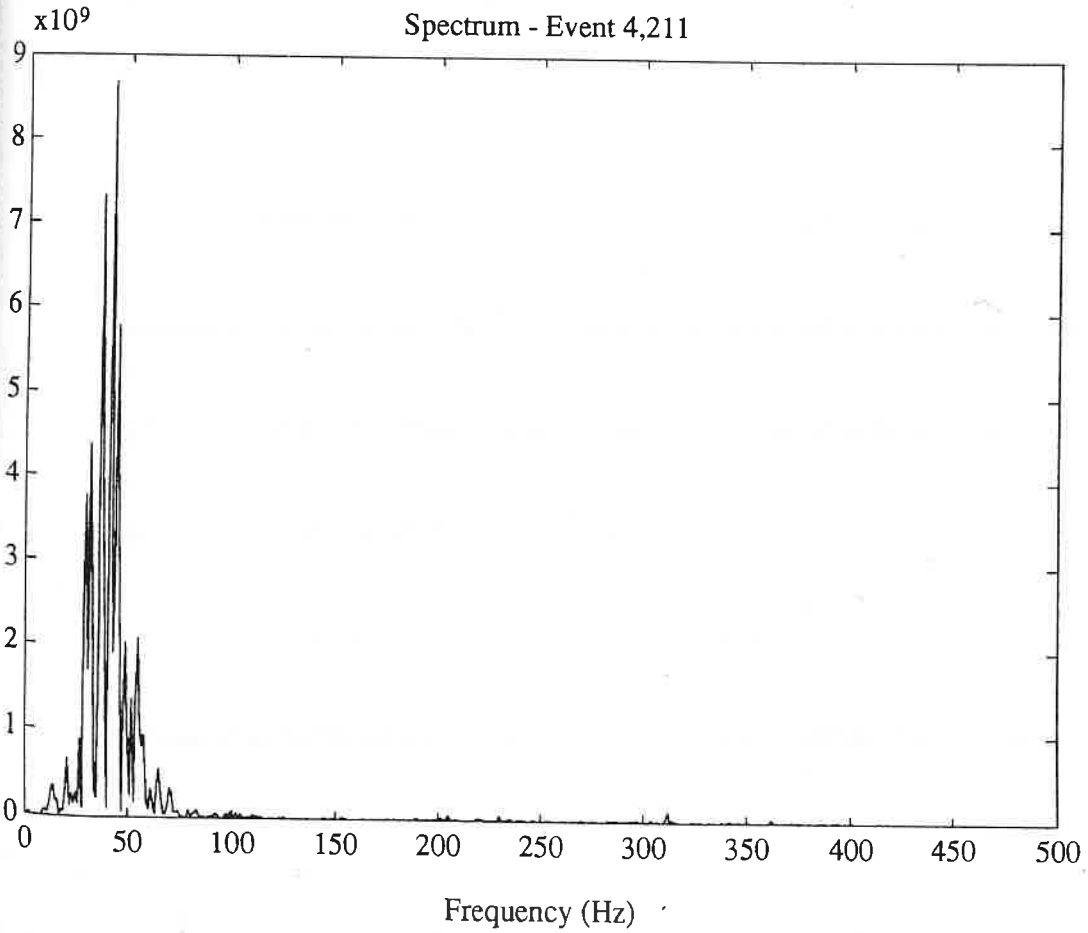

Figure 5.6a The power spectrum of an earthquake with a clear Airy phase.
Figure 5.6b The power spectrum of an earthquake without an Airy phase.

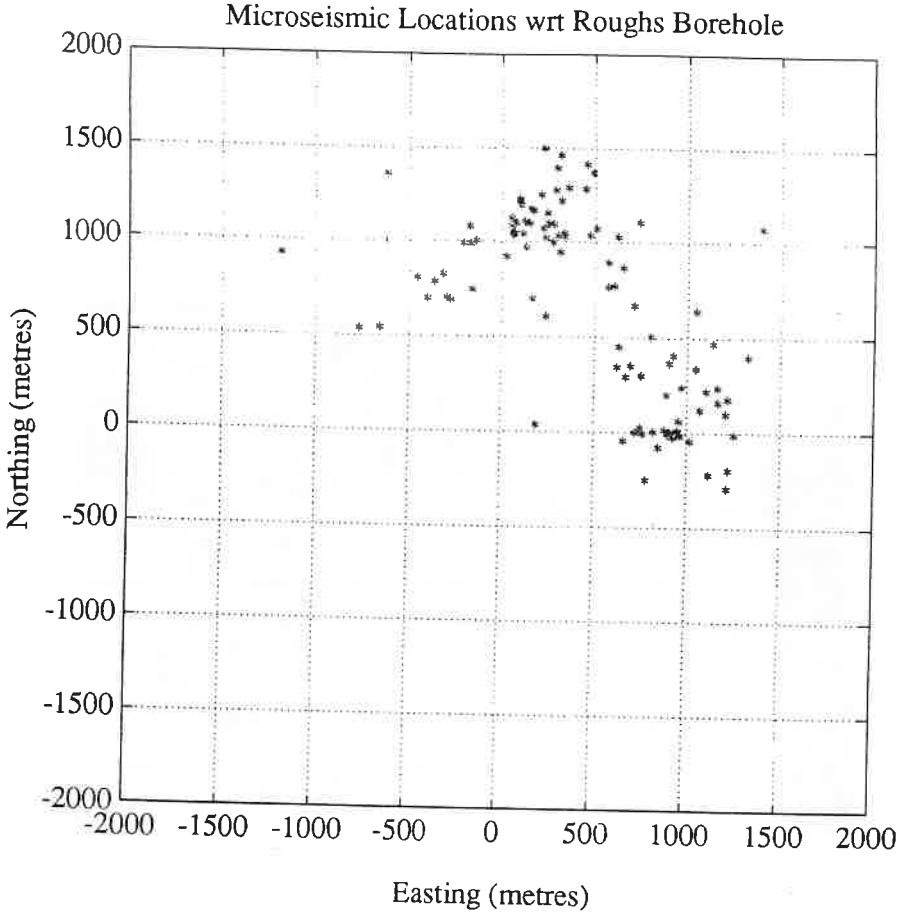

Figure 5.7 Diagram to show the epicentres of the earthquakes recorded at The oughs borehole 5th - 9th September 1994. The coordinate system is centred on e borehole.

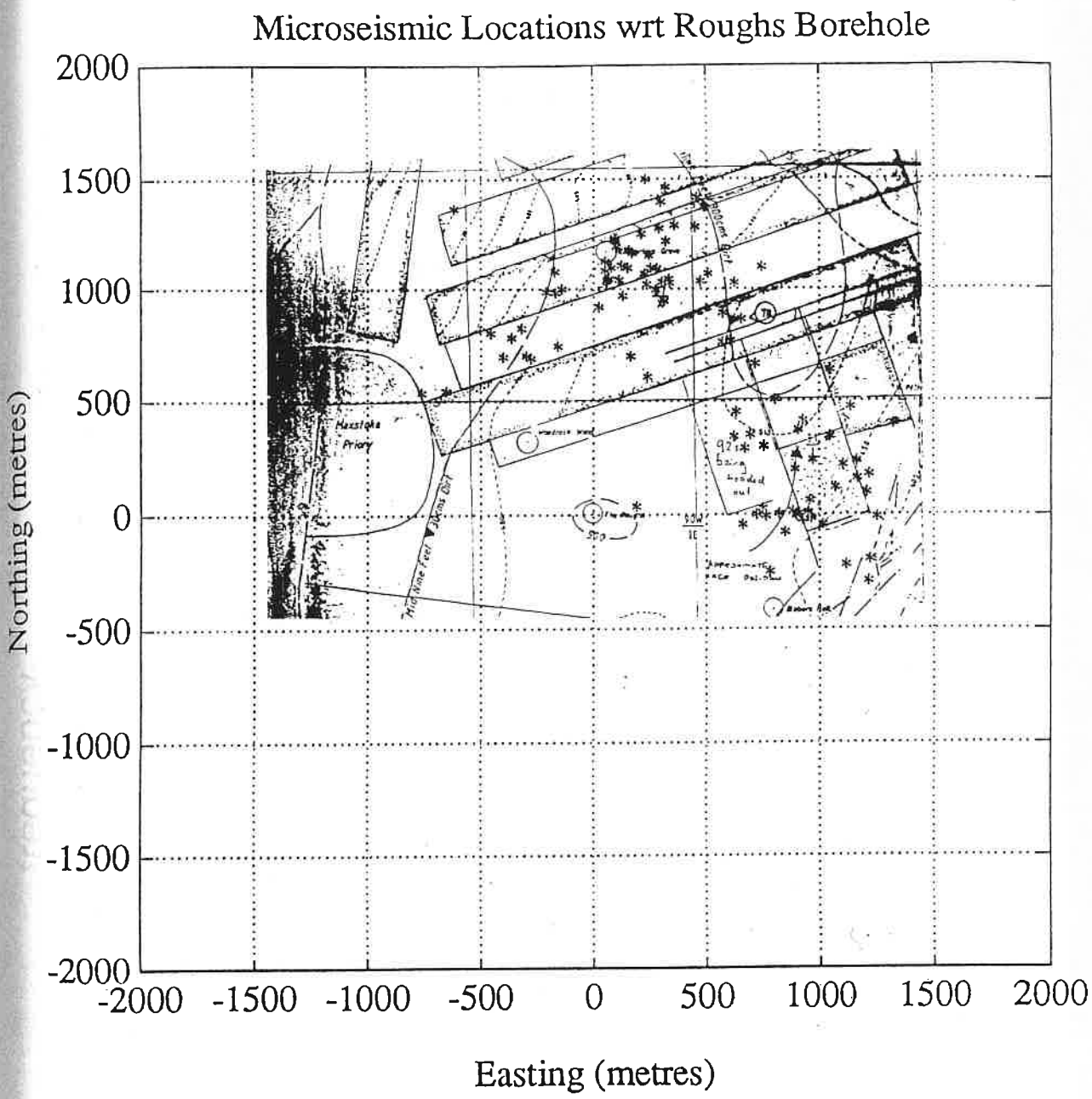

Figure 5.8 Figure 5.7 with the locations of the workings of Daw Mill Colliery superimposed.

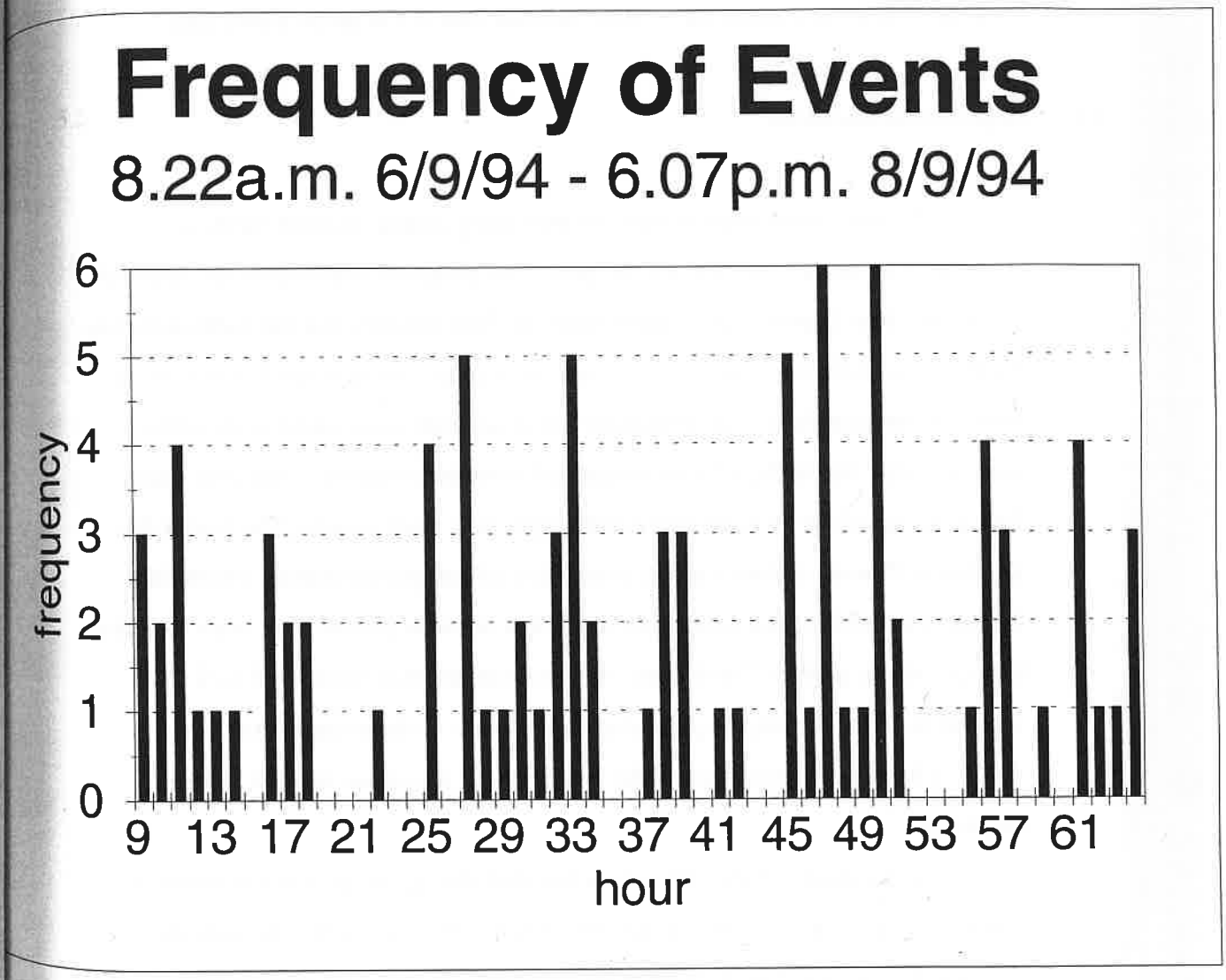

Figure 5.9 Seismicity rate per hour at Daw Mill Colliery for the period 6th to 8th September 1994.

area of worked out coal as discussed later. There was a remarkable similarity between events within types which suggests that similar travel paths have been encountered. If this is so it may be possible to generate high-resolution relative locations using techniques developed in geothermal monitoring where locations with accuracies of 1 metre have been obtained over a 150 metre travel path

5.5.3 Hypocentral Locations

The micro-earthquakes were located using a back-azimuth method developed by the University of Liverpool. This program implements the Spectral Matrix method of polarisation determination. This assumes that the earthquake has either come from or is going to the direction of polarization of the P-wave. With only one detector there is an ambiguity in the azimuth sense and it is therefore assumed that the earthquake has originated from the direction of the coal mine. The accuracy of the location will depend upon two main criteria. The first is the amount of P-wave included in the calculation of the spectral matrix which finds the direction of the polarisation. To check that no other phases have been included, hodograms are plotted. The distance to the event depends upon the P to S separation. This can only be picked using a mouse to the nearest pixel in MATLAB and will depend upon the judgement of the picker and the screen resolution .

The locations of the >90 events detected during this period are shown in Figures 5.7 and 5.8 . Figure 5.8 has the working plan superimposed onto the events and it is clear that the bulk of the activity is located either from the 92 and 91 faces or from the very long panels to the north. The lower frequency events detected appear to come from the older workings and it seems likely that they have been affected by transmission through worked-out areas and that this is the reason for the lack of Channel phases for these events.

5.5.4 Histogram of Seismic Activity

The seismic activity in events per hour are plotted in Figure 5.9 as a stacked chart for the days 6, 7 and 8 September 1994. It is clear that the activity has a regular pattern which recurs on a daily basis. This is a common feature of mining-induced seismicity, reflecting the patterns of extraction during shifts and is further confirmation that this activity is being generated by the Daw Mill extraction.

5.6. Assessment of Performance

5.6.1 Reliability

During the period of testing the machine, once set up correctly, worked without problems for a week of continuous running and appeared to be reliable and stable. It was not clear what life cycle they would have in a field situation and it was necessary to have adequate cards in case a failure did occur. However, during more than 18 months of monitoring no failures have occurred.

5.6.2 System Noise Level and Dynamic Range

The noise level of the system is very low and is certainly well below the ambient seismic noise level in this experiment which was of the order of 100 nanometres per second which is equivalent to 3 microvolts for the SENSOR SM7 geophone. The upper boundary of the dynamic range was not tested during this period as no large events occurred. It seems likely that any mining induced event will be satisfactorily encompassed within the 24 bit dynamic range.

5.7 Modifications made or desirable in the light of field experience

5.7.1 Channel offset

The offset level of the A-D recorder is of rather more concern as this can be several hundred nanovolts. The calibration of the channels is very important. Calibration without using a shorting plug meant that each channel had a significant offset from zero. However performing the calibration with a shorting plug reduced the offsets considerably (table 2). A shorting plug that completely removed any offset would be ideal, or some mechanism for removing them from the signal before triggering takes place. Although at this site, the small offsets were not a serious problem they could be if event amplitudes were very low.

Channel Number	Offset with no shorting plug (µm/s)	Offset with shorting plug (µm/s)
1	-2355	-50
2	-1750	250
3	850	150
4	-2650	250
5	-750	100
6	-1200	-300
7	0	0

Table 1 Offset voltages of the recorder when it is initialise with and without a shorting plug.

In the light of this modifications were made to the equipment in order to remove the offsets in the data before triggering.

5.7.2 Time to store data

Due to the nature of the FLASH cards writing process there is a lengthy wait-state as the machine stores the last event to memory. This means that if there are two events close together, the second event will be missed. The recorder takes approximately 1 minute to store an event containing 1000 samples. With low seismicity rates this may be adequate but in order to accommodate high event rates the recording process was altered so that data were stored to the flash-card in a less-processed format with full decoding occurring in the post-processing software. The alteration means that it now takes 17 seconds to store an event (of length 1.5 seconds) to the flash card. This change in the format of the data stored on the flash cards means that a new program was needed to convert the hex files to ASCII files. For this purpose we have used a program written in-house at Liverpool. The program FLASH2 produces data in the same format as the RDFLASH program.

5.7.3 Triggering off selected channels

As described above, an event is declared when the signal on any channel rises over a certain value. It is desirable to be able to select channels enabled for triggering so that if one channel is particularly noisy, it can be discounted from the triggering algorithm. This modification was made to the equipment.

5.7.4 Master/Slave Priorities

Initially the SP1 was configured so that it could either be a MASTER or a SLAVE but not both. However it was felt to be important that any machine could declare an event and request the others to trigger and so the instruments have been modified to this specification.

5.7.5 Triggering Algorithm

At the present time, the triggering is based on a simple threshold level and an event is declared when the signal from any channel rises over a certain value. Consequently many electrical spikes were recorded. These could have been avoided if a more sophisticated triggering algorithm had been used. We suggest an algorithm based on a ratio of the energy in a short time window corresponding to the duration of the P-wave compared to the long term energy avaeraged over a period longer than the duration of the event (STA/LTA Allen 1969). This discriminates against events with small energy content (eg spikes) and events with emergent onsets and should be implemented if the processing power is available.

5.7.6 Pre-trigger length

The micro-earthquakes that have been monitored generally travel along and around the coal seam and as a consequence the P-wave is usually quite small. It happened several times that the P-wave was too small to trigger on and triggering occurred on the S-wave. Hence the event was recorded, but as the P-S time was greater than 250 samples only the latter part of it was captured. If there were a longer range of pre-trigger length, it would be possible to record the whole event. Modifications were made to permit pre-trigger levels of 250, 500 and 750 samples and this was found to be satisfactory for all eventualities.

5.7.7 Geophone sensitivity range

The geophone sensitivity range is not great enough to include Willmore seismometers which have a sensitivity of about 550 V/m/s. However this type of detector was not deployed during this experiment.

5.8 Conclusions

After a lengthy initial period the equipment was delivered and software was made available for down-loading data. The equipment has performed satisfactorily with some criticisms as detailed above. It is perhaps true that in some cases the specification was inappropriate and that the implementation was as specified. With the modifications outlined above the equipment has considerable potential for detecting and monitoring microseismic activity from long-wall coal faces.

6 BOREHOLE INSTALLATIONS

6.1 Geophone Emplacement

Two boreholes were drilled specifically for this experiment by British Drilling and Freezing Co Ltd. Their details are as follows with all positions in metres below ground level unless otherwise stated

Name	Cant's Thorns #1	Cant's Thorns #2
Easting	470760	471244
Northing	321855	322002
Start Depth	121.45 AOD	141.1AOD
Total Depth	505	515
Bottomed in:	Coal Measures	Coal Measures
Geophone 1:	71	87.5
Geophone :2	171	187.5
Geophone 3:	271	287.5
Geophone 4:	371	387.5

Their locations with respect to Panel 101 is shown in Figure 6 1 together with other boreholes in the area. The simplified stratigraphy encountered in these borehole for the 120 meters immediately above the seam is shown in Figure 6.2 . Both encountered significant igneous sills which are described in a later section. The geophone assemblies were constructed and installed by IMCL and details of the geophone assembly details can be found in Appendix 1. Each borehole contained four geophone packages with 6 individual geophone elements with the following notional orientations:

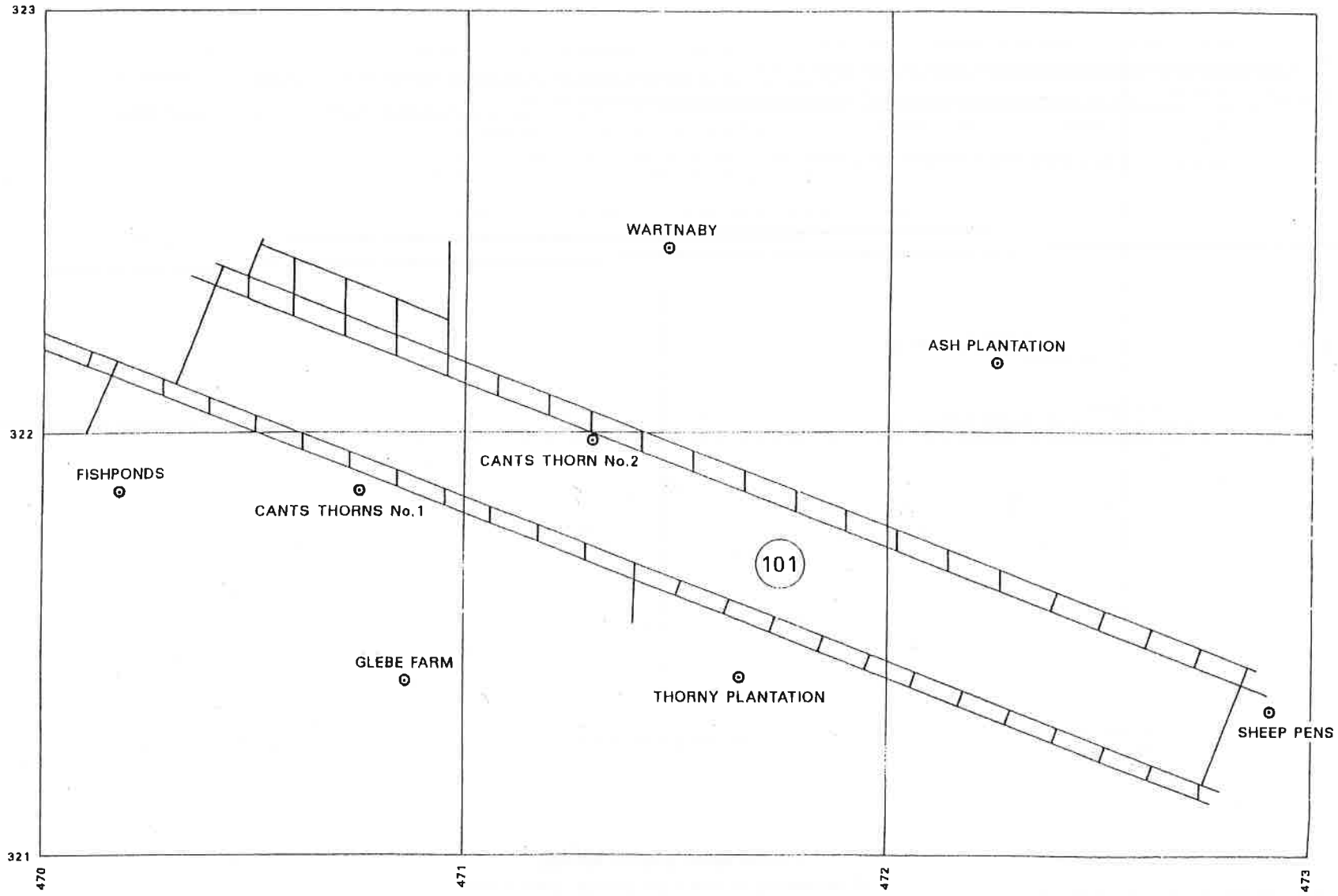

Figure 6.1 Borehole location plan for Asfordby mine.

ASFORDBY MINE
SECTION OF STRATA ABOVE DEEP MAIN
101's FACE START TO CANT'S THORN No.2
(DATUM = DEEP MAIN ROOF)

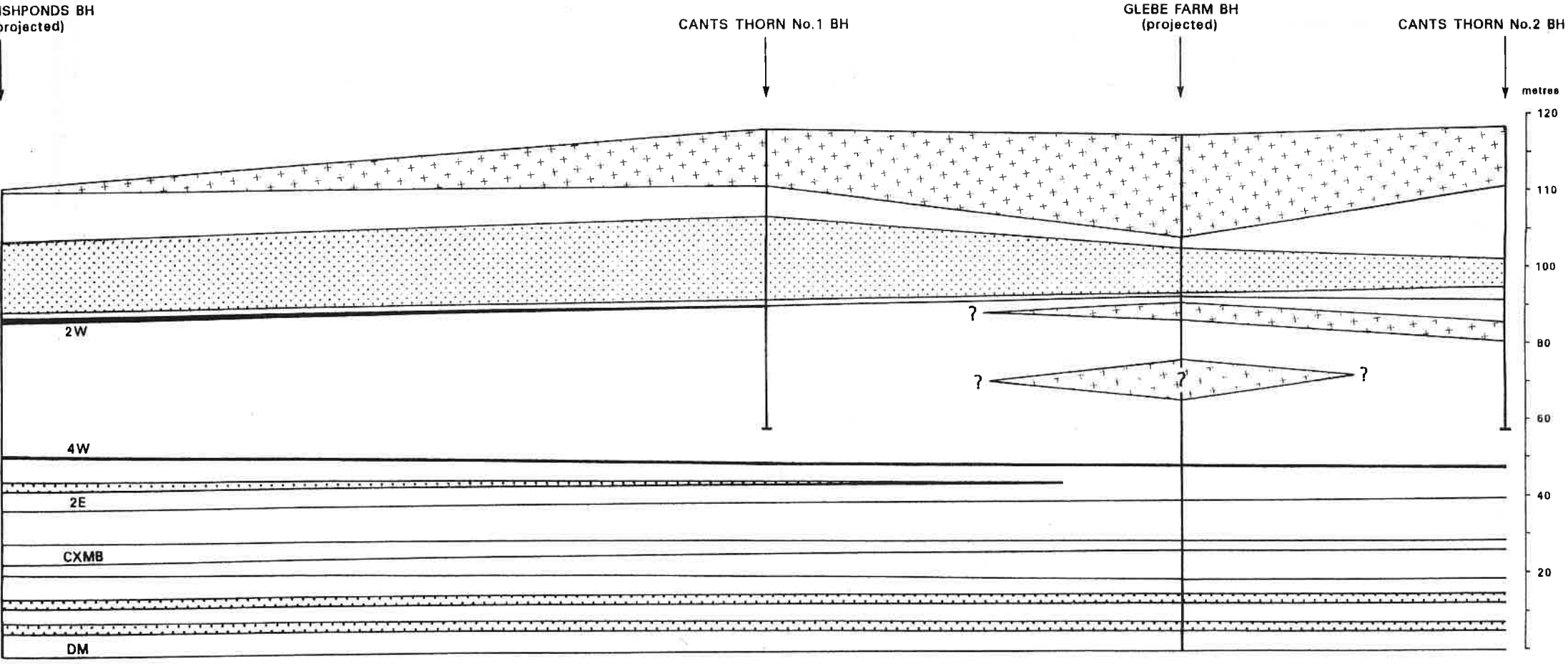

2W = Second Waterloo Seam
4W = Fourth Waterloo Seam
2E = Second Ell Seam
CXMB = Clay Cross (Vanderbeckei) Marine Band
DM = Deep Main Seam Roof

Horizontal Scale 1:2500

KEY

Sandstone

Igneous

Figure 6.2 Asfordby mine - section of strata above deep main 101's face start to Cant's Thorn No. 2. (Datum = Deep Main roof)

Element No:	Orientation
1	Vertical
2	Vertical
3	North
4	West
5	North-West
6	South-West

Because of the number of conductors present in the cable. only Vertical #1 and the four horizontal elements were connected to the recording system.

Fishponds Borehole (Figure 6.1) is a pre-existing borehole which contains a six-element geophone sonde at Deep Main seam level. This was also used for monitoring because of its close proximity to the start position for panel 101.

6.2 Orientation of Geophone Assemblies

In order to obtain an accurate orientation for the borehole geophone assemblies it is necessary to fire shots from one borehole into the other. This was carried out from Cant's Thorn #2 into Cant's Thorn #1 during the night of 2 May 1995. Ten shots were fired from the bottom of the hole progressing upwards in order to preserve the hole condition as long as possible. Shots were fired at the following depths below ground level:

Shot Number	Depth (Metres)
1	510
2	464
3	418
4	372
5	307
6	280
7	234
8	188
9	142
10	96

The data were recorded on a BISON Seismograph by IMCL personnel. Using the polarisation of the P-waves (See later analysis section) it is possible to deduce the apparent azimuth of the shot with respect to the recording geophone and the correction which is required to re-orient the data into coordinated with respect to OS Grid can be calculated. The orientations of the geophones as determined from the shot data are given in Table 4.

	sonde1			*sonde2*			*sonde3*			*sonde4*			
	2 & 3	4 & 5	Difference	2 & 3	4 & 5	Difference	2 & 3	4 & 5	Difference	2 & 3	4 & 5		*Difference*
shot1	-60.67	74.56	-135.23	-75.15	-60.1	-135.25	41.68	-86.98	45.3	65.26	19.86		45.4
shot2	-59.22	75.52	-134.74	-75.38	-60.03	-135.41	41.14	-86.32	45.18				0
shot3	-60.76	74.48	-135.24	-76.05	-58.84	-134.89	40.24	-85.17	44.93	63.96	19.45		44.51
shot4	-60.27	74.82	-135.09	-75.57	-60.37	-135.94	41.68	-86.88	45.2	64.76	21.68		43.08
shot5	-60.16	74.84	-135	-76.37	-59.17	-135.54	42.31	-87.35	45.04	58.6	13.57		45.03
shot6			0	-75.34	-59.58	-134.92	41.67	-86.48	44.81	58.21	13.63		44.58
shot7	-59.85	75.05	-134.9	-76.11	-59.65	-135.76	41.33	-86.07	44.74	57.34	12.62		44.72
shot8	-59.34	75.68	-135.02	-76	-60.04	-136.04	41.09	-86.15	45.06	57.56	12.89		44.67
shot9	-59.83	75.23	-135.06	-75.31	-60.41	-135.72	40.63	-85.53	44.9	57.79	13.07		44.72
shot10			0	-74.47	-61.21	-135.68	40.15	-84.95	44.8	58.42	13.72		44.7
Mean	-60.013	75.0225	-135.035	-75.575	-59.94	-135.515	41.192	-86.188	44.996	60.211	15.61		44.60111
Correction	76.91	-58.11		92.47	76.84		-24.3	103.08		43.32	1.29		

N. B. True Orientation of Shot from Borehole is 16.895 degrees north of east or bearing 73.105 degrees from North

Table 4 Orientation of the geophone elements in Cant's Thorns 1 Borehole determined from shot firing in Cant's Thorns 2 Borehole.

6.3 Logistic Operations

The VIBROSOUND SP1 recorders were deployed at Cant's Thorns 1 (2 instruments recording all four sondes) and at Cant's Thorns 2 (1 instrument recording the lower sonde) and at Fishponds Borehole (1 instrument recording the 6-channel inseam geophone sonde). In each case the channels were recorded as follows. The orientations are nominal and were determined correctly from well shots as described in Section 6.2.

Recorder Channel Number	Geophone Orientation
1	Vertical
2	North
3	West
4	North-West
5	South West
6	Not Used

Table 5 Configuration of geophone elements in Fishponds Borehole

Recorder Channel Number	Geophone Orientation
1	Vertical 1
2	North 1
3	West 1
4	Vertical 2
5	North 2
6	West 2

Table 6 Configuration of geophone elements in Cant's Thorns Boreholes

The equipment was deployed in waterproof enclosures buried 750 mm deep in the ground with wooden boards over them to prevent animals or humans interfering with them . In fact there were no problems with interference or vandalism.

The instruments have their own internal batteries but for this purpose they were powered from external 75 Ampere-Hour Lead Acid batteries. These themselves were provided with extended operation by charging with a Solar-Panel. This gave a recording lifetime of in excess of 1 week. The instruments were calibrated with a shorting plug each time they were re-initialised to remove any offsets on the A-D interface. The acquisition software removed any residual nanovolt level offsets before triggering and recording on the 20 Mbyte Flash Cards occurred.

The VIBROSOUND recorders were set-up with the following recording parameters:

Sampling rate	**1000**
Pre-Trigger	**500 samples**
Gain	**1**
Total Number of samples	**1000 or 1500**
Geophone Sensitivity	**28.8 Vsm^{-1}**

The flash-cards and batteries were changed weekly by IMCL personnel and were sent by Courier to the University of Liverpool, Microseismological Group for analysis. The cards were then erased and returned to IMCL for re-use. This system was perfectly satisfactory for the purposes of this experiment. The equipment functioned well during the recording period with the only difficulty arising from electrical pick-up from the other cables present in the borehole. These problems were eventually resolved by shorting out pairs of connectors which were not being used for any signals. The regular visits by IMCL staff and periodic inspections by University of Liverpool personnel ensured good system performance.

7 DATA ANALYSIS

7.1 Data Pre-Processing

i On receipt of the data the cards were read in PCMCIA format into a PC as a hexadecimal file (*.HEX) and were then converted using FLASH2 (Diskette in Rear Envelope) from hexadecimal into ASCII files of data with a DOS extension of .VIB and a corresponding Log file with event time parameters.

ii Because of the long cable runs and the presence of telluric return flows to power-stations there was a considerable amount of 50 Hz electrical pickup. In some circumstances it is possible to simply filter this out either with analogue or digital filters but as this frequency lies within the bandwidth of signals of interest this was not possible. A noise-adaptive filtering technique was used in preference which requires a considerable amount of signal processing but gives very good 50 Hz rejection.
A sinusoidal signal with a variable frequency in the region of 50 Hz and a certain amplitude and phase was compared with the noise signal in the 250 point of pre-trigger before the true event. A least squares error function was generated from the sums of the squared residuals between the test signal and the noise. This error function was then minimised using a Simplex optimisation technique (see Appendix 3) in which the Frequency, Amplitude and Phase of the test sinusoid were the parameters to be optimised. The optimal sinusoid was then projected forward for the duration of the event and the explicitly predicted signal was removed from the data. Figure 7.1 gives an example of the data before and after filtering . It is apparent that there has been a very efficient removal of the 50 Hz noise. Figures 7.2, 7.3 and 7.4 show examples of Microseismic Events

detected from Fishponds, Cant's Thorns 1 and Cant's Thorns 2 boreholes respectively.

7.2 **Hypocentral Locations** and **Polarisation Analysis**

The procedures and the software for carrying out these analyses are described fully in Appendix 3.

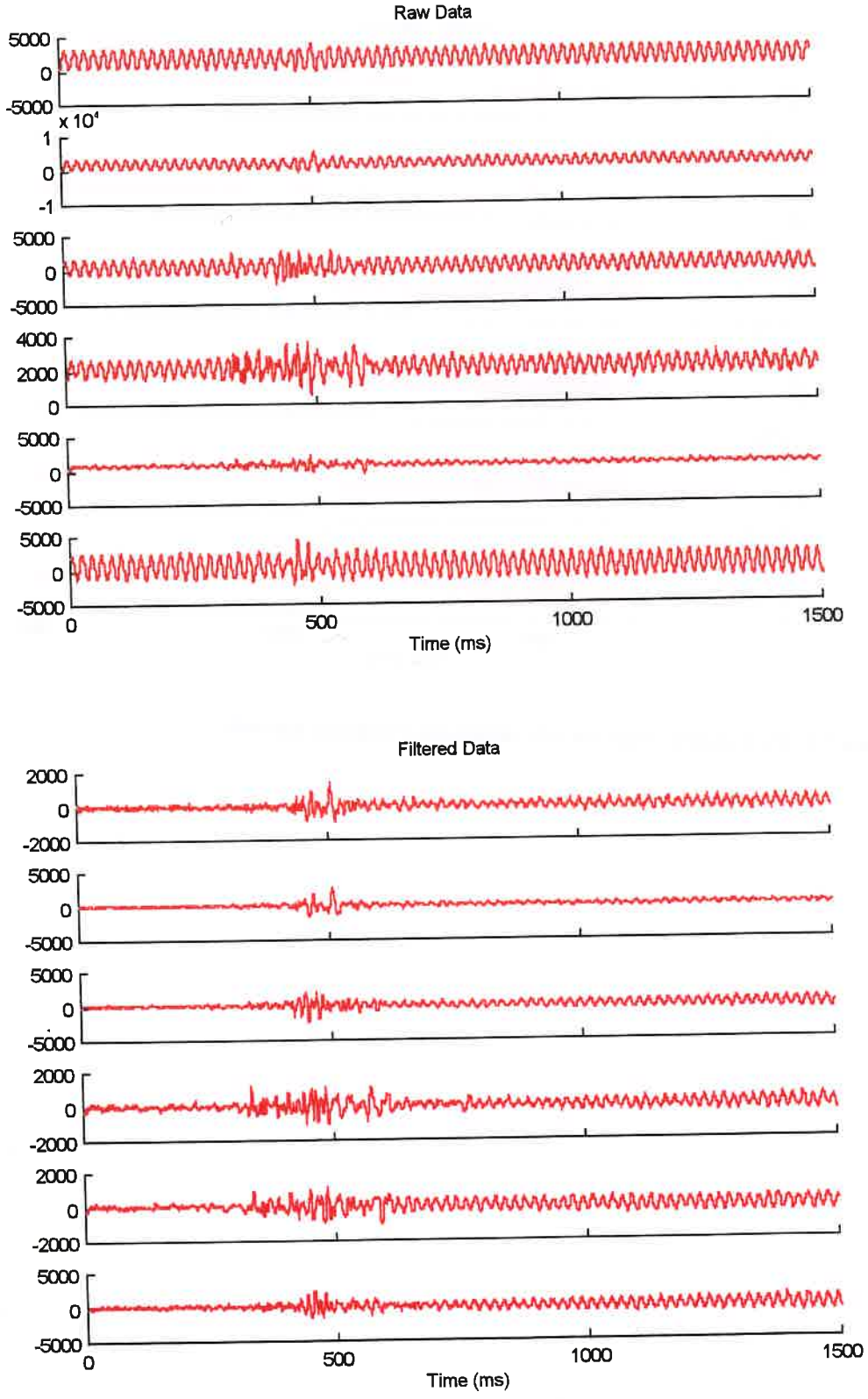

Figure 7.1 Microseismic Events before and after filtering to remove 50 Hz noise generated by telluric currents.

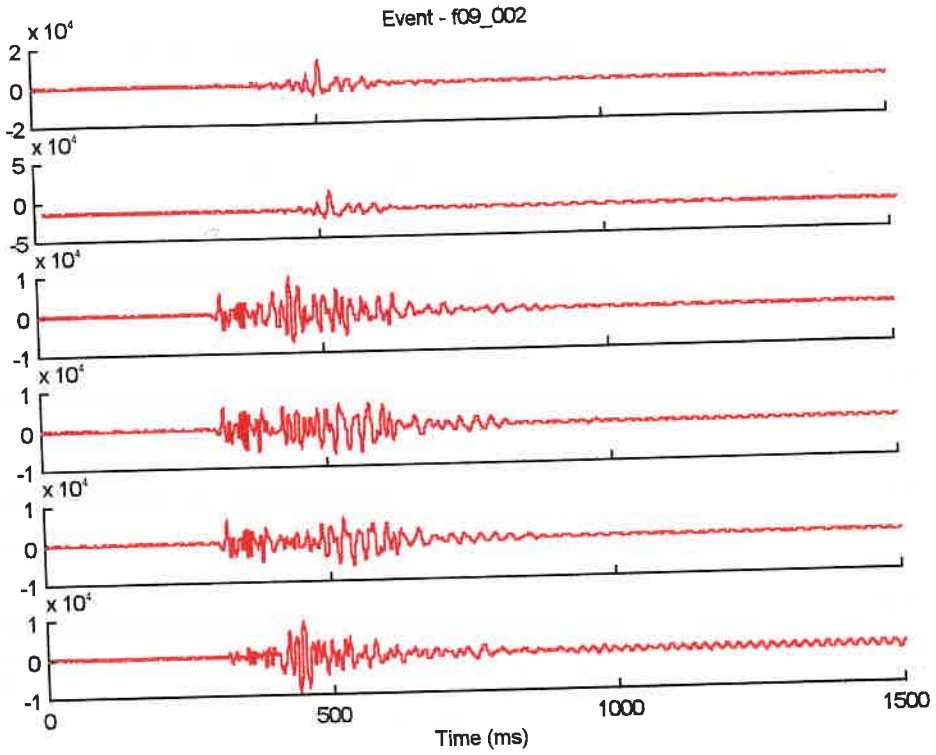

Figure 7.2 Microseismic event f09_002 detected in Fishponds borehole.

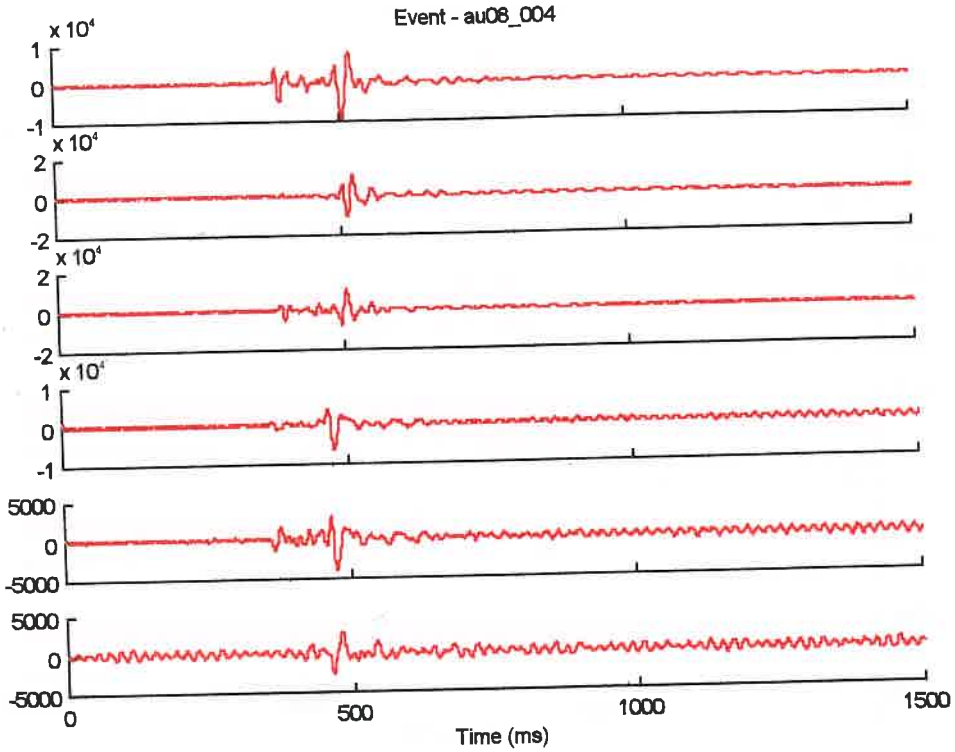

Figure 7.3 Microseismic event au08_004 detected in Cant's Thorn No. 1 borehole.

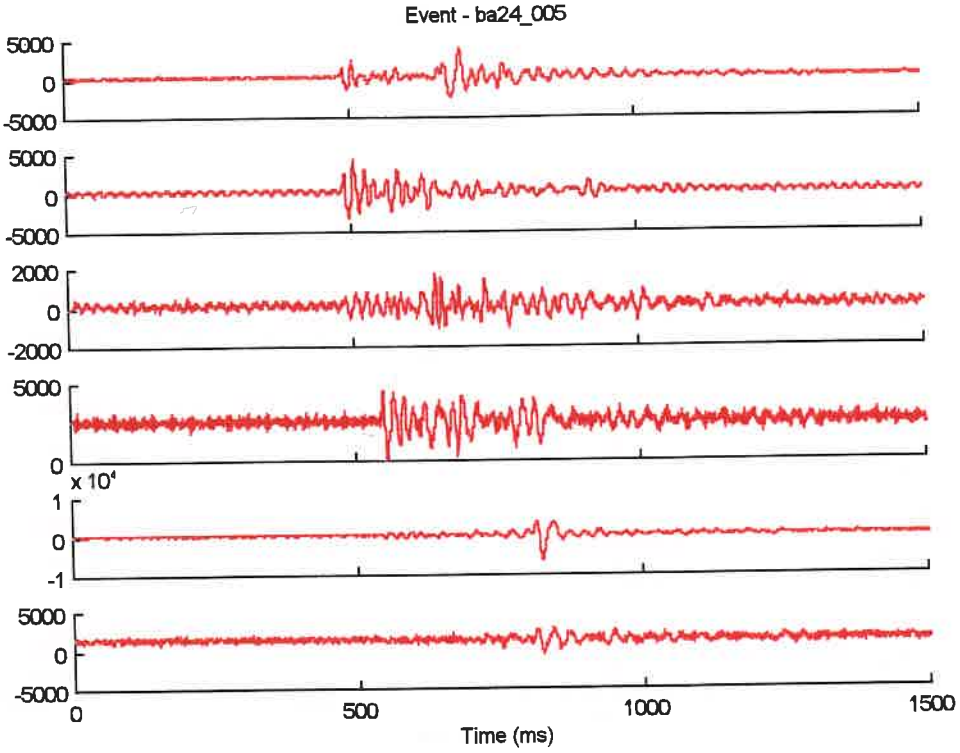

Figure 7.4 Microseismic event ba24_005 detected at Cant's Thorn No. 2 borehole.

8 REVIEW OF MAIN RESULTS

8.1 Mining Activity on Panel 101

Extraction from Panel 101 commenced on 15/4/95 and the rate of advance is shown in Figures 8.1 and 8.2 with the advance figures shown in Table 7. In the following description , weeks are numbered such that **week zero** ended on 22 April 1995, **week one** ended on 29 April 1995 as shown in Table 7.

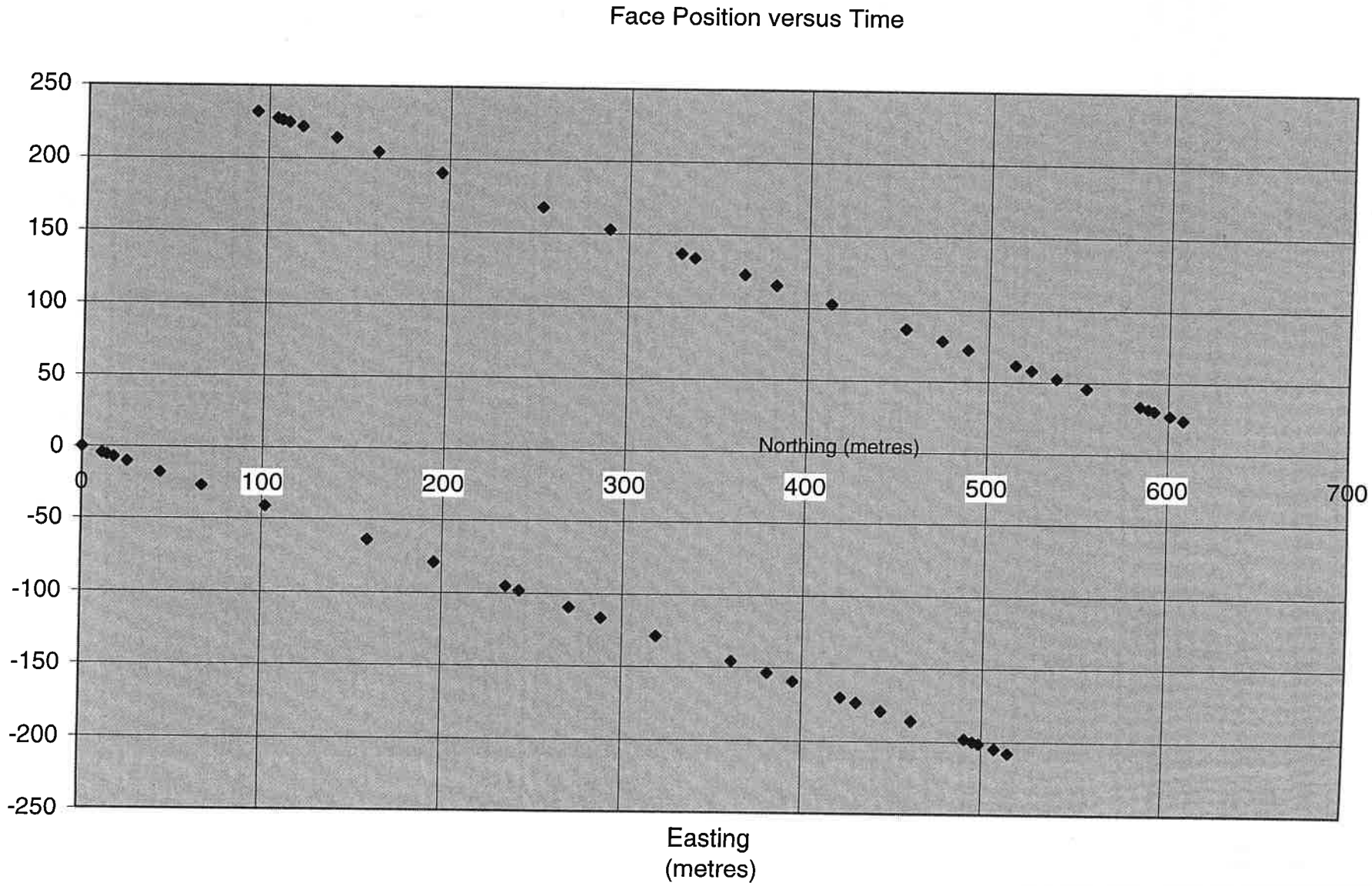

Figure 8.1 Advances for Panel 101, Asfordby from April 22 1995 until January 6 1996

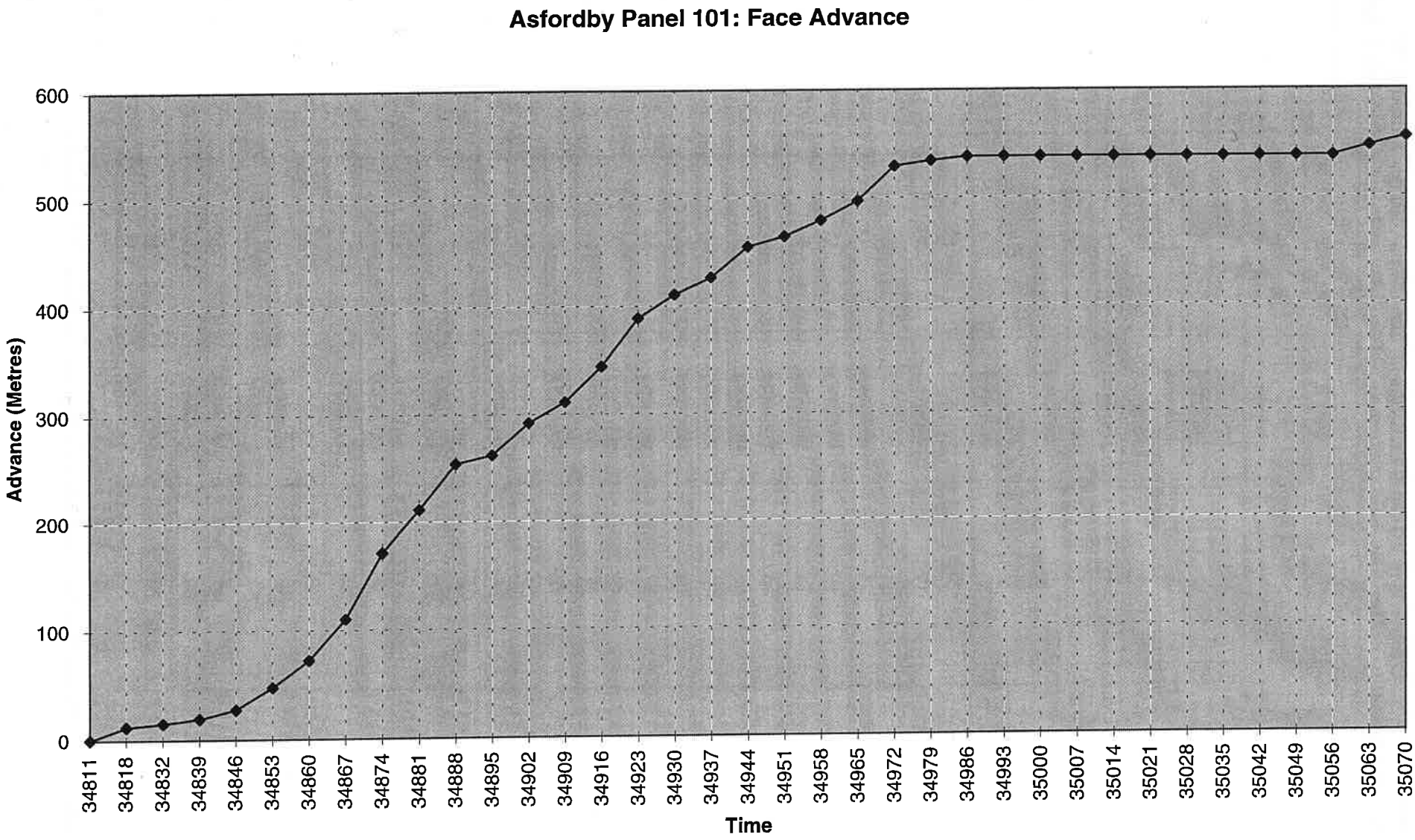

Figure 8.2 Cumulative advance rates (metres) for Panel 101, Asfordby from 22 April 1995 to 6 January 1996

Week Number	Date	Advance (m)
0	04/22/95	**0**
1	04/29/95	12
2	05/13/95	15
3	05/20/95	19
4	05/27/95	27
5	06/03/95	47
6	06/10/95	72
7	06/17/95	110
8	06/24/95	171
9	07/01/95	211
10	07/08/95	254
11	07/15/95	262
12	07/22/95	292
13	07/29/95	311
14	08/05/95	344
15	08/12/95	389
16	08/19/95	410.5
17	08/26/95	426
18	09/02/95	454.5
19	09/09/95	464
20	09/16/95	479
21	09/23/95	497
22	09/30/95	529
23	10/07/95	534
24	10/14/95	537.6
25	10/21/95	537.6
26	10/28/95	537.6
27	11/04/95	537.6
28	11/11/95	537.6
29	11/18/95	537.6
30	11/25/95	537.6
31	12/02/95	537.6
32	12/09/95	537.6
33	12/16/95	537.6
34	12/23/95	537.6
35	12/30/95	547
36	01/06/96	555

Table 7 Week Numbers and Advance Figures for Panel 101 Asfordby

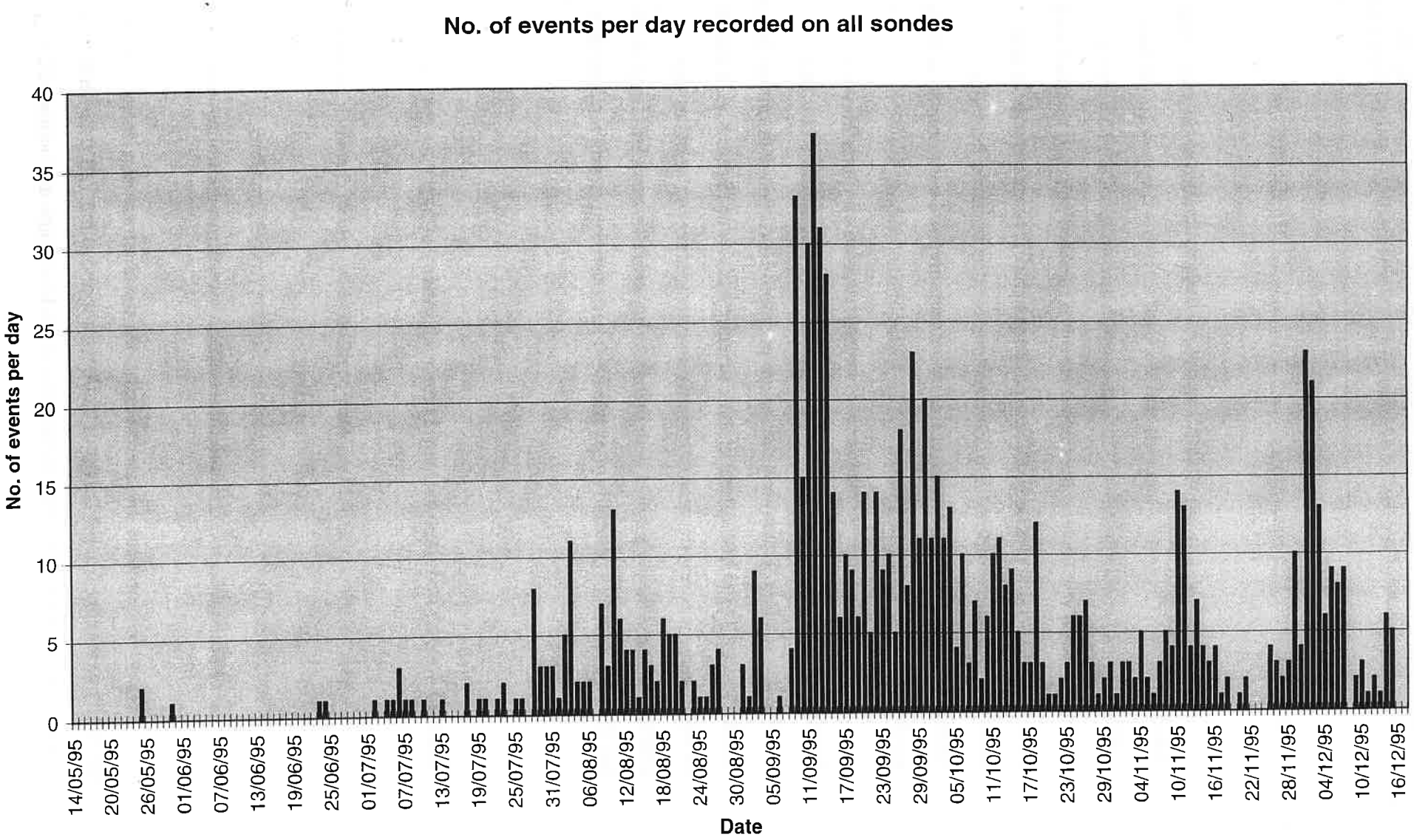

Figure 8.3 Number of events per day detected at Asfordby Colliery.

8.2 Mining-Related Microseismicity

Although significant activity (especially early in the life of the face) was detected on the Fishpond's borehole and the Cant's Thorns 2 Borehole, the best controlled data was obtained by the sondes contained within Cant's Thorns 1 borehole principally because the ray paths to these sondes travelled in intact rock in advance of the face rather than through the goaf to Fishponds Borehole and excellent orientation information was available for this borehole from the calibration shots. The discussion of the spatial and temporal variations in activity are therefore predominantly based on this high-quality data set.

There were only 12 microseismic events recorded on Cants Thorn 1 Borehole until Week 14 (5 August 95) when the face had advanced by 344 metres, just slightly further than the square position . The change in seismicity can clearly be seen in the histograms of microseismic activity of Figure 8.3. It should be noted that the levels of microseismicity detected during the whole of this interval was considerably lower than that experienced from other UK Long-walls (eg Coventry) where hundreds of events have been detected during a single shift.

Figures 8.4 to 8.16 all show the weekly microseismicity in four views:

Top Left:	Plan, face position at the end of the week marked
Top Right:	Advance Direction
Bottom Left:	Perpendicular Section from Main Gate
Bottom Right:	Three-dimensional view from the south-west

Figure 8.4 for week 14 clearly shows the development of a linear zone of seismicity extending from a height of c 400 metres above the Tail Gate and some 50 metres in advance of the face to the edge of the Main Gate at a height of 200

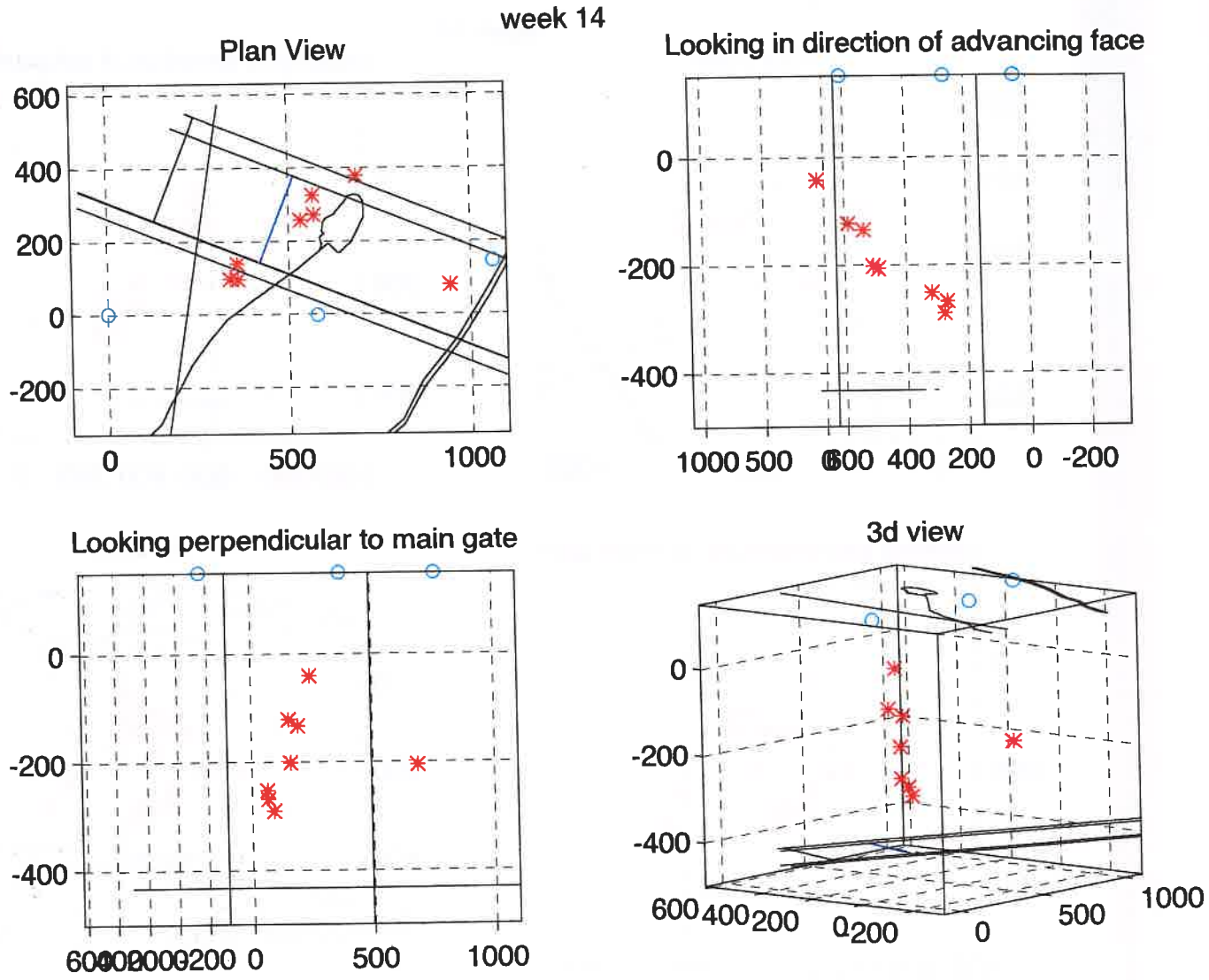

Figure 8.4 Events located using Cant's Thorns 1 Borehole - Week 14

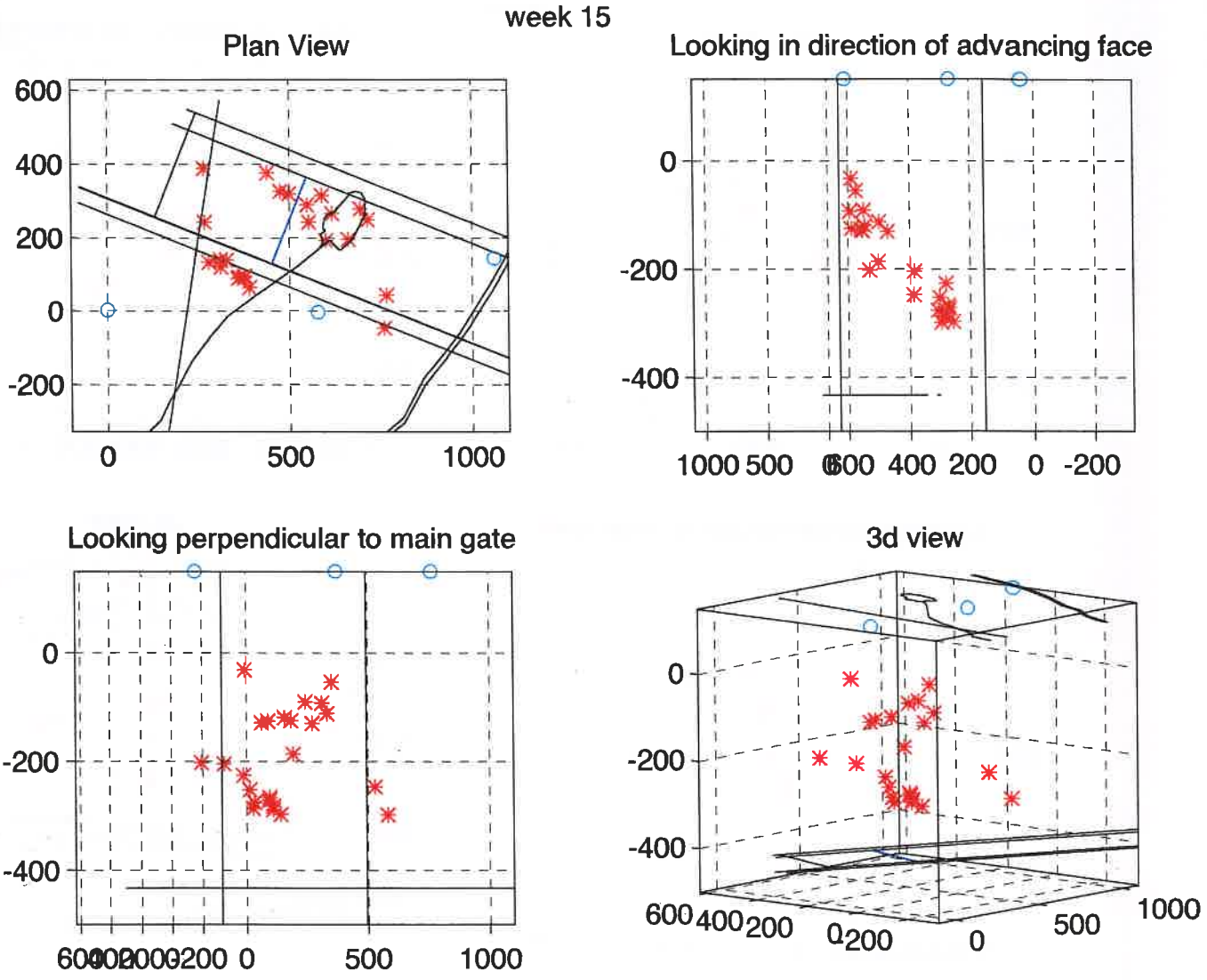

Figure 8.5 Events located using Cant's Thorns 1 Borehole - Week 15

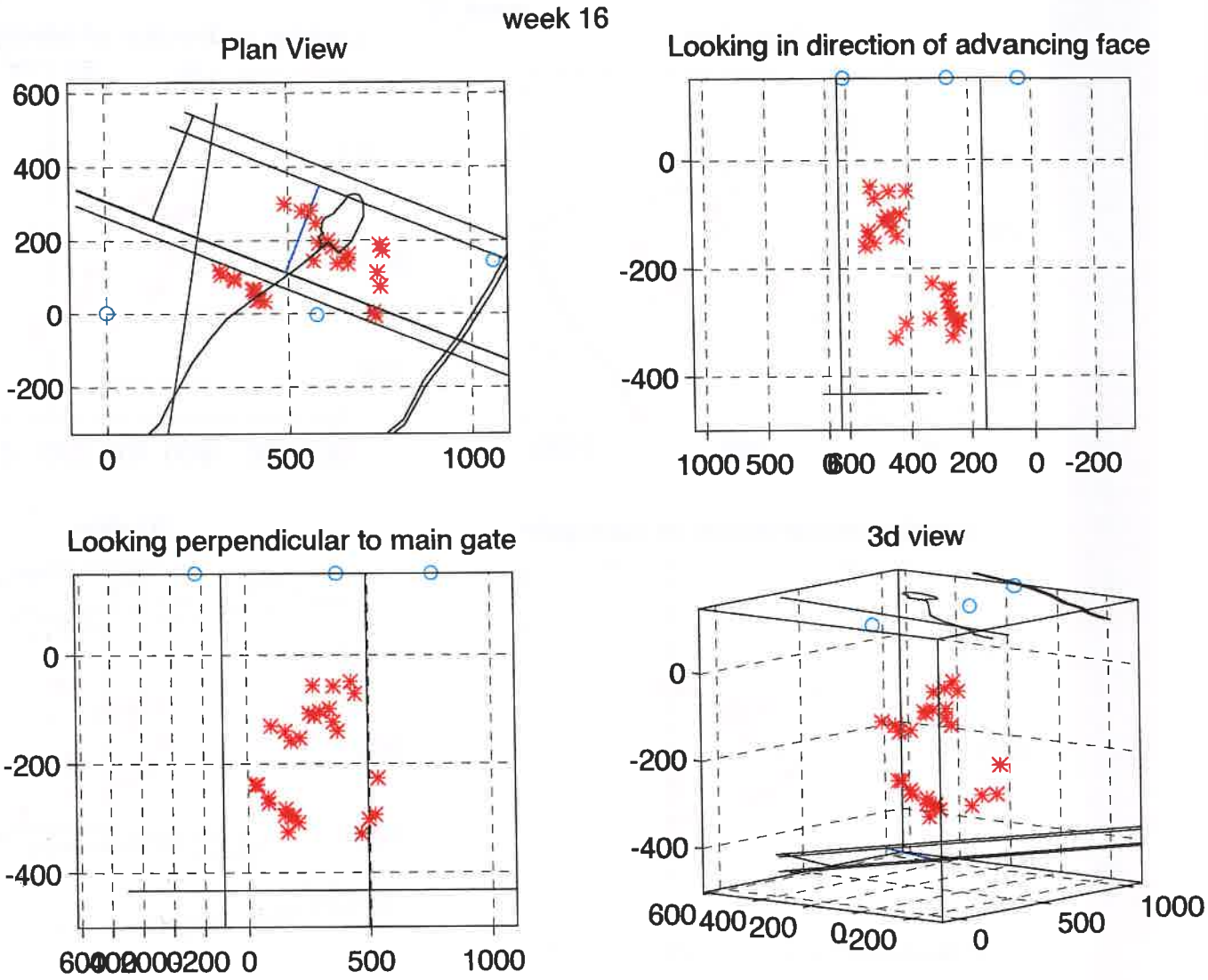

Figure 8.6 Events located using Cant's Thorns 1 Borehole - Week 16

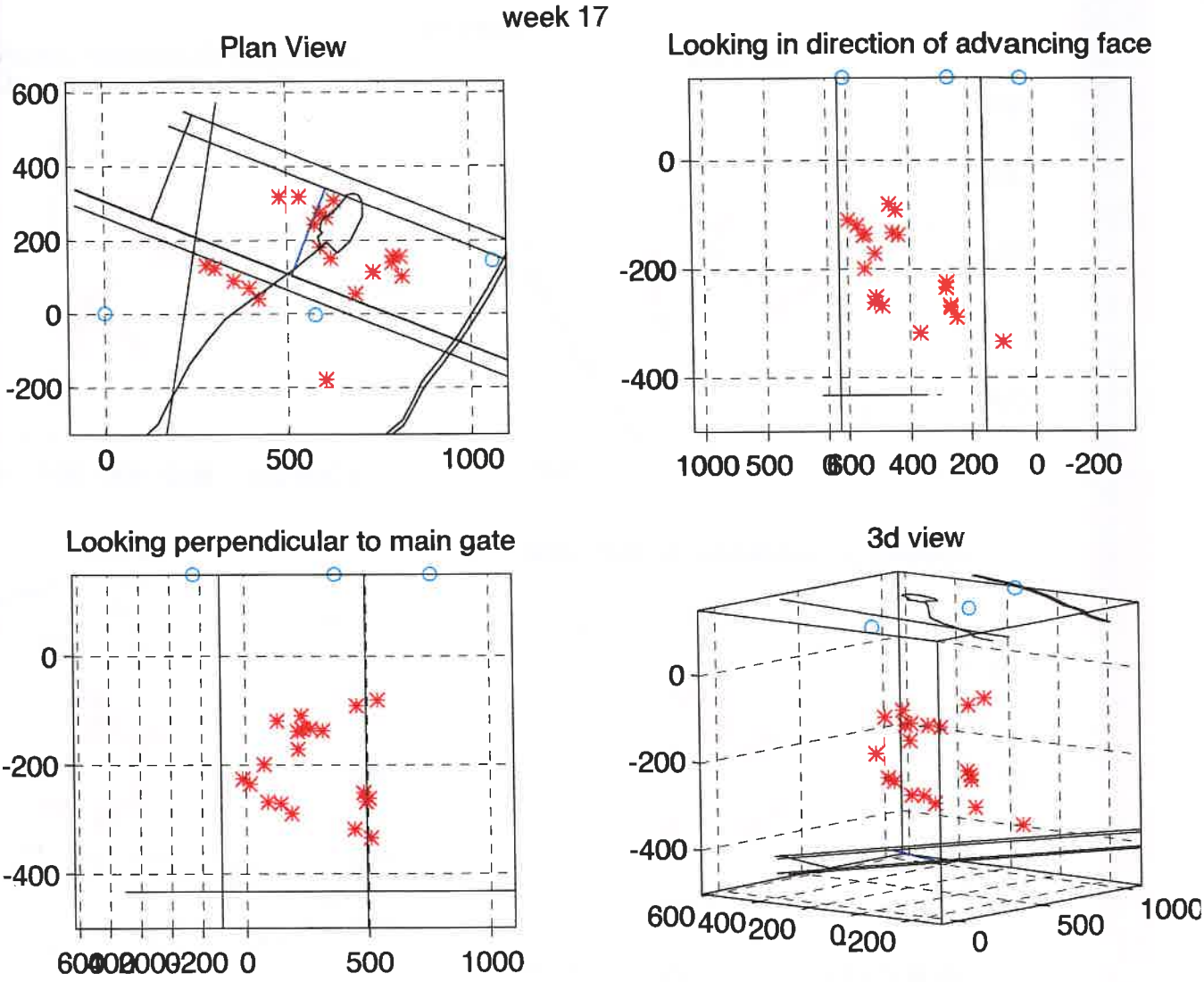

Figure 8.7 Events located using Cant's Thorns 1 Borehole - Week 17

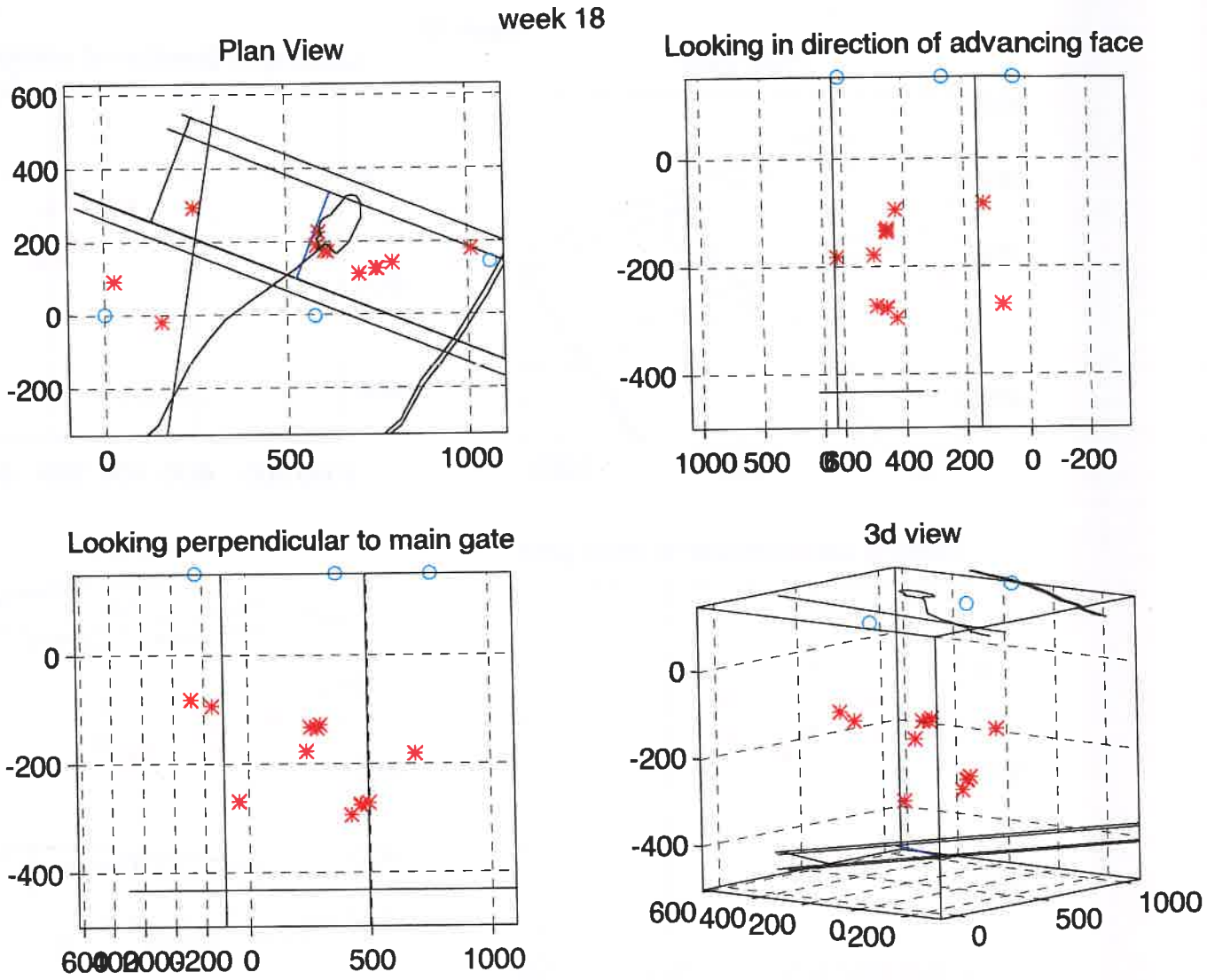

Figure 8.8 Events located using Cant's Thorns 1 Borehole - Week 18

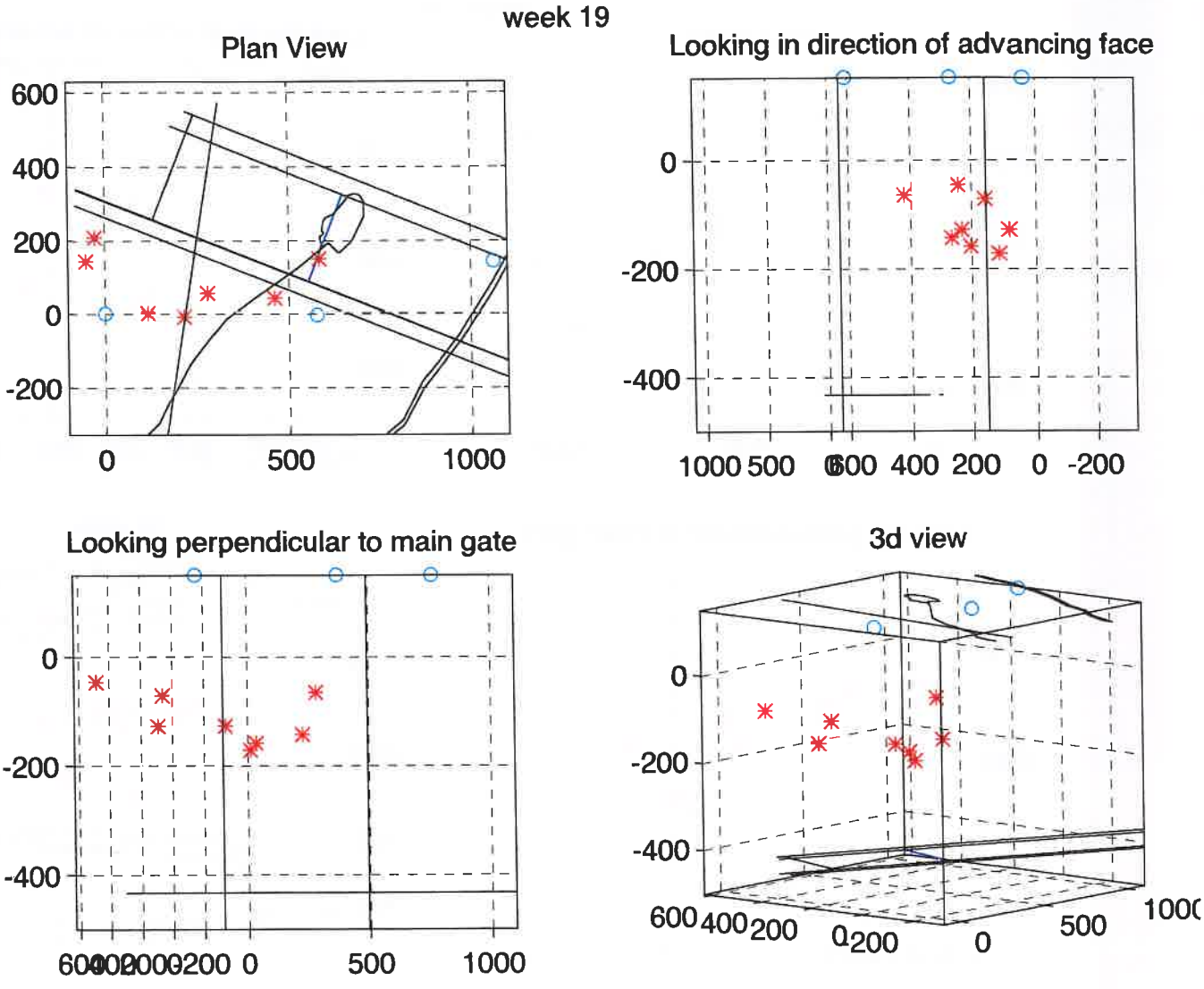

Figure 8.9 Events located using Cant's Thorns 1 Borehole - Week 19

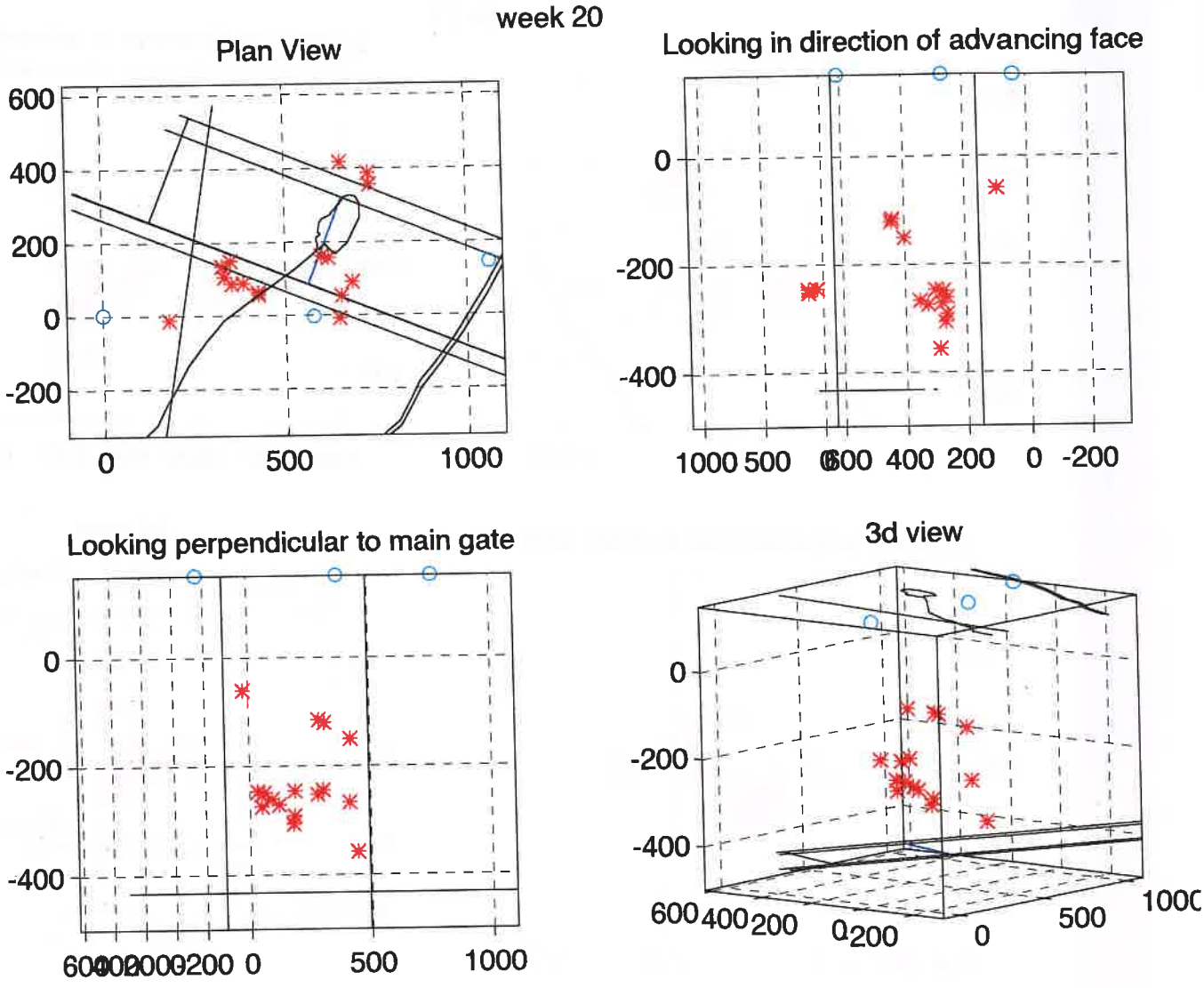

Figure 8.10 Events located using Cant's Thorns 1 Borehole - Week 20

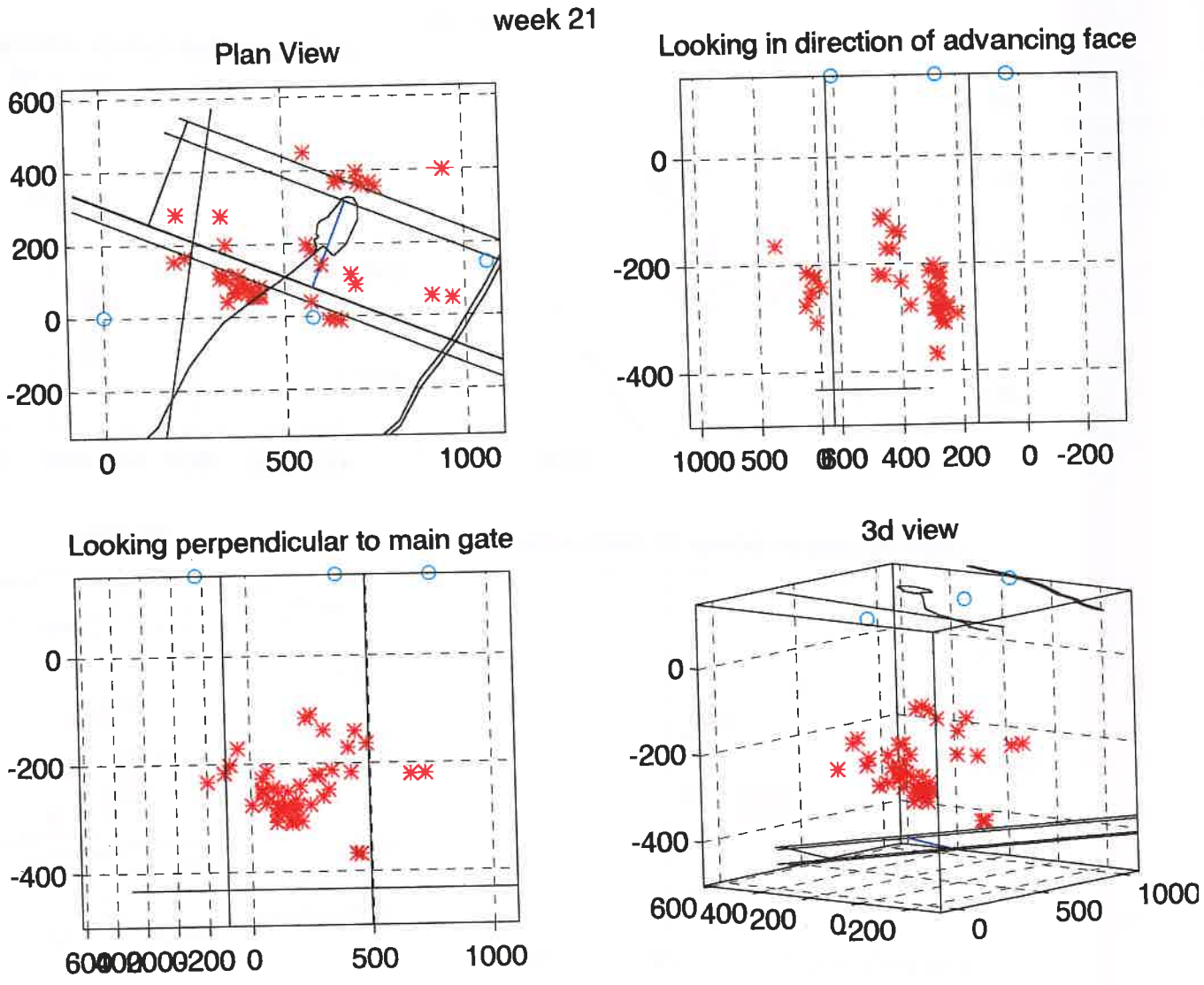

Figure 8.11 Events located using Cant's Thorns 1 Borehole - Week 21

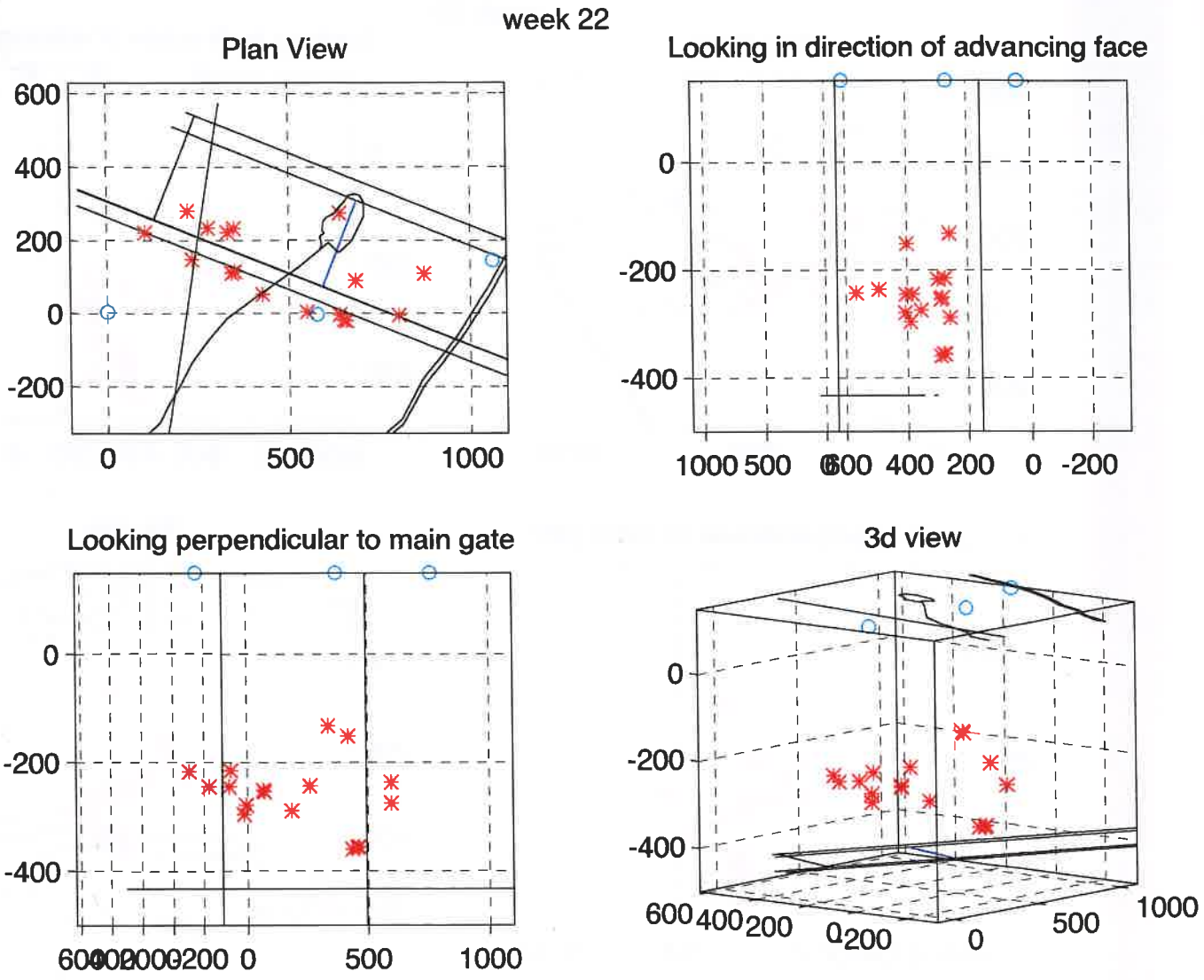

Figure 8.12 Events located using Cant's Thorns 1 Borehole - Week 22

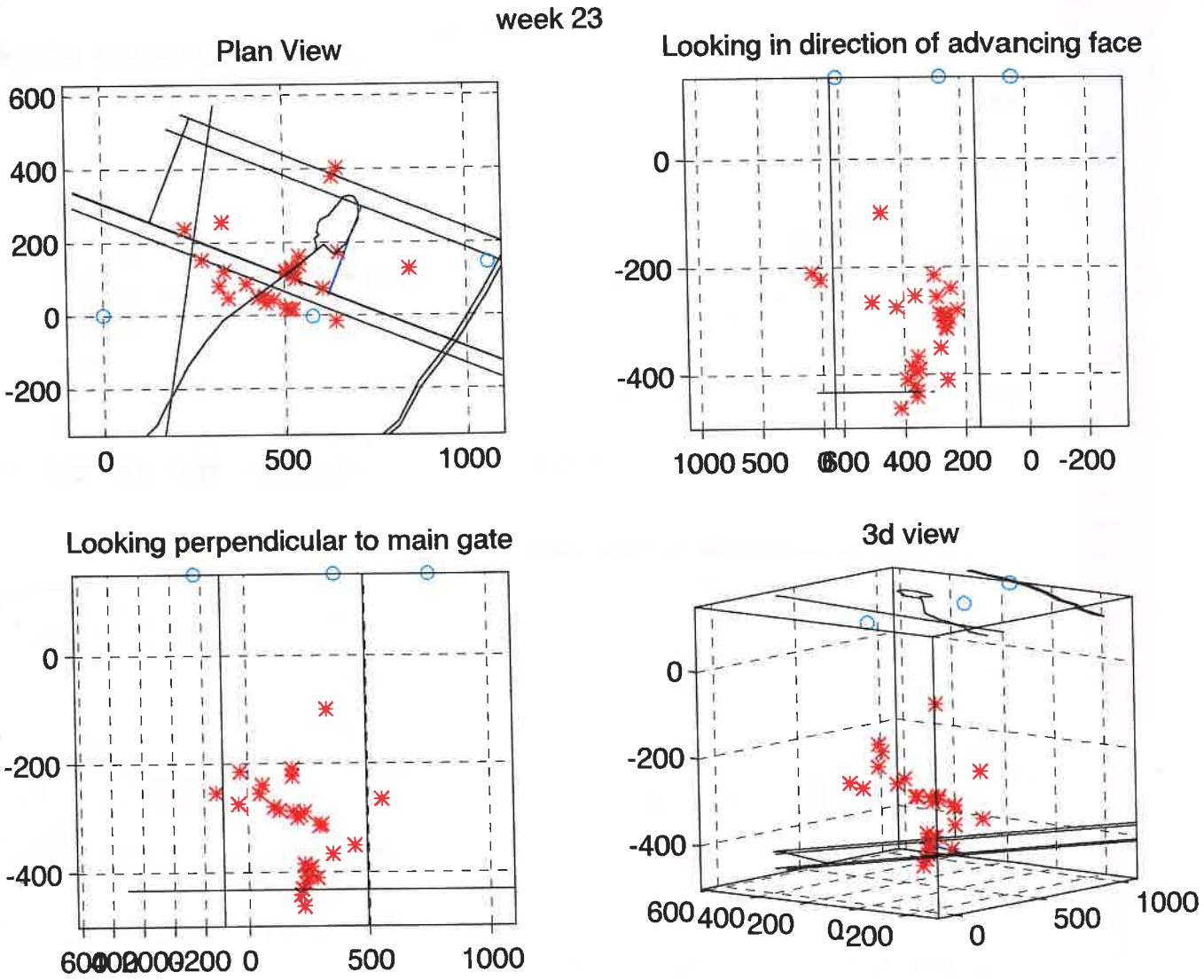

Figure 8.13 Events located using Cant's Thorns 1 Borehole - Week 23

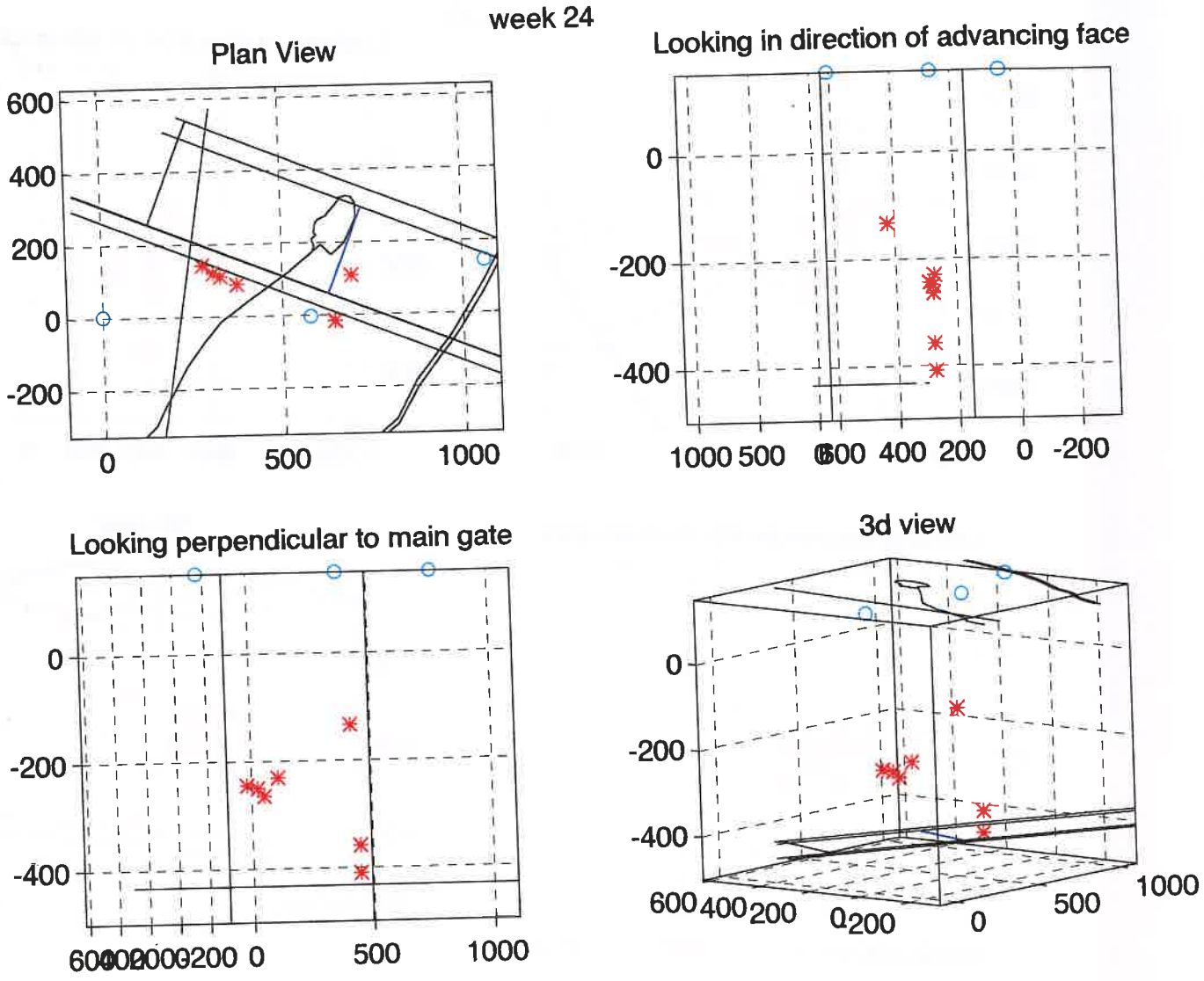

Figure 8.14 Events located using Cant's Thorns 1 Borehole - Week 24

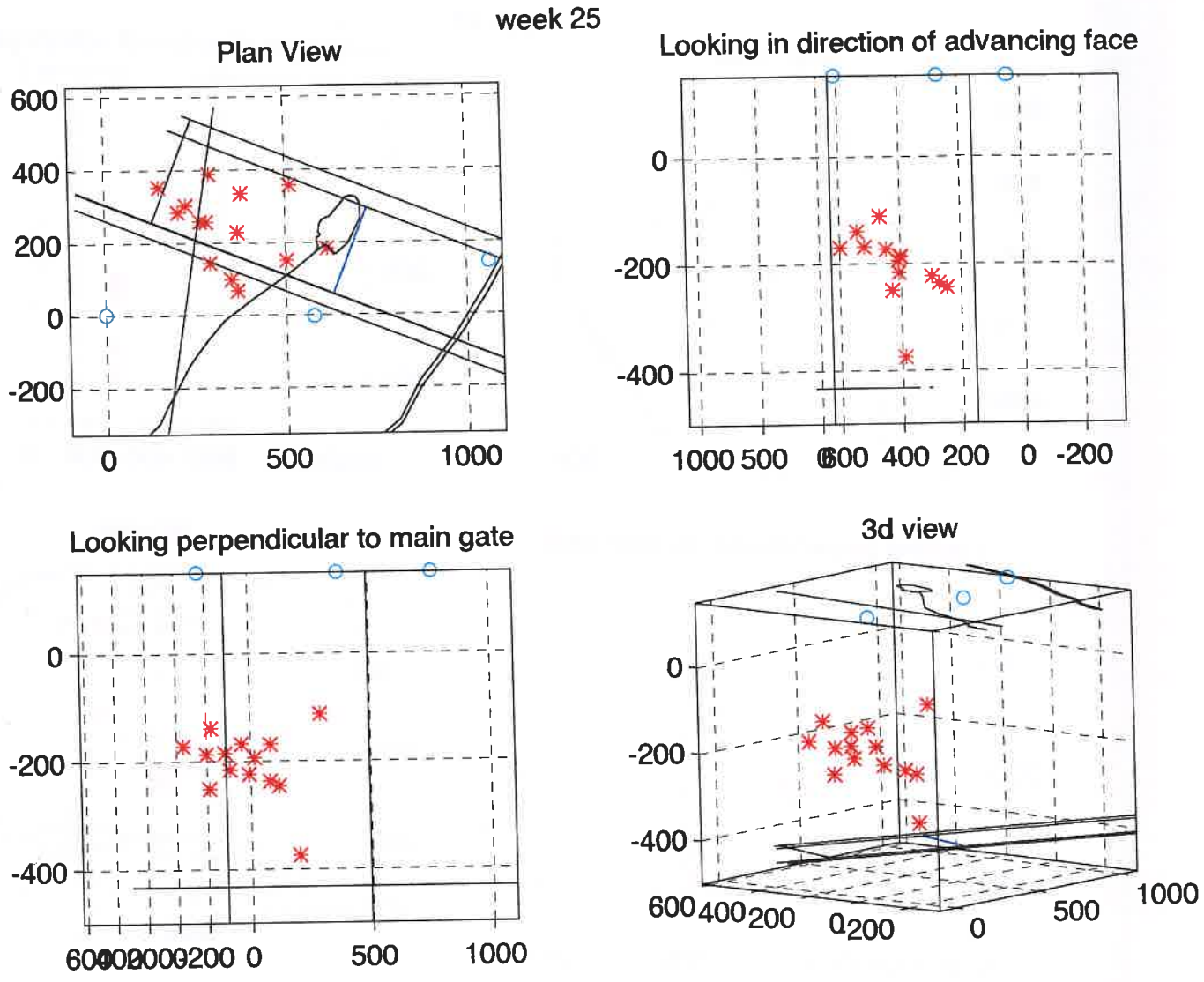

Figure 8.15 Events located using Cant's Thorns 1 Borehole - Week 25

metres. This lineation becomes more pronounced in Figure 8.5 for week 15 with additional seismicity developing behind the face on a backward-hading surface.

Weeks 16 and 17 (Figures 8.6 & 8.7) show seismicity clustering in two distinct zones , the first located over the edge of the Main Gate from 100 to 200 metres above the face and the second at a height of 250 to 400 metres above the face. No activity is occurring in the immediate region of the extracted zone at this time. The view from the Main Gate clearly shows the presence of a zone where activity is not present bounded by linear regions of intense seismicity. The higher cluster is clearly associated with the face position but the lower is developing parallel to the Main Gate. Weeks 18 and 19 (Figures 8.8 & 8.9) show more diffuse seismicity distributed over a wide area with only a tentative relationship to the face position.

However during week 20 (Figure 8.10), (20/9/95) activity again returns to the edge of the Main Gate with a further zone developing over the Tail Gate. During week 21 (Figure 8.11) (27/9/95), there was a tremendous increase in seismicity with clear zones of failure developing over both the Main and Tail Gates form a height of c 250 metres above the seam to a height of 100 metres above the seam. The three-dimensional perspective view indicates that a discrete block of roof rock is becoming bounded by fractures on three sides. During week 22 (Figure 8.12) the fracture fringing the Main Gate extended over a region some 500 metres long extending all the way from the start position of the face to slightly in advance of the present face position at an advance of 529 metres. At this stage the zone of fracture damage has not penetrated down to the immediate roof above the extracted zone.

During week 23 (Figure 8.13) , the first week in October, seismic activity propagated downwards , intersecting seam level right at the edge of the Main Gate some 70 metres behind the active face position with activity apparently extending for a short distance (c 20 metres) into the floor. A major through-going fracture architecture clearly developed at this time establishing fracture pathways between the higher strata and the seam. A reduced level of activity persisted into week 24

(Figure 8.14) which was mainly confined to a narrow zone above the Main Gate. Activity during week 25 (Figure 8.15) was rather more diffuse and probably relating to the relaxation of the strata above the failed zone. Minor activity continued after this time although the face advance (Figure 8.1) had ceased. This is to be expected as the rock mass accommodates to the changed stress regime brought about by the development of a major set of bounding fractures.

Figure 8.16 is a synoptic view of the total microseismicity during the period 5/8/95 until 30 December 1995 which shows a funnel-shaped fracture damage architecture has developed in the roof which has then become localised in a narrow zone of seismicity extending down to the seam. Throughout this period very little activity has occurred close to the seam , on the Tail Gate side of the face with most activity concentrating around the Main Gate. The plan and perspective views clearly show the existence of a zone in the centre of the panel where no activity appears to have occurred. Clearly, fracturing is becoming localised and major discrete blocks bounded by fractures are forming. These are then free to subside along the fractures which are extending almost up to the ground surface and it is possible that this could be manifest in well-defined surface subsidence at some later date.

8.3 Seismicity in a Face Frame of Reference

It is often instructive to view mining-induced seismicity in a frame of reference which is relative to the moving face position as this tends to demonstrate any relationships between zones of failure and the front stress-abutment zone. This could be clearly seen for the events detected from Coventry Colliery (Figure 3. 9) and especially from Gordonstone Colliery, Bowen Basin Queensland, Australia (Figure 3.10 to 3.14). In both of these cases there was a very clear spatial relationship between instantaneous face position and the locus of the cloud of events surrounding the face. Figure 8.16 shows a plan view and

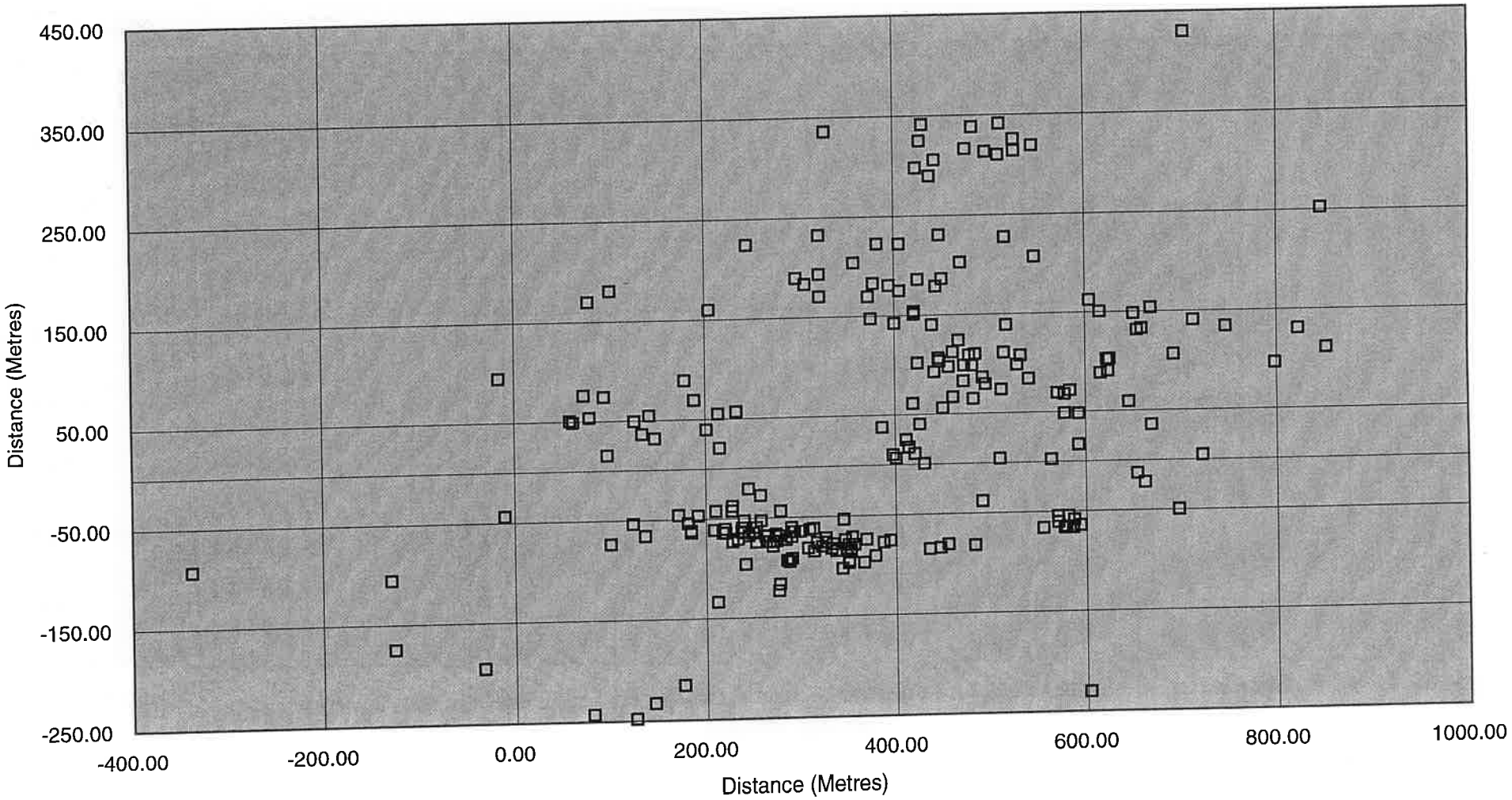

Figure 8.16 Hypocentral locations, Asfordby face 101. Plotted in geographic frame of reference.

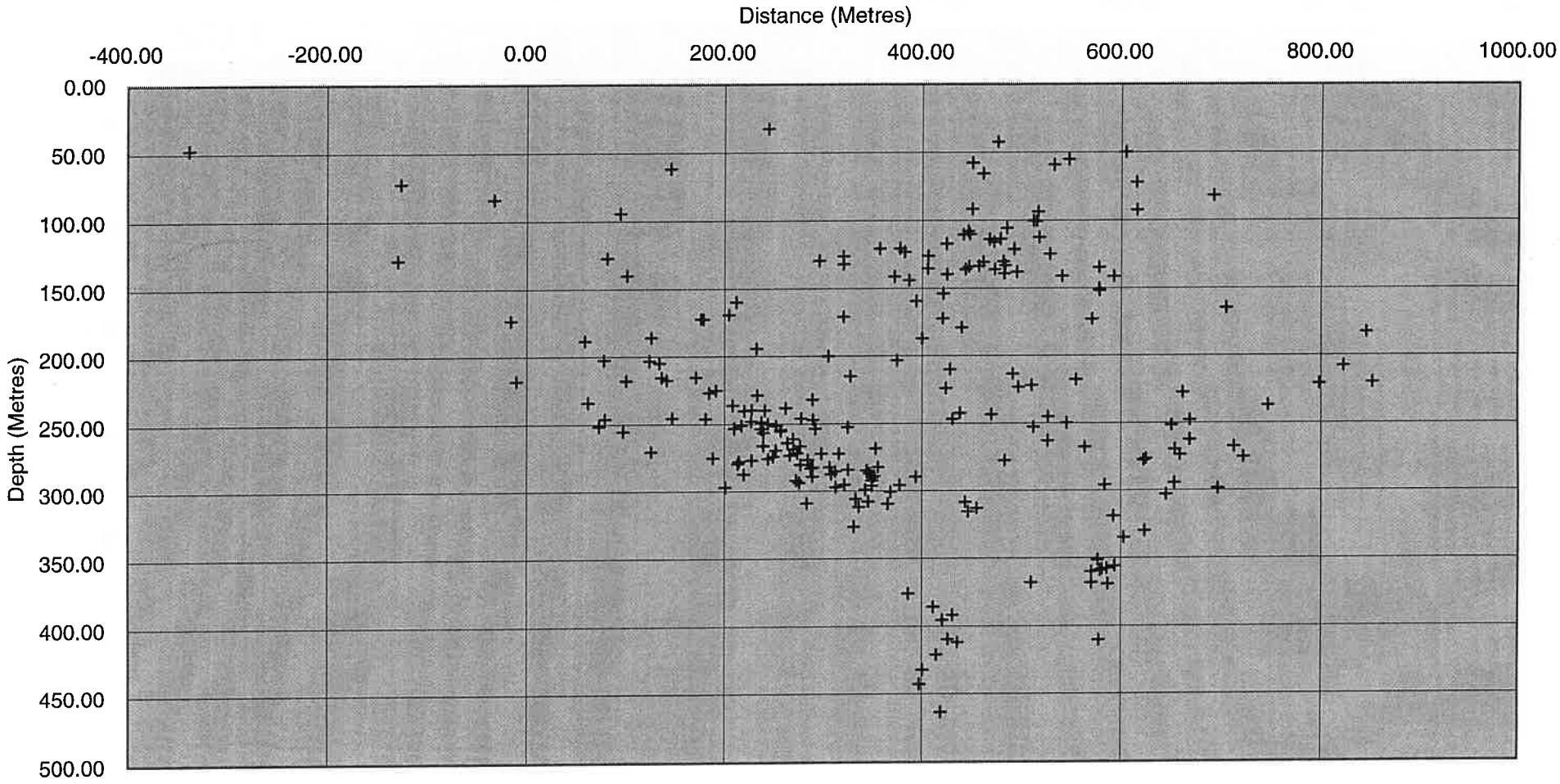

Figure 8.17 Hypocentral Locations, Asfordby Face 101. Plotted in Geographic frame of reference

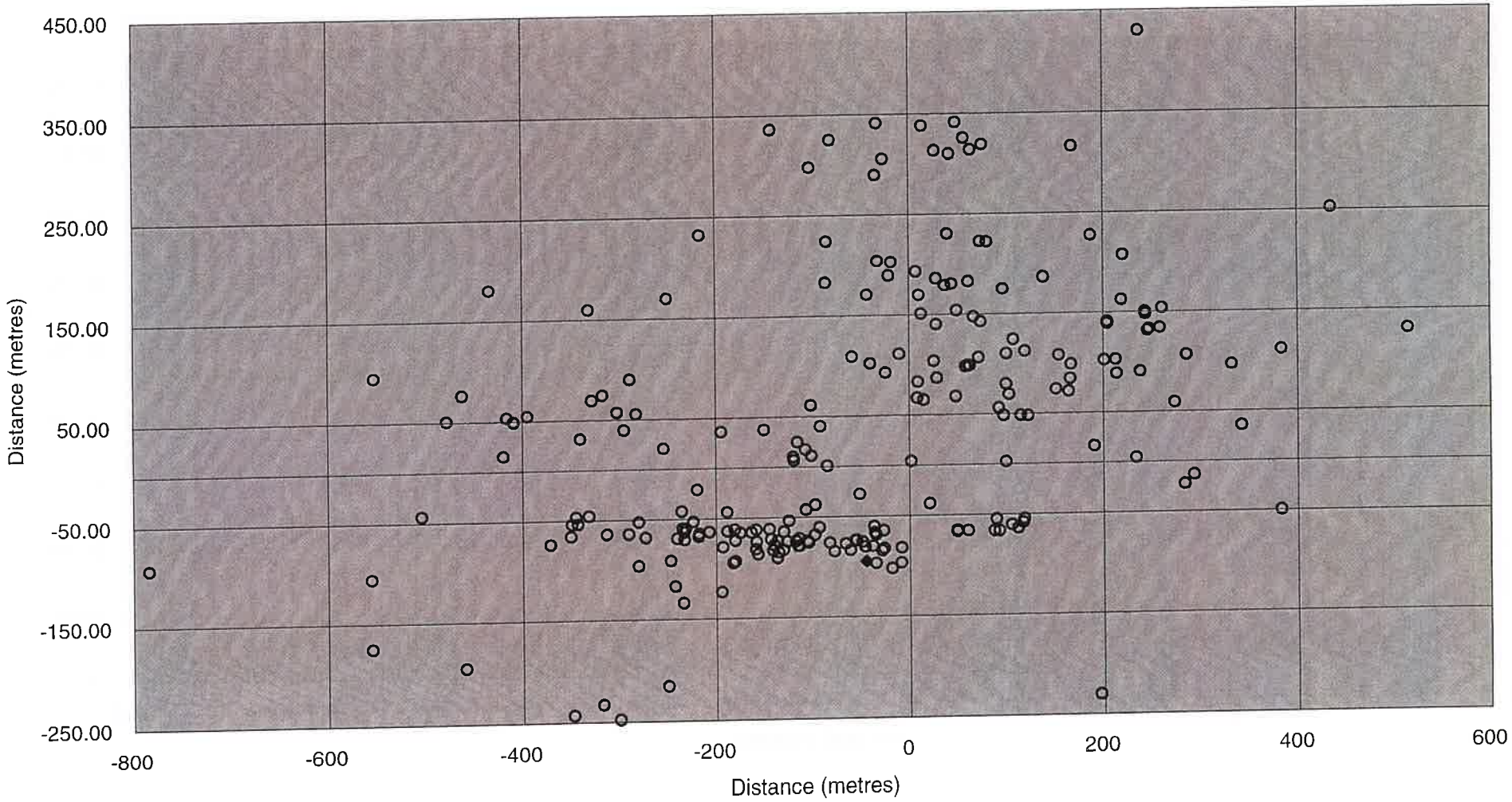

Figure 8.18 Hypocentral Locations, Asfordby Face 101. Plotted relative to face position

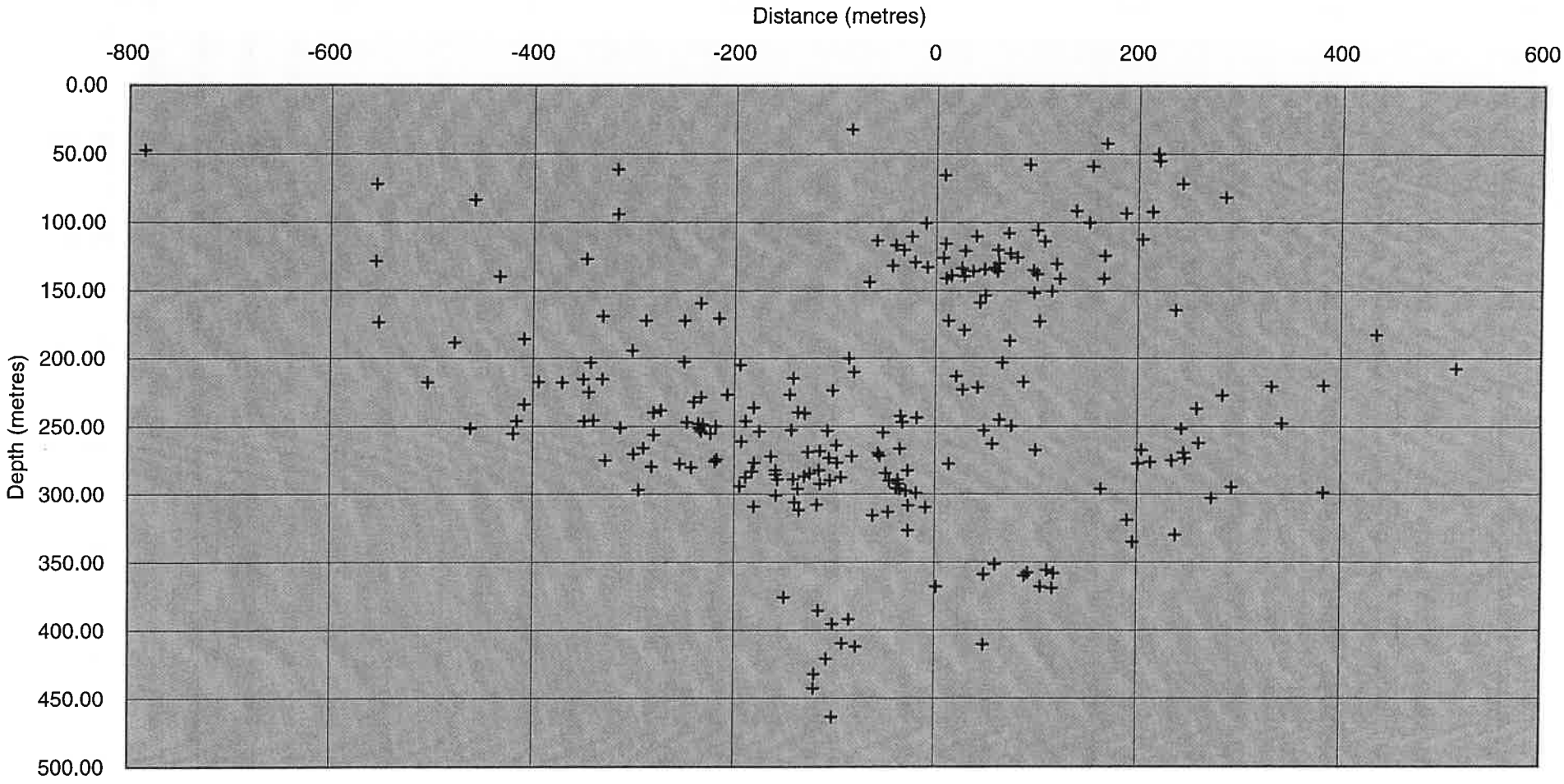

Figure 8.19 Hypocentral Locations, Asfordby Face 101. Plotted relative to face position

Figure 8.17 a cross-section along the Main Gate through the total seismicity detected on Cant's Thorns 1 borehole in the normal geographic frame of reference and Figures 8.18 and 8.19 show the same activity when plotted in a frame of reference with respect to the face. The seismicity is more tightly clustered in geographic coordinates, in contrast to the Gordonstone results and even in a face-frame of reference has a distribution of activity over a width of 700 metres and a length of 1400 metres. This seems to indicate a very strong stratigraphic or structural control on the loci of the seismicity. However, while both show the same general 'tree-shaped' pattern the plot in the 'face-frame', (Figure 8.19) has three clearly defined zones of seismicity activity:

i A surface inclined backwards and rising away from the face position

ii A shallowly-inclined zone extending out more than 500 metres in front of the face to a height of 200 metres above the seam.

iii A steeper zone inclined at about 45 degrees which extends about 200 metres in front of the face and rises to more than 400 metres above the seam.

These are almost certainly related to the principal failure surfaces which have developed in the rock-mass as a result of the extraction of the coal-seam and which have clearly influenced a very large volume of the overlying strata. It seems likely that these failure surfaces have some real relationship to the pattern of stress developed around the long-wall under the interactions between the ambient stress, the mining-induced stress and the laterally-heterogeneous geology and that further geomechanical modelling should be able to explain their Rock-Mechanical significance. It seems likely, given the discrete failure surfaces which appear to have formed above this face that Distinct-Element methods rather than Finite-Element methods might be fruitful.

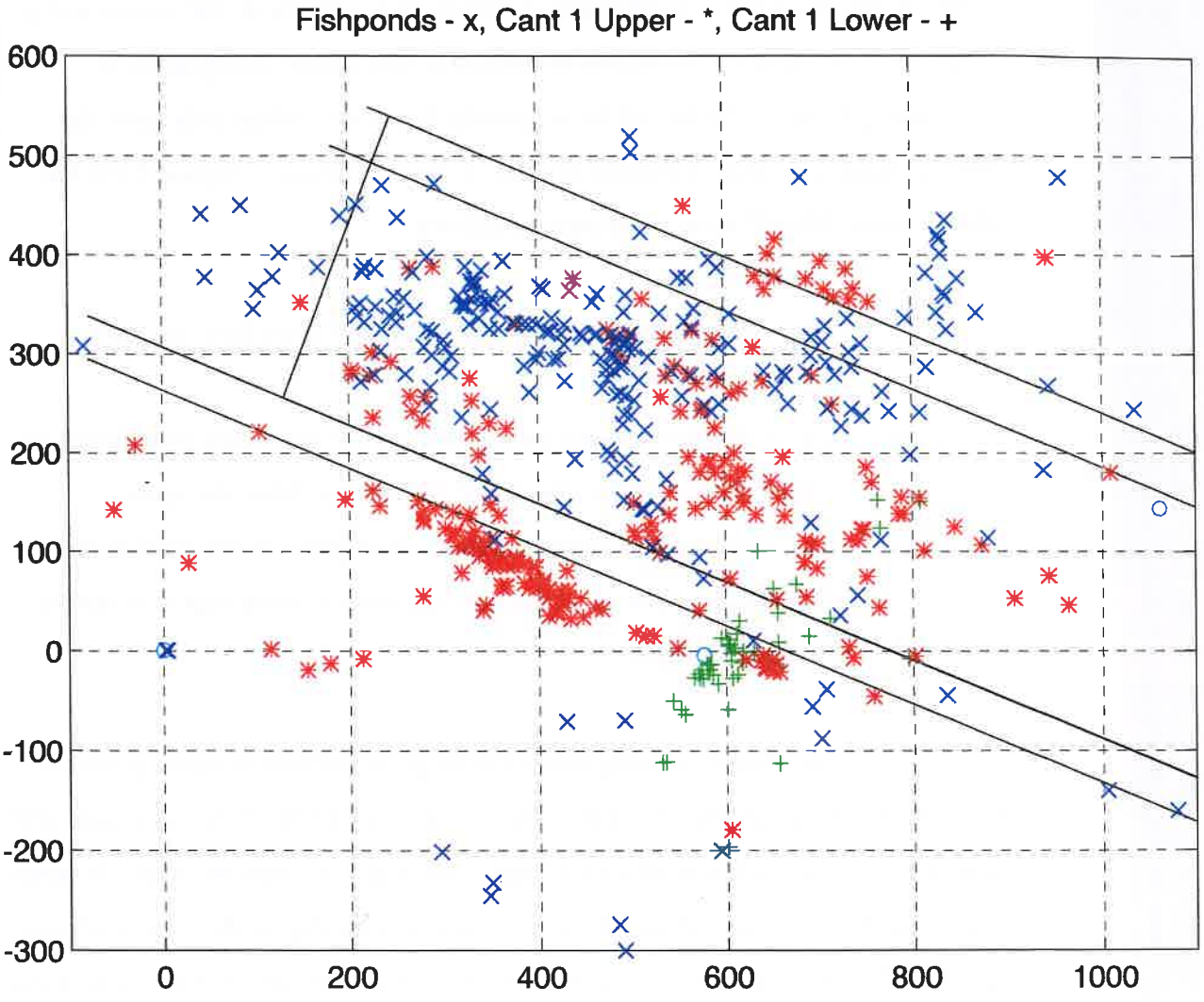

Figure 8.20 Microseismic event locations for Asfordby. Shown are events detected at Fishponds and Cant's Thorns 1 Boreholes.

8.4 Hypocentral Locations from Fishponds and Cant's Thorns boreholes

Figure 8.20 is a composite plot of the hypocentral locations of events detected from Fishponds , Cant's Thorns 1 and Cant's Thorns 2 boreholes. While the best data are derived from Cant's Thorns 1 and the inclusion of the other data will tend to slightly degrade the image quality the distribution clearly outlines a rhomb-shaped area within the panel which is bounded by seismicity but has very few failures within it. This can be seen on Figure 8.16 but the inclusion of the Fishponds data has helped delineate the north and western edges. It seems likely that fracturing around the margins of this rhomb which lies principally within the Sherwood Sandstone has effectively detached a major block of roof rock with dimensions of approximately 200 metres by 200 metres and that this has been free to subside as a distinct element without normal mature caving developing.

8.5 Failure mechanisms associated with the development of the fracture architecture

If there are sufficient seismic stations surrounding a rock volume it is possible to utilise features of the seismic waveforms such as relative P and S-wave amplitudes and polarities to determine the orientation of the individual fractures associated with each microearthquake and to discriminate whether the events are associated with tensile failure or shear failure. While the present data-set is not adequate to give a full description of the fracture process it is possible to make some simplifying assumptions which permit the principal parameters to be determined. The full details of this analysis procedure are contained in Appendix 3. However, in summary we make the assumption that the fractures have a shear mechanism with a vertical failure plane. With these constraints it is possible to determine the azimuth of the planes containing the failure. Figure 8.21 shows a plan view, with the face superimposed, with the azimuth determined for all of the microseismic events which can be solved during the life of the face. The events

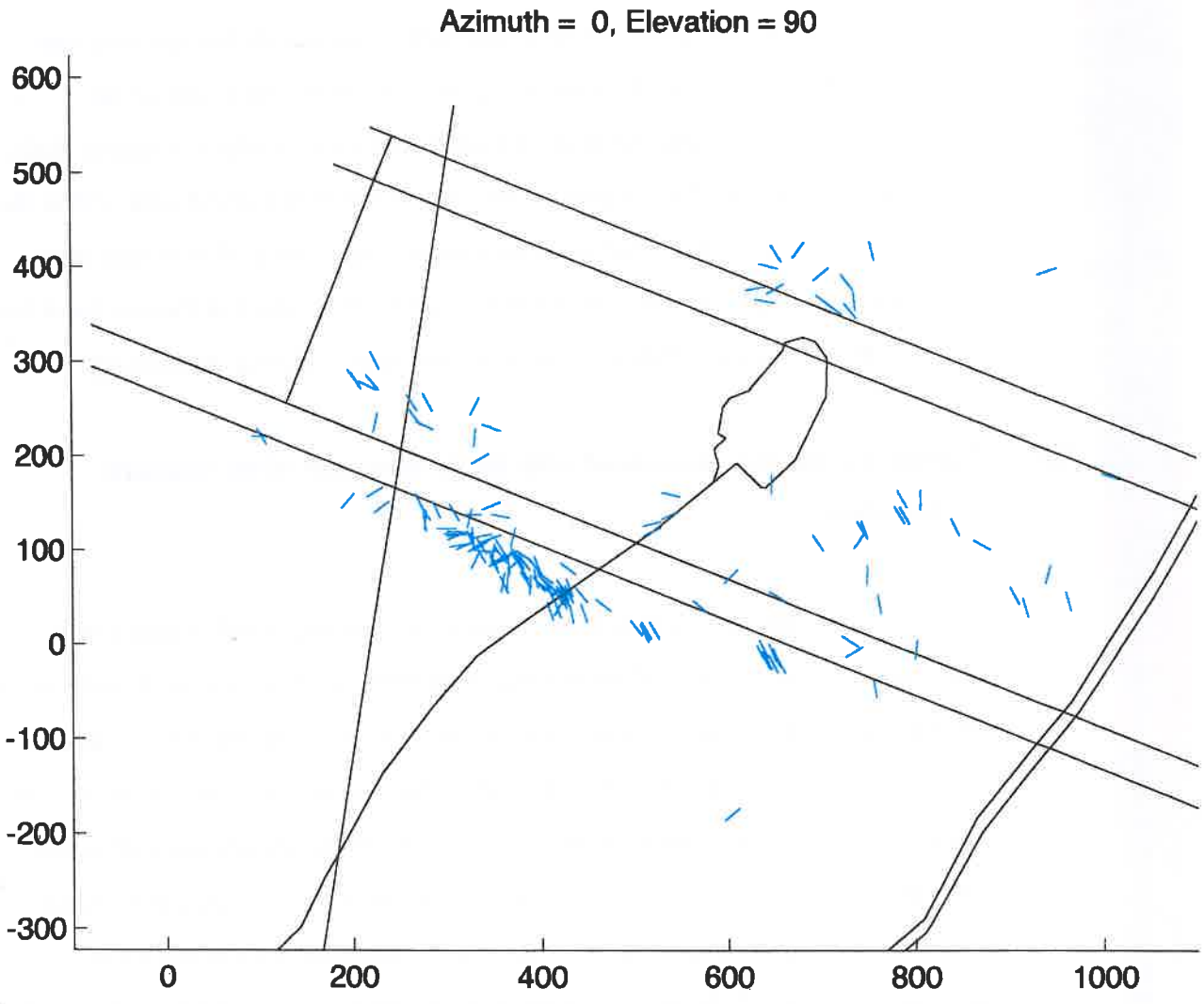

Figure 8.21 Location of microseismicity at Asfordby Colliery showing the orientation of the fracture planes (assuming vertical fractures).

show some variation but as the Radar Plot of Figure 8.22 shows the principal orientation is along the direction 300 to 315^0 at a shallow angle of about 20^o to the bounding fracture as delineated in Figure 8.20 . The orientation of the failure planes is very close to the principal stress directions derived from borehole breakouts and overcoring obtained during the exploration phase of the Asfordby development (Whitworth *et. al.* 1994) which is shown in Figure 4.5 . Figure 8.23 shows a perspective view of the same data which demonstrates that the orientation of the fractures does show some variation with depth. The geometric relationship between the individual fractures and the through-going bounding fracture is very similar to that seen in laboratory studies of rock-failure where the individual events lead to stress concentrations around their tips which interact and eventually coalesce to form a through-going process zone (Lockner 1993) which eventually progresses to complete failure. With sufficient geophone coverage of the seismically active zone it would be possible to determine the complete seismic-moment tensor with a full description of the fracture process.

8.6 Relationship between Underground Mining and Roof Control Events and Microseismicity

The Deep Main seam which is being worked by panel 101 lies at a depth of c. 545 metres (435 metres below O.D.) beneath the surface with a thickness of c 2.8 metres . The generalised geological section in the area was shown in Figure 4.2 together with a detail of the roof strata in Figure 4.3. Several igneous sills with a combined thickness of up to 45 m are present between 60 and 100 metres above the seam. These are jointed with occasional joints which may contain water. Overlying this is the Sherwood Sandstone , a medium to coarse-grained sandstone which is a major aquifer over the whole of Central England. This lies approximately 100 to 120 metres above the Deep Main seam beneath the western portion of Panel 101.

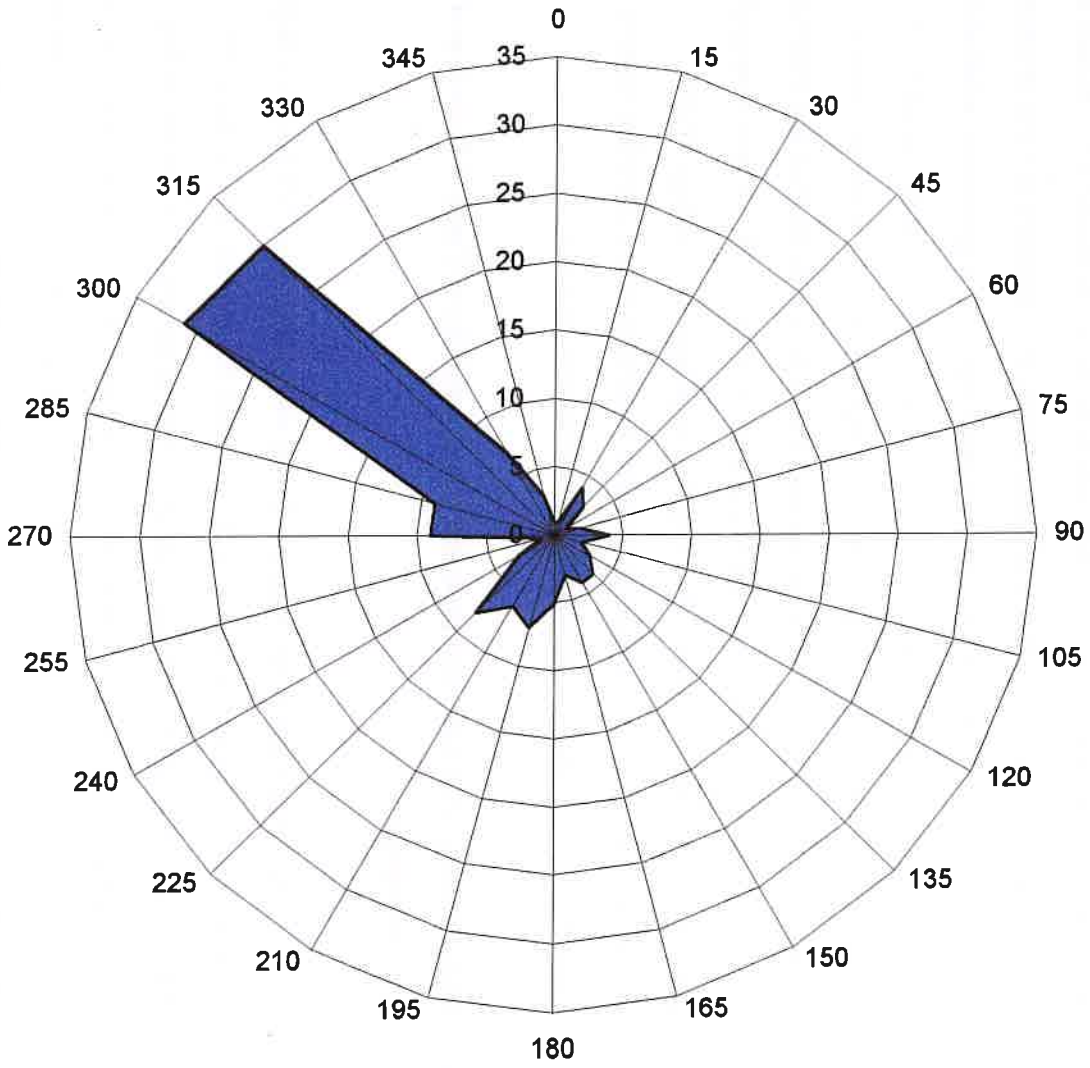

Figure 8.22 Fracture azimuths for microseismicity detected around Panel 101, Asfordby Colliery.

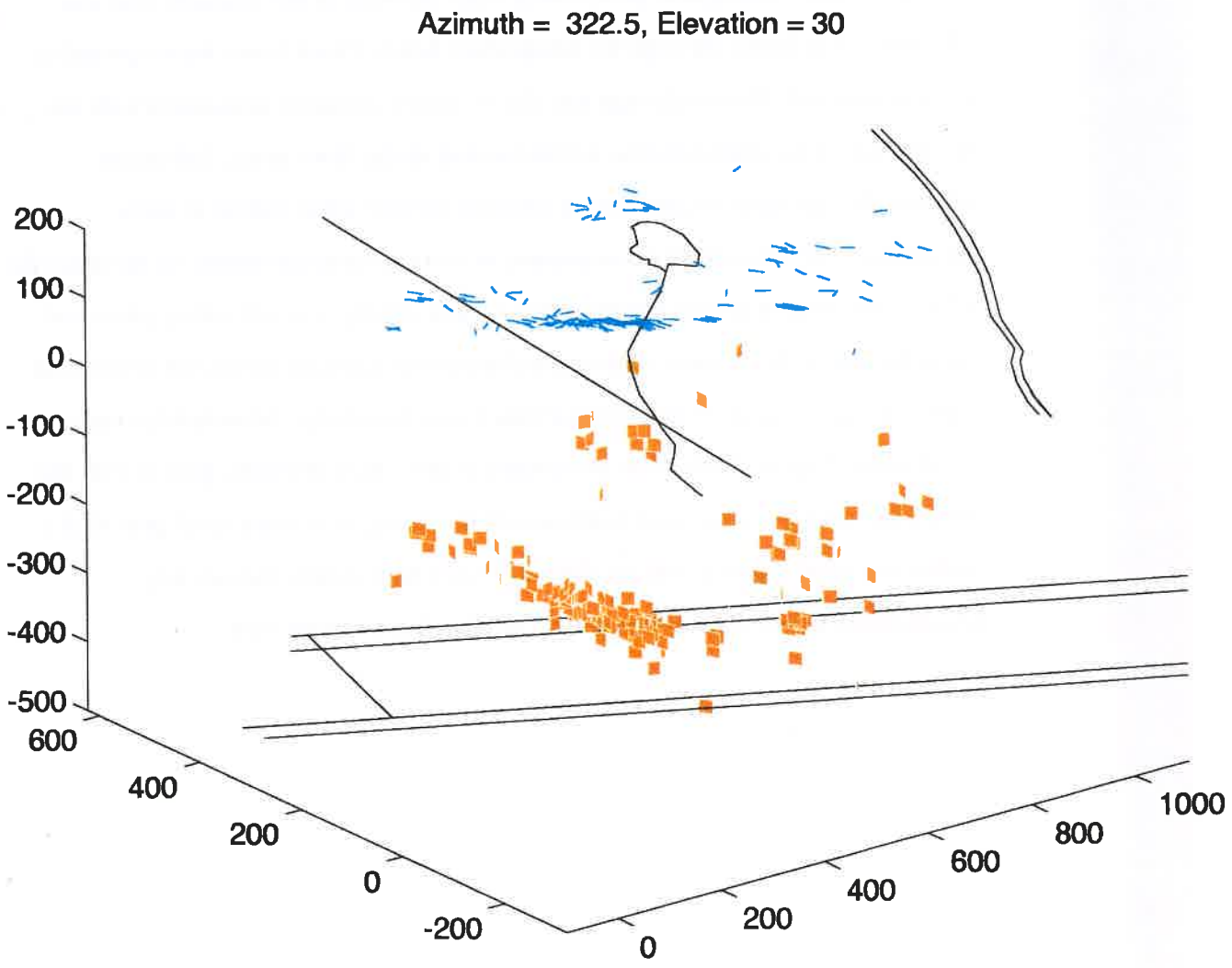

Figure 8.23 Perspective view of microseismicity at Asfordby Colliery showing the orientation of the fracture planes.

The principal mining events which occurred during the life of this face are shown in Table 8. Enhanced levels of seismicity occurred from 11 September, some two weeks before the first weighting on the face, with the bulk of the seismicity occurring within the Sherwood Sandstone strata and very little activity in close proximity to the face. The activity during the first week in October appears to have propagated downwards from the base of the volcanic sills and Sherwood Sandstone through the Deep Main Seam. Floor heave was reported in conjunction with the weightings and this is almost certainly associated with the occurrence of the microseismic events located in the floor strata. Enhanced activity also occurred in association with the second water *inflow* in early December. The absence of microseismic activity in close proximity to the seam for most of the mining period suggests that normal caving was not taking place and the presence of the failures with vertical shear mechanisms within the Sherwood Sandstone are indicative that a major block was detaching, bounded by fractures on all sides (Figure 8.20) . The movement of this block probably gave rise to the weighting, and the associated extension of fracturing near seam level provided a hydrogeological pathway for the Permo-Trias which waters had already accumulated in bed separations above, to percolate onto the face.

Date	Face Retreat	Event
18 March 1995	0	First Cuts
5 July 1995	241	Poor Roof
15 July 1995	270	Poor Roof
12 August 1995	388	Poor Roof
30 August 1995	442	Poor Roof
8 September 1995	460	Poor Roof
17 September 1995	481	Poor Roof
1-7 October 1995	534	Weightings
12 October 1995	539	Water Inflow / Weighting
25 November 1995	539	Restart
30 November 1995	540	Second water Inflow
2 January 1996	546	Full Production
5/6 January 1996	555	Final Weighting

Table 8 Principal mining events on Panel 101 Face, Asfordby Colliery

9 CONCLUSIONS AND RECOMMENDATIONS

- A 24-bit portable microseismic recorder with 20 Mbyte storage capability on Flash cards has been developed which has the capability of detecting and recording mining-induced microseismic events induced by Long-Wall Extraction. This device operates on batteries and Solar panels and can record in excess of 400 events which will usually accommodate a week of mining activity.

- Tri-axial borehole geophone packages cemented at 100 metres intervals between the surface and seam-level can satisfactorily detect mining-induced microsesimicity up to 1000 metres away because of the low ambient microseismic noise at these depths.

- Monitoring during the extraction of coal from Panel 101 of Asfordby Colliery has given tremendous insights into the fracture processes occurring around a Long-Wall face in an undisturbed regional stress-field with complex Geology. Seismic activity occurred primarily within the overlying Sherwood Sandstone aquifer and volcanic sill rather than as normal caving close to the seam level. This activity was generated by fracturing which delineated the margins of a detached block of rock , 200m by 200 m which subsided as a discrete unit causing periodic weightings on the face. Eventually fracturing propagated downwards to the face generating a hydrogeological pathway permitting the ingress of water onto the face.

- Analysis of the source mechanisms of these events has been possible using the high-quality digital tri-axial data and has delineated the azimuths of the individual fractures associated with each microseismic event and their eventual coalescence into bounding fractures.

- The microseismic monitoring has permitted an understanding of the geomechanical behaviour of the rock-mass above Asfordby Panel 101 which was

not possible without the knowledge of the fracture-architecture revealed by the microseismicity

Microseismic monitoring holds the potential of being able to determine and delineate the full extent of the fractured zone around a longwall panel, eventually in real time and at relatively low cost. The data provided by such a system will significantly increase our understanding of the mechanisms leading to strata failure and permit continuous assessment of rock mechanical behaviour while mining. If the technology can be proven under United Kingdom conditions the development of real-time, online monitoring devices to give warning of incipent roof failure and the extent of propagating roof and floor fractures will be a reality.

Appendix 1

Borehole Geophone Assembly Details

CANTS THORNS N°1 & N°2 BOREHOLE

BOREHOLE GEOPHONE DRAWINGS

ASFORDBY FEB 95

CONTENTS

Ammendments

SHBT Tool added 24/2.

John Cowgrove
23.2.95

Final 22/2/9

Stripe cables every 25
stripe and measure from
base of hole ie zero
at the base of the sinker

Bull dog the cables togeth
every 30 M.

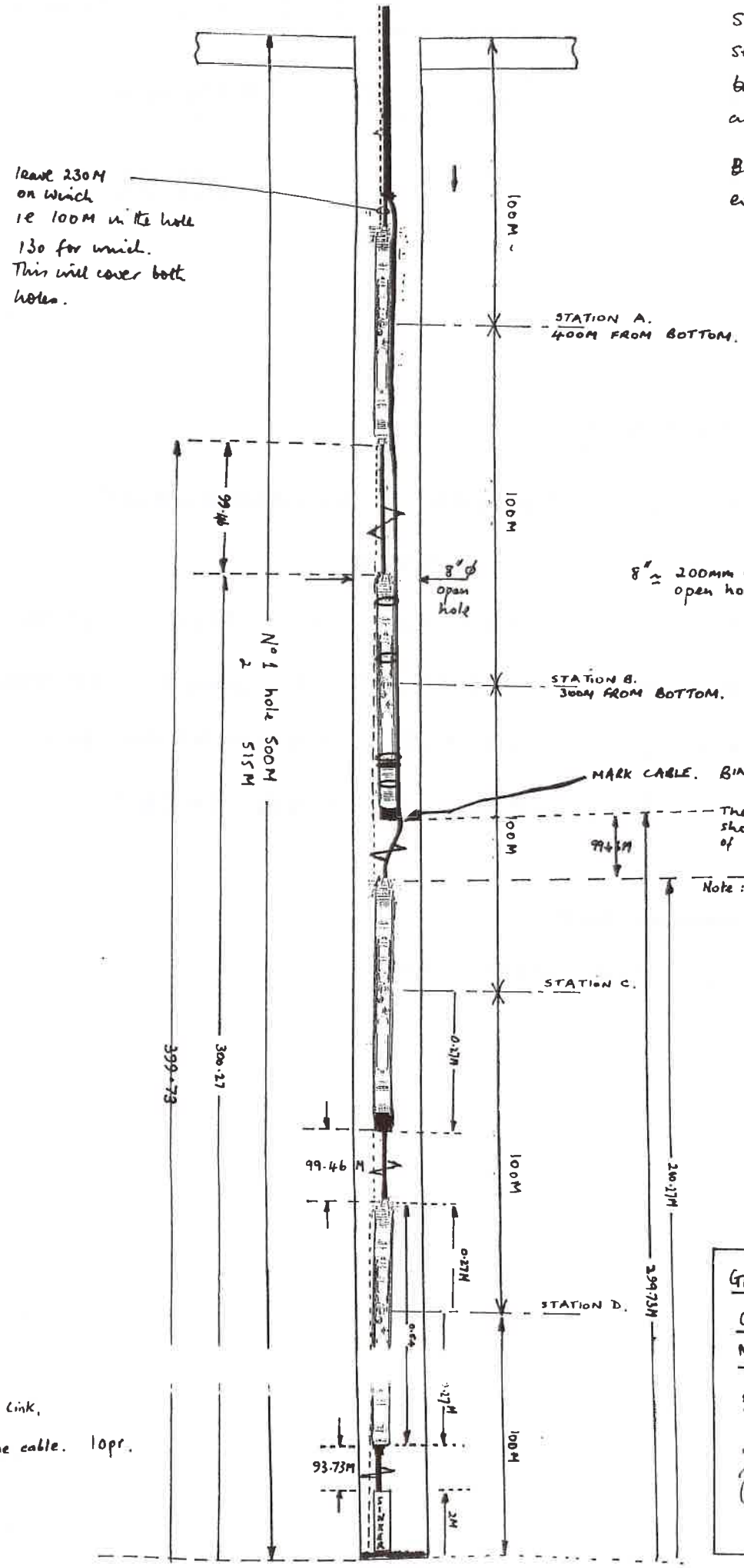

GENERAL ARRANGEMENT

CANTS THORNS

No 1 & No 2

ASSEMBLY

DWG 1

22.2.95

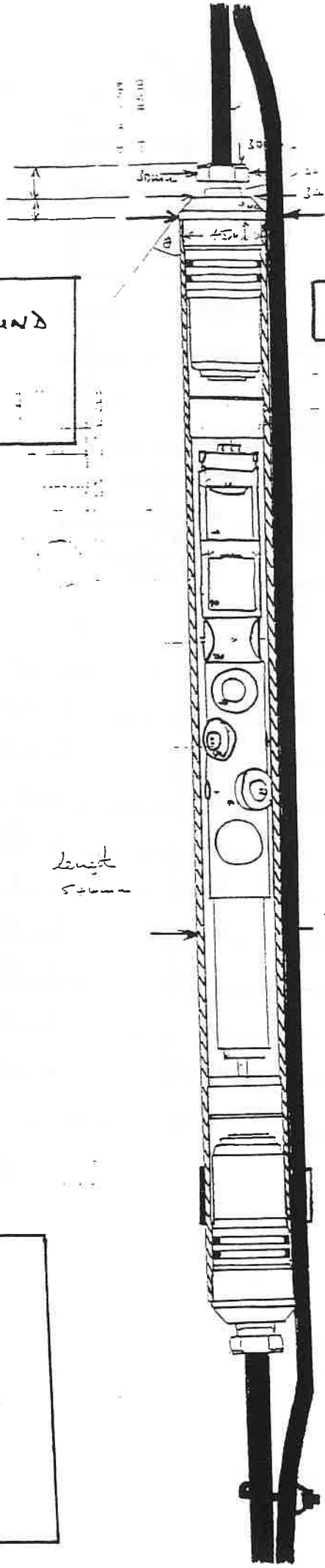

GEOPHONE AND BOUND CABLE WILL OCCUPY 64.5mm Ø.

~~49~~ + 11.5 + 2 + 2
A B C D.

= 64.5mm

A = O.D of Gland
B = O.D of Cable
C = 1 mm of tape
D = laser lead

.CLEARANCES

.DWG 2

CANTS THORNS
Asfordby Borehole.

Micro Seismonitor

Arrangement.

Final

13th Feb 95

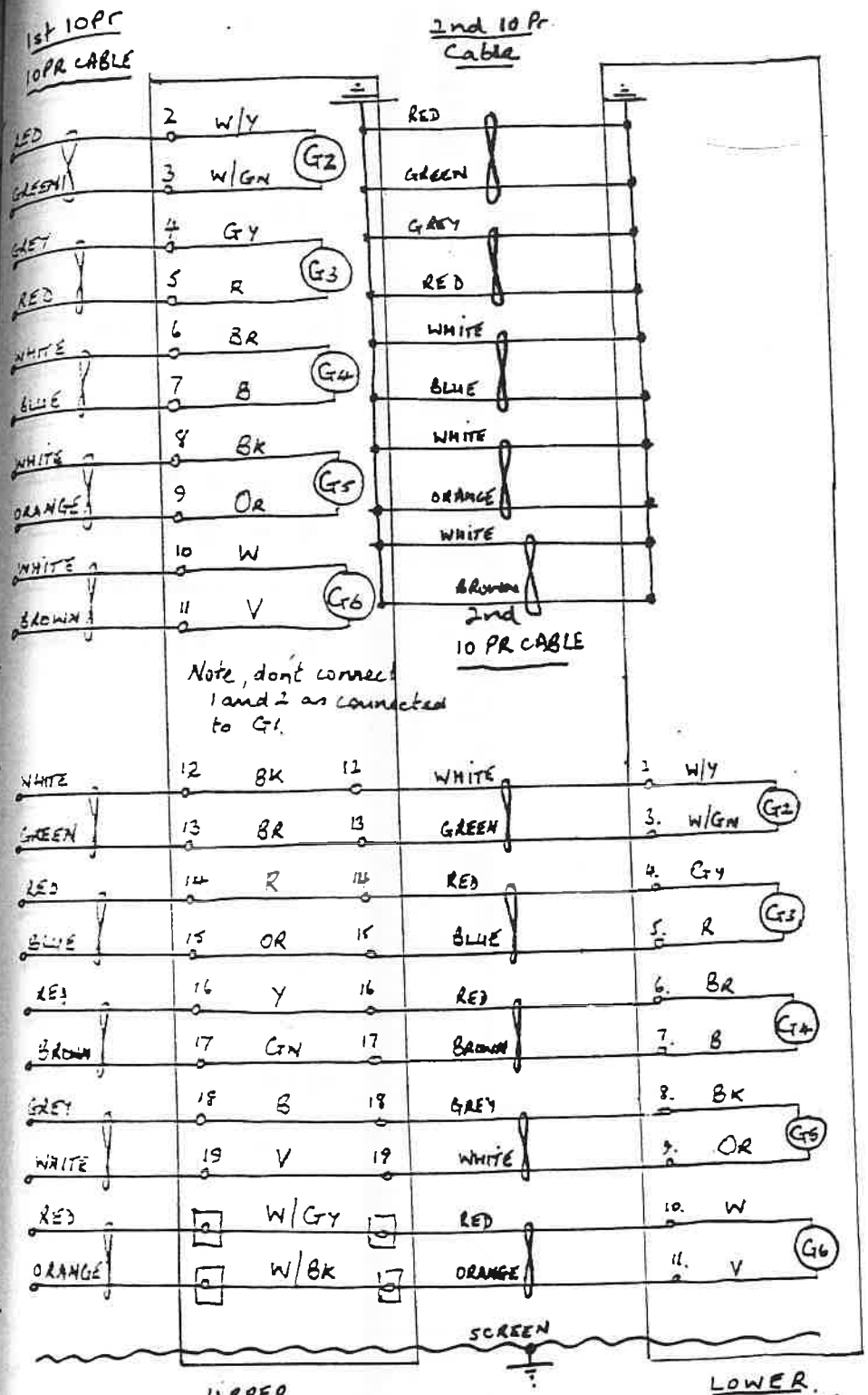

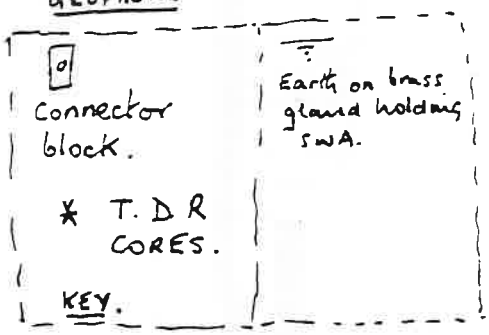

DWG 3
CANTS THORNS
ASFORDBY

DIAGRAM SHOWING THE CONNECTION OF THE UPPER PAIR OF GEOPHONES.

Jr. 22 Feb 9
Final

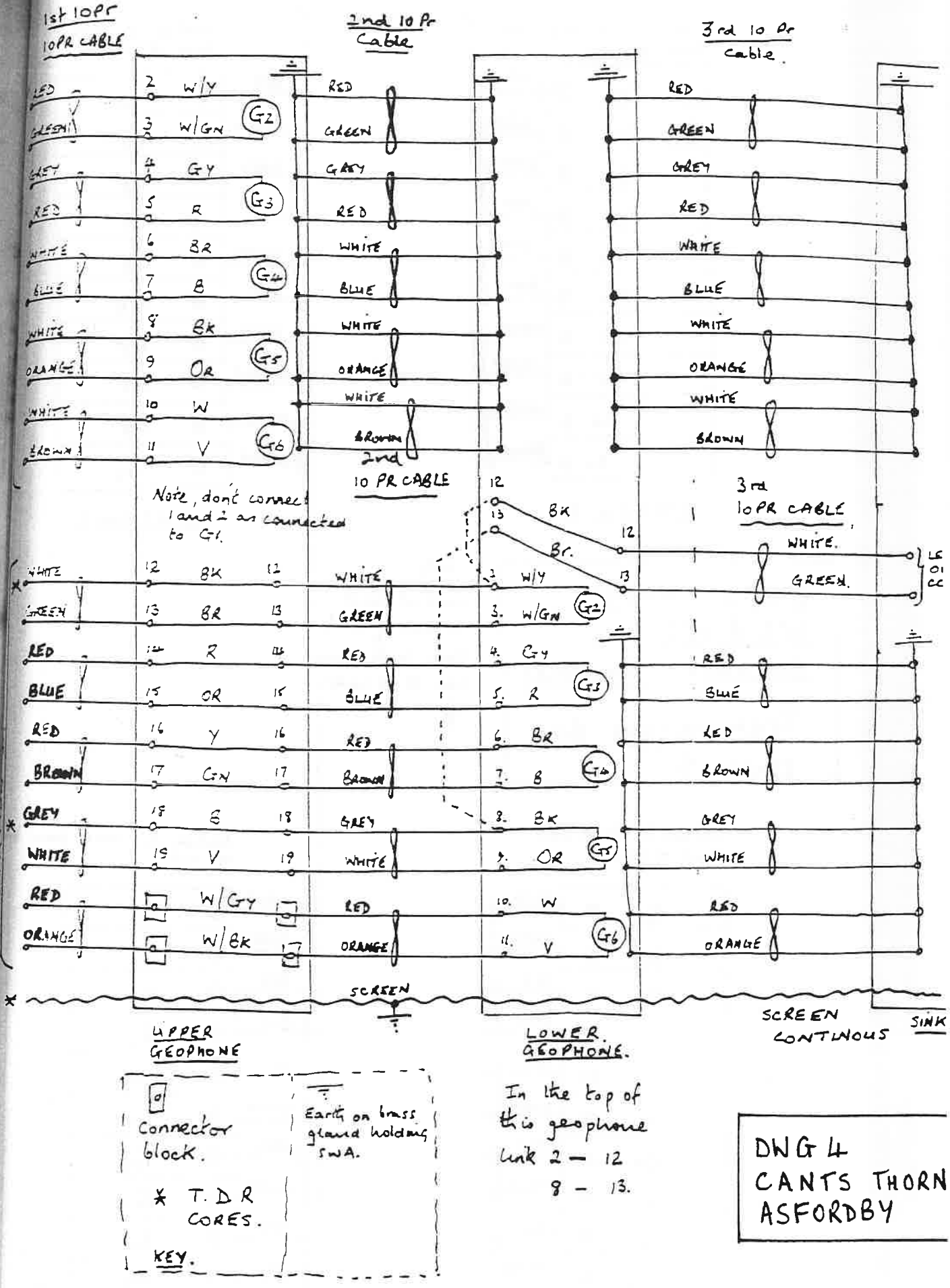

DWG 4
CANTS THORN
ASFORDBY

DIAGRAM SHOWING THE CONNECTION OF THE LOWER PAIR OF GEOPHONES.

22 feb 9

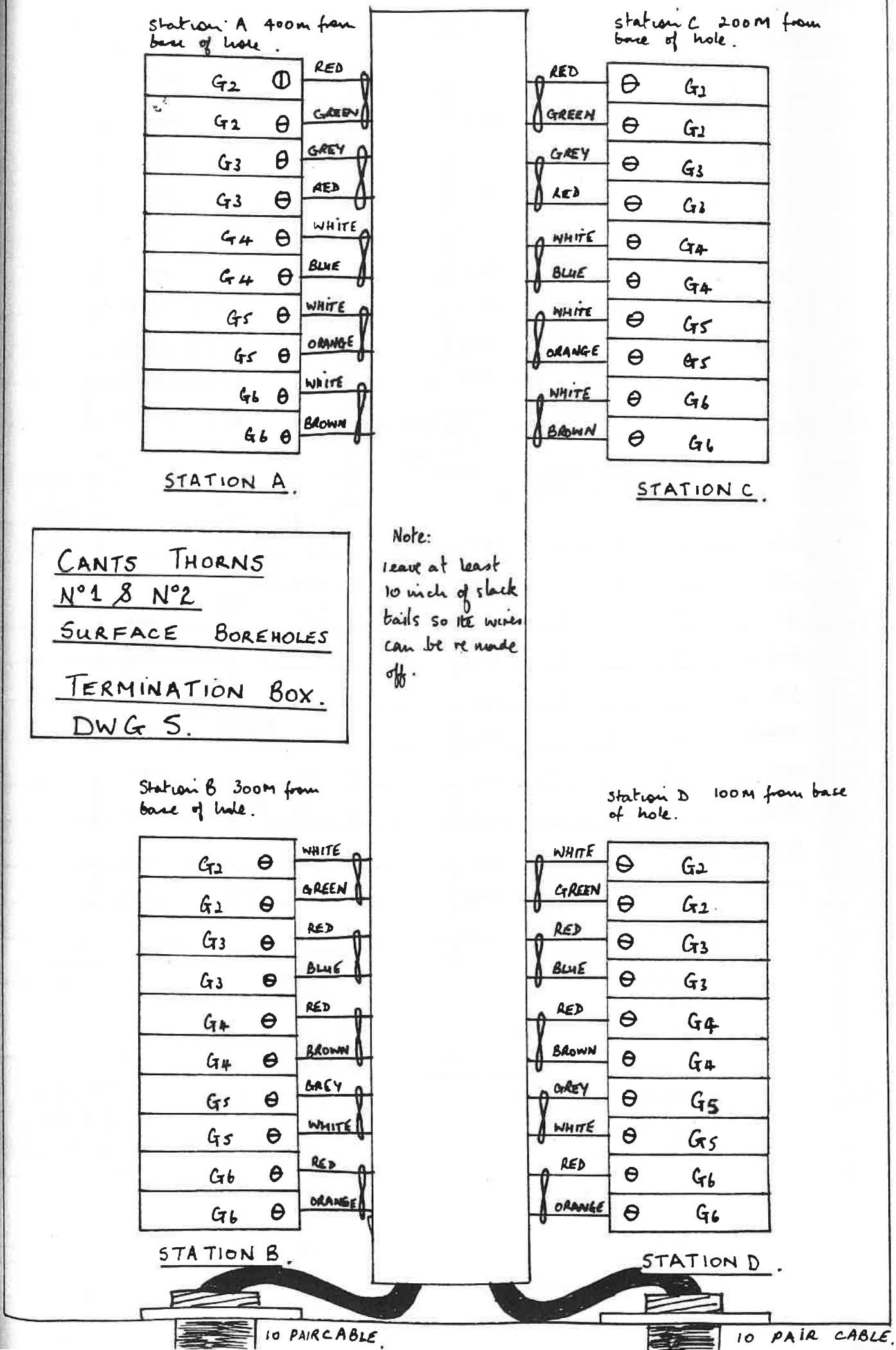
Station A 400m from base of hole.
G2 ⊖ RED
G2 ⊖ GREEN
G3 ⊖ GREY
G3 ⊖ RED
G4 ⊖ WHITE
G4 ⊖ BLUE
G5 ⊖ WHITE
G5 ⊖ ORANGE
G6 ⊖ WHITE
G6 ⊖ BROWN
STATION A.
Station C 200M from base of hole.
RED ⊖ G1
GREEN ⊖ G1
GREY ⊖ G3
RED ⊖ G3
WHITE ⊖ G4
BLUE ⊖ G4
WHITE ⊖ G5
ORANGE ⊖ G5
WHITE ⊖ G6
BROWN ⊖ G6
STATION C.
CANTS THORNS
N°1 & N°2
SURFACE BOREHOLES
TERMINATION BOX.
DWG 5.
Note:
leave at least 10 inch of slack tails so the wires can be re made off.
Station B 300M from base of hole.
G2 ⊖ WHITE
G2 ⊖ GREEN
G3 ⊖ RED
G3 ⊖ BLUE
G4 ⊖ RED
G4 ⊖ BROWN
G5 ⊖ GREY
G5 ⊖ WHITE
G6 ⊖ RED
G6 ⊖ ORANGE
STATION B.
Station D 100M from base of hole.
WHITE ⊖ G2
GREEN ⊖ G2
RED ⊖ G3
BLUE ⊖ G3
RED ⊖ G4
BROWN ⊖ G4
GREY ⊖ G5
WHITE ⊖ G5
RED ⊖ G6
ORANGE ⊖ G6
STATION D.
10 PAIR CABLE.
10 PAIR CABLE.

CABLE LENGTHS SHEET

FROM	TO	L
WINCH	STATION A	230M + TAILS
STATION A	STATION B	99.46 M + 2 TAIL

UPPER GEOPHONE PAIR

.FROM	TO	L.
WINCH	STATION C	400 M + TAILS
STATION C	STATION D	99.46M + 2 TAIL
STATION D	SINKER	93.73M + TAIL

DWG 6
CANTS THORNS
ASFORDBY
FEB/MARCH 95.

John Gregson 23.2.9

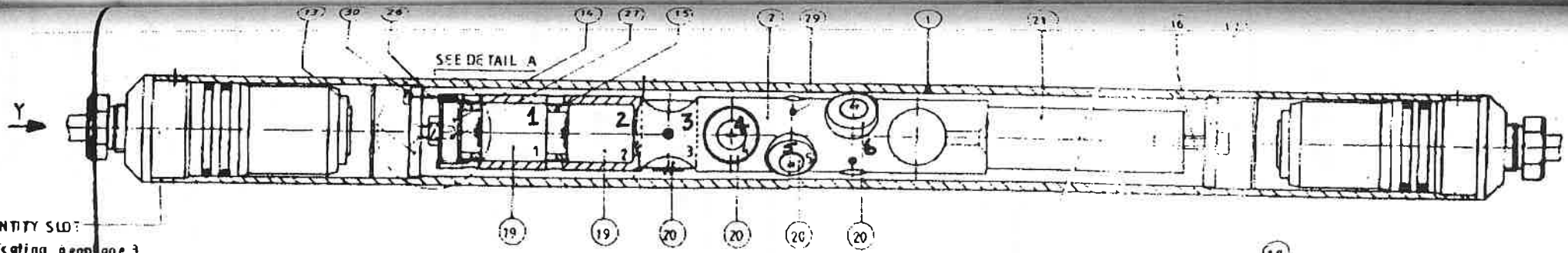

IDENTITY SLOT
indicating geophone 3

SBHT-2 Tool
6 Geophones (total length)
626 mm

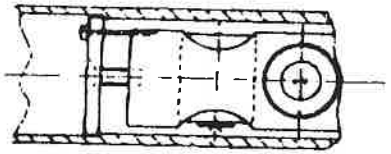

DETAIL A

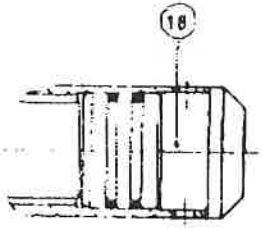

Note.
terminals of G3 are on the same side as the slot.

PCB	Code		
0	G1	V	+ Y
1	G1	V	− GN
2	G2	V	+ Y/W
3	G2	V	− Gn/W
4	G3	N	+ GY
5	G3	N	− R
6	G4	W	+ BR
7	G4	W	− B
8	G5	N-W	+ BK
9	G5	N-W	− OR
10	G6	S-W	+ W
11	G6	S-W	− V
12	Thro'		
13	Thro'		
14	Thro'		
15	Thro'		
16	Thro'		
17.	Thro'		
18.	Thro'		
19.	Thro'		

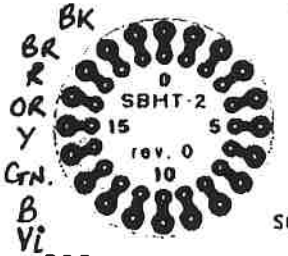

SCALE 2:1

PCB

FOR CONNECTIONS SEE SEPERATE SHEET

VIEW Y

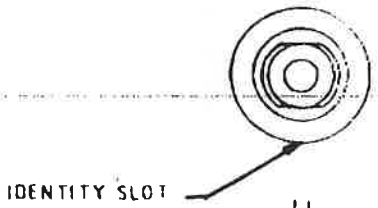

Connect microampere meter plus to positive wire of the geophone
The first movement of the meter will be positive when the unit is moved in the direction of the arrows
(for geophones 1 and 2 see sectional view)

Four extra wires not connected to pcb.

R/BK
R/W
B/W
Gy/W.

SM11 inserts.
These inserts measure 360 Ω with no additional wire.

REMOVE ALL BURRS AND SHARP EDGES

		UNLESS OTHERWISE SPECIFIED ALL DIMENSIONS ±0.1 mm ANGL. ±1°	SBHT-2 SLIMLINE BOREHOLE ASSEMBLY GEOPHONE.
MATERIAL			
ORDER SN 12268		9050	1
SCALE		SHEET 2 OF 2 SHEETS	A3

23/02/95 16:03 WESTERN-SENSOR NL 071 617145 002

ORDER : SN 12268

Number of SBHT-2 tools: 6
Installed geophones
vertical: 1 and 2
horizontal: 3, 4, 5 and 6
(For numbering see drawing 9050, sheet 2)
Gamma detector : Not requiered.
Case : Double ended
Total length : 626 mm

PCB WIRING SBHT-2 ORDER: SN 12268

PCB CODE	GEOPHONE No.	Position	Polarity	INTERNAL WIRE COLOUR
0	1	vertical	+	Yellow
1	1	vertical	-	Green
2	2	vertical	+	Yellow/White
3	2	vertical	-	Green/White
4	3	north	+	Grey
5	3	north	-	Red
6	4	west	+	Brown
7	4	west	-	Blue
8	5	north west	+	Black
9	5	north west	-	Orange
10	6	south west	+	White
11	6	south west	-	Violet
12	Thru connection: 01			'Flat cable': Black
13	Thru connection: 02			'Flat cable': Brown
14	Thru connection: 03			'Flat cable': Red
15	Thru connection: 04			'Flat cable': Orange
16	Thru connection: 05			'Flat cable': Yellow
17	Thru connection: 06			'Flat cable': Green
18	Thru connection: 07			'Flat cable': Blue
19	Thru connection: 08			'Flat cable': Violet

4 extra thru connections, not connected to the PCB's: Red /Black

Red /White

Black/White

Grey /White

Appendix 2

An Overview of Microseismic Monitoring in Mining and Other Application

A2 Overview of Microseismic Monitoring in Mining and Other Applications

This review of developments in the field of Acoustic Emission/Microseismic (AE/MS) monitoring includes work not related to mining, because it is probably in these other spheres of work that the greatest developments have been achieved in terms of equipment and technology. These developments are now being transferred to mining applications and can be used to improve the AE/MS monitoring of mines. Research in AE/MS monitoring is taking place on an international scale, with many countries having made significant contributions to the development of the subject. The areas in which AE/MS monitoring have been used include geothermal power, underground storage of natural gas and various wastes (e.g. chemical and nuclear), stability of nuclear power stations, stability of dams, flood control and irrigation. This section omits United Kingdom coal-mine monitoring which is discussed separately in the body of the report because of its particular relevance to this project.

A review of the beginning of the use of AE/MS techniques is given by Obert (1977) and Hardy (1977) in the proceedings of the First Conference on Acoustic Emission/Microseismic Activity in Geological Structures and Materials (Hardy & Leighton 1977). The material in this review will be presented on a country-by-country basis in alphabetic order.

A2.1 Australia

Major developments have taken place in Australia, with microseismic monitoring systems being deployed in both hard-rock and deep coal mines.

A2.1.1 Hard-Rock Mining Applications

Godson, Bridges and McKavanagh (1980) report the initial operation of a 32-channel automated system for the on-line detection and location of rock noise, which was used to monitor the Mount Isa Lead-Zinc and copper mine, although a great many problems were experienced in the commissioning of the system.

A2.2 Coal Mining Applications

McKavanagh and Enever (1980) were recording signals in the 100 Hz to 5 kHz range prior to outbursts of coal and methane in West Cliff Colliery, New South Wales. They report a reduction in the rate of microseismic activity in the 10 minute period immediately prior to the outbursts. Grezl, Leung and Ahmed (1984) built on this work and deployed underground systems at both Leichardt and Metropolitan collieries with accelerometers in the coal rib and a system bandwidth of 2 Hz to 1.5 kHz. They clearly

detected in-seam channel waves which gave characteristic coal dispersion curves. Enhanced background seismicity occurred for 17 days before a 25 tonne outburst again with a reported reduction in activity several shifts before the outburst.

A2.3 Canada

A2.3.1 Hard-Rock Mining Applications

The use of sub-audible noises as a prediction of rockburst occurrence was first suggested in 1923 by Hodgson (1958), of the Dominion Observatory, Ottawa, but it was not until 1937 that investigations were conducted by the U.S. Bureau of Mines, in shallow workings where rockbursts had occurred. In October 1941 Obert used equipment, developed by the U.S. Bureau of Mines, at Sudbury and Kirkland Lake (Lakeshore Mine) (Pakalnis 1984), with up to 100 geophones being used at any one time by the end of 1943.

Further work continued in Canada under the auspices of INCO at Sudbury with equipment having a frequency response from 300 to 3000 Hz. Although many events were detected in this bandwidth, no reliable precursors were identified, with the possible exception of an upward shift in frequency of the recorded events prior to rockbursts.

A portable listening device was built in 1942 and rock–noise was monitored sequentially for three minutes at a time at 160 stations at all levels of the mine taking three days to cover the entire mine. Notwithstanding this early work, acoustic emission monitoring research resumed in Canada in 1979, after a gap of some 37 years since the pioneering work of Obert and the results are reported by Bourbonnais (1984). A research system based on the USBM's RBM was deployed at East Malarctic Mine, NW Quebec, which recorded some 1600 microseismic events and two large rockbursts. There was an observable pattern of a build–up in acoustic emission followed by a quiescent period immediately before the rock–burst. Only limited data were, however, obtained.

Microseismic activity associated with pillar bursting has been reported from Campbell Red Lake Mine, Ontario, (Neumann and Makutch 1989) and their system is based around an Electrolab MP-250 48-channel microseismic system with 32 geophones and 16 accelerometers with processing carried out on a PDP11-23 system.

A 16-channel MP-250 microseismic system, designed and constructed by Electro–Lab, has been used to monitor the deepest openings between the 6600 to 7000 feet levels at Creighton Mine, Ontario by INCO Ltd. Although this had location capabilities, it could not provide premonitory warning of rockbursts and additional activity at higher levels justified an expansion of the system to 48-channels, (Oliver and McDonald, 1989).

Talebi *et. al.*. (1990) describes a two PC based monitoring system produced by Queen's University, Ontario, for the Strathcona mine in the Sudbury Basin, Ontario. The system was designed to monitor the microseismicity associated with stope development in the nickel mine. Importantly the monitoring system recorded whole waveform signals from five clusters of three component sensors, having a frequency response of 50Hz – 5kHz, installed around the stope, and 16 single component sensors of the existing automatic multichannel monitoring system (Electrolab MP250).

The Queen's University acquisition system was capable of digitising up to 32 channels of data using two personal computers. The acquisition system utilised two computers configured with 1 MHz 16 channel 12 bit A/D boards, developed by RC Electronics. Digitisation was performed at a sampling rate of 20 kHz. Events were recorded using a trigger logic unit developed by Queen's University, which sent a TTL pulse to the computers, based on user selected criteria, for example signal level, duration, number and designation of channels.

At the Denison Mine near Elliott Lake, Ontario, a portable high frequency data acquisition system was used, monitoring in the range 50 – 400 kHz. The sensor used in the monitoring trials was a piezo–electric transducer. The signal was digitised by a microcomputer using a digitising board with a 12 bit A/D converter and a sampling rate of one million samples per second, to avoid aliasing the high frequency components (Calder *et. al.*. 1990). Computer processing of the incoming data was controlled by a priority based multi–tasking program. Signal processing involved signal conditioning in the time domain and frequency calculations in the frequency domain. The precursor analysis of the captured microseismic events was based on features extracted from the wave form and the frequency content. Pattern recognition techniques were used to characterise the different waveforms. Unfortunately, the range of detection of the system was no more than 5m. As the range of detection was so low, areas in need of such high frequency monitoring need to be determined. This could be provided by numerical modelling and/or event location systems and/or the experience of mining personnel. The analysis of the peak waveform magnitude and the centre frequency did not reveal any significant precursory behaviour prior to a rockburst.

Hedley *et. al.*. (1989) discuss the source mechanisms and stress drops associated with a series of fault–slip rockbursts (largest with magnitude 2.8) at Falconbridge Mine using an 8-channel underground system. At both the Denison and Quirke Mines, in Ontario, triaxial velocity gauges, with a frequency response of 2-250 Hz were used, installed in the floor of drifts and stopes (Hedley 1990). This is complemented by five geophone sets at the surface, with a frequency response of 8-300 Hz. These were grouted in shallow boreholes, of the order 4m below the surface and on rock outcrops.

Within the Sudbury area a local, three station, digital seismic network has been set up. It monitors the mines of two major mining companies, those of INCO Ltd and Falconbridge Ltd. The system uses short period Teledyne–Geotech S13 vertical component seismometers, including a 60Hz package, in surface vaults. At the outstations the data is digitised producing 16 bit data samples from a 12 bit A/D converter with a minimum detectable ground motion of 2mm/sec. The dynamic range of the system is 126 dB with a frequency range of 1–16Hz. The outstations are linked to a central processing centre by dedicated telephone lines. The incoming signals are connected to a PDP 11/73 computer, which monitors continuous data from the outstations, and saves any triggered events using a STA/LTA trigger algorithm. The data is transferred to Ottawa where data processing and analysis is performed on a MicroVAX II (Plouffe *et. al.*. 1990).

Rio Algom's Quirke Mine, near Elliott Lake, Ontario, is monitored by a microseismic surface network. The sensors are located in shallow boreholes and originally consisted of 5 triaxial accelerometers. These were, however, subsequently replaced by geophones (Semadeni *et. al.*. 1990). Signal analyses are performed, both in the time and frequency domains. Event locations are determined by an Electrolab MP250 source location system operated by the Quirke Mine. The vertical axes of the five surface sensors are connected to the MP250 to augment the underground array. Parameters such as first motion, P- and S–wave arrival times, peak particle velocity, seismic energy and attenuation are determined. Some of the seismic source parameters determined are corner frequency, frequency plateau, seismic moment, source radius and stress drops.

The other major use of microseismic monitoring in the Canada has been in Potash Mines in Saskatchewan, where seismic events of magnitude 3.6 have been recorded. A permanent underground monitoring system has been installed at the Cory Mine of PCS mining (Vance & Mottahead 1989). This was again an Electrolab MP-250P system with 16 geophones linked to an IBM–PC.

In Saskatchewan, local seismic networks are operated to monitor potash mines. A local seismometer array, consisting of six vertical component geophones were established on the surface about 1km above the mining horizon of the Cory Mine, (Prugger and Gendzwill 1988). Signals were recorded digitally on cassette tape and played back on an Apple II-plus microcomputer. Source location is performed by a simplex algorithm.

Prugger & Gendzwill (1993) conclude that events recorded at the Cominco Fertilizers mine at Vanscoy are best modelled by a single vertical force directed either up or down. The suggested mode of failure is one of roof-slab delamination and/or floor heave in mined out rooms, and possibly pillar shortening for events that occur over pillars.

A2.3.2 Other Applications

The Queens University Group have also deployed their microseismic network at the Underground Research Laboratory, operated by the Atomic Energy of Canada Limited, which is a potential nuclear waste repository and effectively a mine in granite. An integrated laboratory and field program has investigated source mechanisms, and has been able to characterise field events as approximately 70% shear, 5% tension and the rest mixed mode. The group has developed presentation software for tomographic representation of microseismic activity in three dimensions (Feignier & Young 1992, Young and Maxwell 1992)

A2.4 China

The Peoples Republic of China has more than 1,000,000 men working at risk from outbursts in some 100 mines. Roof failures in hard rock mines are also a major problem; Li (1989) reports the case of the Pangushan Tungsyen Mine in Jiangxi province where **373 stopes collapsed successively over the course of a few days!**. Microseismic monitoring, however, is still in its relative infancy in China. Li (1989) describes two portable, single–channel AE monitoring facilities which have been used in both hard–rock and coal mines the first with a frequency range of 20-20Khz and a sensitivity of 90mV/g. and the second, hand–held unit with a bandwidth of 800-1600 Hz and described results showing some increase in AE rates prior to rock failure, but with other failures occurring without any apparent warning. He does, however, report an anomalous increase in emitted energy some two days prior to a coal burst at the Mentougu Mine. Apparently, similar systems are presently employed in a number of mines in China. A more comprehensive joint study of the relationship between acoustic emission and gas emission during drilling was carried out co–operatively between the Fushun Coal Research Institute and Hokkaido University at Yangquan First Coal Mine using accelerometers deployed in boreholes with monitoring being conducted on a Dunegan/Endevco 300 AE monitor (Zhang *et. al.*. 1987).

A2.5 Czechoslovakia

Mining induced seismicity in the former Czechoslovakia is experienced in four mining districts. Rockbursts are most severe in the Ostrava-Karvina coal district. The first rockburst was reported in 1917 and the strongest and most disastrous rockburst occurred on April 27, 1983 (Holub *et. al.*. , 1988). Seismic monitoring in mines was started in 1977 and a regional seismic network has been in operation since 1988 (Konecny, 1989).

A2.6 France

A2.6.1 Coal Mining Applications

Dechellette *et. al.*. (1984) and Revolar *et. al.*. (1986) have described the operation of a 4-channel underground system in the Provence coalfield, France, and have established relationships between face advance and energy released per shift. They have attempted to identify the onset of outburst–prone conditions using departures from this relationship, and their results appear to show high negative residuals prior to an assumed rockburst, which they ascribe to the storage of elastic energy prior to release in the rockburst.

During the last ten years two different techniques have been applied to the monitoring of seismic activity associated with mining at Charbonnages de France. Revalor *et. al.*. (1990) have described the phenomena of rockbursts in French coal mines as the catastrophic failure of the coal seam, which they in turn describe as a "coal bump". In such cases the roof remains intact but the floor is noted to heave and there is a low emission of gas accompanying the events.

A first approach is the "seismo–acoustic monitoring" method which has been applied to one longwall face, where, based on the energy release rate, dangerous areas are detected during the mining operations. The meter uses between 4 and 7 vertical component geophones, capable of measuring a particle velocity in the range 0.3 to 20 mm/sec with a frequency range of 10 to 300 Hz. These are located in either the roof or the floor and are moved periodically as the face advances. The signals are transmitted via telephone cables. A band pass filter is applied to the data with a frequency range of 10 to 300 Hz. The data are processed by an on–line computer which digitises the incoming data at 1500 samples/sec. Triggering is performed by the simple function of exceeding a pre–set level on 2 or more channels. The events are recorded both on a photo–sensitive recorder and digitally as event characteristics.

The second technique is that of "seismic monitoring" in which a larger network is used to locate seismic events and to study their focal mechanisms. This network utilises between 8 and 12 geophones both vertical component and tri–axial and having a frequency range of less than 30 Hz, these are located both at the surface and underground. With this system, the transmission method is more sophisticated using FM modulation and transmitting the signal either by radio telemetry or cabling. The signals are band pass filtered in the range 1 to 20 Hz. Triggering is again performed by the signals exceeding a pre–set level on 3 or more channels. Digitisation is performed automatically with a sampling rate of 50 to 100 Hz. The whole wave form data are recorded on a continuous chart recorder and also stored on magnetic tape or hard disk.

A2.6.2 Other Applications

Sarda (1984) used passive seismic monitoring to determine the orientation of a hydraulic fracture, that was aimed at connecting two wells in a coal

gasification project. Water was injected into a sandstone/coal sequence in open hole conditions using a packer assembly, at a depth of 1050 metres. Three TABS (Tri-axial borehole sonde) tools, containing accelerometers, were situated in an observation well about 100 metres away from the treatment well. The TABS tools were anchored at separate points in open hole conditions at reservoir depths. The system detected over 600 events, in the frequency range 1 to 2 kHz, and more than 400 were located. A change in the event clustering was noticed after the pump rate was increased. Natural fracturing may have been playing a role in determining pressure and fluid movement directions. The high frequency of the events is associated with the use of accelerometers and possibly the small scale of the fracture.

Talebi *et. al.*. (1989) discusses two hydraulic injection tests for investigating the possibility of extracting heat from deep hot dry rocks (granite). In the first experiment, four three-component accelerometers set in two adjacent boreholes (30 m apart), recorded several tens of events whose locations migrated away from the well bore with increasing injection of the gel. The events had clear P and S wave phases with frequencies between 200 and 5000 Hz. The location of the events suggested a rather limited sub-vertical hydraulic fracture and that the source of the events was along pre-existing fracture planes. In a second experiment, in which water was injected at a depth of 440 m, only a few events were recorded on the 14 three-component geophone stations, which were situated at the surface and below ground. These events also had P and S wave phases, in the frequency range 50 to 1000 Hz, and source analysis gave similar source mechanisms - shear along pre-existing fracture planes.

Deflandre *et. al.* (1995) report the use of microseismic monitoring and repeated VSP 's for monitoring the stability of an underground gas storage reservoir at Germigny-sur-Coulumbs in the Paris Basin

A2.7 Germany

Will (1980) describes a 12-channel underground system which recorded 100,000 events in a four month period in a mine on the Ruhr, while Will (1984) also reports the development of a portable, intrinsically safe, instrument for monitoring the seismic seam–reaction during destressing drilling which was developed jointly by WBK (Bochum) and Lennartz.

WBK and Lennartz have now developed a fully digital PCM underground system which can multiplex 24 channels deployed as 6 x 4 geophone packages and then telemeter these to the surface for on–line analysis on a MicroVAX II. The DMT system is designed to be intrinsically safe for use in coal mines (Will & Rakers 1990).

A2.8 India

Major rockbursts have occurred in the Kolar Gold Mines, South India, since the beginning of the century and both surface and underground seismic networks have been used to monitor them. The underground network has a bandwidth of 0 to 5kHz and covers an area of 100 x 100 metres (Subbaramu *et. al.*., 1985) with 7 Geospace sensors and the surface system covers an area of 6 Km by 3 Km again with 7 Geospace sensors.

A2.9 Japan

A2.9.1 Coal Mining Applications

Outbursts have been a major problem in Japan, with an explosion occurring at the Oyubarhi Mine, Hokkaido in 1981, with 93 lives lost. A two channel underground system was installed in Akabirqa and Ohyubari mines and seismo–acoustic activity monitored during advance boring for methane drainage (Nakajima *et. al.*. 1984). Isobe (1974), Isobe *et. al.*. (1976, 1977, 1979, 1980, 1984) report a combined surface and underground system employed at the Sunagawa Coal Mine near Bibai, where three rockbursts occurred in 1968, which were detected by a seismic observatory more than 100 Km away, with Richter magnitudes of 1.9 to 2.8. They have carried out comprehensive studies of the energy releases associated with hydraulic coal mining of steeply inclined coal seams. They also claim an accuracy in their hypocentral locations of 7-10 metres.

Sato *et. al.*. (1988) describe a system which has detected more than 20,000 events with local magnitude greater than -2.5, occurring during the extraction of two longwall seams at the Horonai Mine, Hokkaido. Mining at the Horonai Mine is conducted at depths between 985 and 1125m and monitoring has been conducted since 1980, using an underground array of accelerometers or geophones, or by using a near surface array of geophones (Sato and Fujii, 1990). The mine wide seismic array developed consisted of 10 stations, of which 6 to 8 stations are placed on the surface and the remainder placed in underground roadways near the mining panels.

Geophones with built–in pre–amplifiers were used. Detected seismic signals were digitised at the recording station, whilst signals detected by surface stations were immediately digitised at the site with the digital signals being transmitted to a recording station. Any seismic signal, exceeding a preset level, was recorded automatically by a triggering method on a standard magnetic tape. The seismic events are located using an interactive least squares method. Gutenberg Frequency–magnitude relationships were established giving b–values of 1.01.

At the Miike Coal Mine, which is an undersea coal mine, pure coalbursts have occurred with no associated gas, while working below 550m with an immediate sandstone roof. A 12 channel source location system was installed to monitor the microseismicity. It consisted of 12 seismometers situated in roadways

surrounding the district being monitored, amplifier, filters, A/D converters and a mini–computer (Kaneko *et. al.*., 1990).

A2.9.2 Other Applications

Niitsuma *et. al.*. (1989) report on the acoustic emissions measured by triaxial downhole equipment following build up tests of geothermal wells in the Kakkonda field. The geothermal fluid circulation is in fractured and highly permeable Neogene sedimentary rocks. Following the shutdown operations of production wells at the Takinoue geothermal power plant, more than 150 acoustic emission events were located with a triaxial sonde in a shallow borehole (15 m deep). The events were located using the hodogram technique, at depths of between 400 and 1300 metres below the ground surface. Niitsuma *et. al.*. (1989) concluded that the AE sources were concentrated near fault planes, considered to be a result of the extension of the cracks during in-service operation and previous build-up tests. The AE analysis indicated that the crack had propagated along faults and the pre-existing fracture zones.

Sato *et. al.*. (1988) described the analysis of events displaying shear wave splitting to estimate the azimuthal orientation of the natural fractures. Fracture density was calculated from delays between the shear-wave polarisations.

A2.10 Poland

Seismicity induced by underground mining is a well-known long-studied phenomenon in Poland, observed in the Upper Silesia coal basin (e.g. Gibowicz, 1984) and in the Lower Silesia coal basin (e.g. Gibowicz & Cichowicz, 1986) where mining has been carried out for many decades, and in the Lubin copper district in Lower Silesia (e.g. Gibowicz, 1985) where mining was started only just over 20 years ago. In both the Upper Silesia basin and the Lubin district, the rockbursts are severe. Several underground seismic networks have been operated by the mining industry in Upper Silesia since the mid-1960s and in the Lubin district since the mid-1970s. Several thousand mine tremors are recorded annually, but only about a dozen of them reach a local magnitude greater than 3. Very seldom does an excessively large tremor, with magnitude exceeding 4, occur (Gibowicz, 1984).

A2.11 South Africa

Detailed AE/MS studies in South African mines began in the early 1960s (Cook, 1963). Since that time, there has been a continuing and comprehensive development of AE/MS techniques and instrumentation. The majority of studies have been specifically related to the rock burst problems encountered in the deep gold mining operations. The proceedings of the first International Symposium on Rockbursts and Seismicity in Mines, (Gay & Wainwright, 1984), held in

Johannesburg in 1982, gives an excellent review of AE/MS studies in South Africa to that date. Spottiswoode (1987) gives a review continuing on from that symposium until 1987. The proceedings of the second and third symposiums on Rockbursts and Seismicity in Mines (Fairhurst, 1990 and Young, 1993) include papers which review further developments in South Africa. Earlier work in South Africa concentrated on the development of instrumentation for the location of microseismic events. In recent years the emphasis has changed, and more studies are now under way investigating matters such as source mechanisms, mine design, rock mass modelling and rockburst prediction and control.

Recently two systems have been developed, and are being marketed commercially, in order to obtain more information about AE/MS events and stress around mines. These systems are :

(1) The Portable Seismic System (PSS) developed by the Chamber of Mines Research Organisation (COMRO), and

(2) The Integrated Seismic System (ISS) developed by ISS international.

The PSS is described by Pattrick *et. al.*. (1990) and has been developed for shaft-wide monitoring and smaller applications to assist in reducing the rockburst hazard. The system allows intensive coverage from 10 metre scale to 10 km scale. The system has been developed to work in conditions of high temperature (up to 40°C) and high humidity because of the harsh conditions encountered in deep gold mines. It is designed for monitoring and analyzing of seismic events down to magnitude M=-2. The data acquisition system comprises a network of transducers and a central data acquisition unit (DAU). This equipment is installed underground in the vicinity of the site to be monitored. The data processing system consists of a personal computer driven by custom software, installed at the surface.

Several types of transducers may be used, including geophones, accelerometers, extensometers and strain gauges. Transducer stations amplify the transducer signals and transmit them via up to 5 km of cable to the DAU. Each transducer station can serve three channels so that triaxial transducers can be used. Plug–in interface cards allow the stations to cater for the variety of transducer types mentioned above. The transducer stations use FM telemetry to transmit signals of bandwidth 0-10 kHz at a dynamic range of about 66 dB, and are powered by local AC mains or by DC supplied remotely via the telephone cable from the DAU.

Signals from up to 16 transducer channels are received, demodulated and digitised by the DAU. The purpose of this unit is to detect and capture seismic events and forward appropriate event information to the PC. The DAU was designed to operate unattended at an underground site within or close to the mining area being studied. It communicates with, and is entirely controlled from, the PC via modems and two pairs of a standard telephone cable. The DAU is based on the Intel 8086 microprocessor chip. The unit digitises transducer signals continuously to 12 bits of resolution on 16 channels at rates of up to 16 kSample/sec/channel.The DAU uses dual port memory of 512 kByte, which

allows event sampling and capture by the data acquisition sub–system to occur simultaneous with, and independent of, event processing by the 8086. At least six events can be stored in the memory before transfer to the PC. Communication between the DAU and PC occurs over a serial data link operating at rates up to 19200 baud. The amount of information about each event that is transmitted to the PC is dependent on the event rate and only when there is a low event rate are the full seismograms transferred.

There are currently several PSS systems operating. At the President Steyn gold mine, in Orange Free State, a PSS system was installed as part of a fault monitoring project. Minney & Naismith (1993) used this system to monitor a pillar. A system has also been installed at Blyvooruitzicht gold mine, in the Carletonville area, by COMRO as part of a pre-conditioning experiment (Stewart & Spottiswoode, 1993).

The ISS is described by Mendecki (1993). The ISS is digital, intelligent and performs online automatic quality controlled seismological processing. An ISS is comprised of transducers, remote stations, a communication system and a central computer. The latter is controlled by an operating system conforming to open systems standards. A remote station may be configured in a standalone mode. Each remote station acquires data from one or more triaxial seismic transducers and a number of non-seismic sensors.

The advantage of a digital system lies primarily in maintaining the integrity of acquired seismological data. With conversion to a digital format as close as possible to the sensors, maximum dynamic range can be ensured. Digital communication between the remote sites and the central computer allows for transmission of waveforms with no amplitude or phase distortion.

The ISS has the largest installed base in terms of mine seismic systems in the world (ISS International, 1993). Installations are primarily in South Africa, on 15 mines, and also in Chile and Canada.

A2.12 United Kingdom

Coal Mining Applications of Microseismic Monitoring in the UK have already been described in Section. Only other application are discussed here.

A2.12.1 Other Applications

A Hot Dry Rock (HDR) geothermal energy extraction system consists of two wells, drilled into naturally heated but relatively impermeable, crustal rock. The wells are connected at depth by a hydraulic fracture system. Cool water pumped down the injection well passes through the fracture system where the surfaces act as heat exchangers. The heated water returns to the surface via the production well. Due to the convenience of a dual well system for observations, the low seismic attenuation of most geothermal reservoirs and the necessity for accurate fracture orientation, such projects provide an excellent opportunity for application of passive microseismic monitoring.

A HDR project was set up in a disused granite quarry at Rosemanowes in Cornwall, jointly financed by the Department of Energy and the EEC, following the 1973 oil crisis. The aim of the project was to see if it would be feasible to drill 6 km down to reach rock containing water at 200°C, hot enough for power generation. Drilling and circulation experiments have been carried out by the Camborne School of Mines combined with the passive seismic monitoring of injection phases to map stimulated regions (Batchelor *et. al..*, 1983 a/b, Pine & Batchelor, 1984, Baria *et. al.*. 1989).

Following the completion of the first two wells (2000 m deep), a massive hydraulic fracture operation was carried out in November 1982. The experiment was terminated after 120 hours and 18,500m^3 of water had been injected. To monitor the seismicity a string of 5 hydrophones were suspended at 75 metre intervals in the observation/production well, 300 metres from the injection well, and a surface array of vertical axis accelerometers and seismometers grouted in 200 metre deep boreholes up to 2 km away. In addition a network of seismometers operated by the British Geological survey was also incorporated into the system. A computerised recording and processing system allowed on-line analysis and event location from this 3D sensor network.

Some 30,000 events were detected (Batchelor *et. al..*, 1983) of which 15% were good enough to be located accurately. The locations showed a progressive growth away from the injection zone, with occasional infilling of previously quiet areas within the cloud of located events. Most of the events were dominated by shear wave coda. The sequence of events showed a definite progression away from the injection well, and unexpectedly downwards to a depth of over 3.5 km. Pine & Batchelor (1984) explained that the downward migration of shear events was due to the high ratio of horizontal stress gradients, the rock joint orientation and the shear strength of the rock. At treatment depths the shear stress gradient was less than the hydrostatic gradient causing downward growth by shear dislocation.

Baria *et. al.*. (1987) describe other events which were not caused by shear dislocation at joints, i.e. they did not show clear P and S wave arrivals. They classified these events into three groups :

(1) long period events - possibly related to tensional extension of a crack due to an increase in fluid pressure in the crack, or related to the transport of fluid from one crack to another.

(2) high frequency events (over 3 kHz) - possibly related to the pressure front moving ahead of the shearing activity, causing some asperities to be crushed as stress adjustments take place.

(3) tube waves - interpreted as being possibly generated by the rapid expulsion of water in the well from a collapsing joint.

A2.13 United States

A2.13.1 Hard Rock Mining Applications

The first rockburst to have occurred in the United States, in a metal mine, is believed to have been in 1904 in the Atlantic Mine in the Copper district of Michigan. At the present time the only area where bursting is a problem is the Coeur d'Alene metal mining district of northern Idaho.

The earliest research on rock bursting conducted by the United States Bureau of Mines (USBM) began in the late 1930's. The microseismic technique was first mentioned as a way of studying rockbursts in the Coeur d'Alene district in 1941 (Bolstad, 1990). It was not until the mid 1960's, after methods for locating the source of seismic activity became available, that microseismic techniques were applied.

Several types of microseismic systems have been developed to monitor rockbursts. The mine wide systems have generally used between 20 to 30 single axis geophones to triangulate the source and triaxial sensors to determine magnitudes.

The Denver Research Centre has used the approach for almost 20 years at the Galena Mine and is now expanding and re–designing its single stope microseismic systems into a mine wide network. The present system routinely monitors one or two stopes, utilising 16 geophones per stope, and has been updated to improve the data quality and minimise data loss. A new modular system has been designed, which uses a 32 channel remote data collection unit for each stope. Of the 32 channels, 16 are set to a low gain and the remaining 16 to a high gain to extend the dynamic range of the system. Each stope module is fed to an underground instrument room where each remote unit has an associated processing computer. Data are then transmitted to the surface through a fibre optic cable. A vertical single channel, short period seismograph is located on the surface and the digitised data can be incorporated into the analysis.

Blake and Leighton (1970) of the USBM obtained much higher frequency information from hard–rock mines in Idaho (Galena Mine, Wallace, Idaho) using accelerometers cemented in underground boreholes with cable transmission to a central recording facility (7-track analogue tape recorder) and they carried out early work on the location of rock noises (Leighton and Blake, 1970).

Acoustic emission monitoring was becoming a widely used tool for mine stability studies and Langstaff (1977) describes a 24-channel minicomputer based system employed at the Star Mine, part of the Coeur d'Alene mining district in Shoshone County, Idaho, at that time the deepest Lead–Zinc mine in North America, with associated serious burst problems. The results were rather problematical, with occasional seismic pre–cursors to bursts, bursts without precursors and precursors without subsequent bursts. Later work reported by Blake (1984), from the Star mine, was similarly equivocal with only 30% of bursts having clear precursors and some very large bursts (Richter magnitude 2.6) appearing to have no obvious associated precursors.

In contrast to these rather disappointing results, Gibbons (1980) has reported small, mid–range frequency, events at about 30 Hz from White Pine copper mine, Michigan and quotes:
"These signals are small in amplitude but consistent in form and frequency content. The mid–frequency events appear prior to less than half of the total falls observed. However, whenever they appeared, a fall followed soon afterwards. In times of quiet, or immediately after a fall, these mid–range signals are virtually non–existent. Their source mechanism probably is either the coalescing of microfractures into larger "microfractures" or layer separations independent of the microfracturing ... "

This study showed that very low frequency signals (25-35 Hz) can be seen just prior to falls of rock in mines. The link between their occurrence and falls seems sound.

A2.13.2 Coal Mining Applications

Leighton and Steblay (1977) describe the work which was being carried out by the USBM in deep coal mines in Western Colorado where coal 'bounces' or outbursts were a major hazard. Geophones with a bandwidth from 15 to 250 Hz were used to detect the events which were discriminated and analysed on the Rock Burst Monitor (RBM). Measurements in the ultra–sonic range were made using the 36-44 KHz band to detect the high frequency signals associated with roof falls, although this was only effective over short distances of about 70 feet because of the rapid attenuation suffered at these high frequencies.

Several microseismic monitoring programmes have also been conducted over the last 20 years in the coal mines of the Eastern Wasatch Plateau, Utah, (Wong *et. al.*. 1990). In 1984 a three dimensional, high resolution network of analogue and digital seismographs was operated in the vicinity of two coal mines beneath Gentry Mountains.

Testing of a prototype high frequency AE/MS monitoring system has been conducted in a number of coal mines and provided an early warning for 20 out of 23 ground failures, with pre–cursor times in the range of 5 to 92 minutes (Hardy & Mowrey, 1976). The system was developed as a Roof Fall Warning System under a USBM Contract, and the commercial development of the system has been undertaken as a one channel high frequency AE/MS monitoring system and has been manufactured by Integrated Sciences. The system is battery operated, self contained, portable and intrinsically safe. This type of system has met with considerable success in coal mines and also Canadian Potash mines.

Probably the highest frequencies used in acoustic emission monitoring were those reported by Leighton (1984a) who used events in the range 40kHz to 110kHz to perform near source monitoring for outbursts at the Coal Basin site with some reasonable results using energy/event ratios rather than straight event counts. Precursors were demonstrated to be present some 15 minutes before impending outbursts with the obvious limitation that the extremely high frequencies used imply severe attenuation over distances as short as 25 metres.

Leighton (1984b) reported the preliminary results from the testing of an automated real–time coal mine bump monitor being developed by the USBM, Denver. A commercial implementation of this was developed as the McPhar Rock Monitor and an assessment of this was carried out by Ersavci (1989) who carried out tests on a long–wall panel in the Kitt #1 Mine, Phillipi, West Virginia which produces metallurgical grade coal (1 Mtonnes per year). Immediate problems with electrical interference were noted which were improved by improved shielding and found that transducer coupling was extremely important at these high frequencies. Notwithstanding these problems he considered that there was some potential for the use of this type of equipment for the detection of roof falls but that much further work was required to obtain consistent results.

Wong (1984, 1985) describes the use of a 16-24 channel high gain, short–period (1Hz) microseismic network in the Paradox basin to monitor seismicity associated with coal mining beneath the Book Cliffs, where events as large as 4.5 magnitude have occurred, and also with subsidence from a Potash Mine. He detected activity ascribed to collapses within the coal mine, triggered earthquakes on pre–existing thrusts beneath the Colorado Plateau and also low–level seismicity associated with the subsidence due to a Potash solution Mine. This mine was subsequently monitored in detail by a 9-station digital, high gain short period network and two types of event were recorded. Firstly, tectonic events like earthquake were experienced and secondly, unusual, harmonic, surface–wave–like events.

A2.13.3 Other Applications

During 1961, a deep injection well was drilled by the United States Army Corps of Engineers to a depth of 12,000 feet (3568 m) into Precambrian bedrock below the Rocky Mountains Arsenal. Contaminated water was injected at the base of the well into a fractured reservoir, over various periods between 1962 and 1966. Soon after injection began, earthquakes were detected in the vicinity of the RMA and recorded on two surface seismometers, one at a station operated by Colorado School of Mines, the other at Regis College, Denver. The earthquakes subsequently became known as the "Denver Earthquakes". Evans (1966) showed convincingly that the fluid injection was linked to the earthquakes. Seismicity did not cease once the well was shut-in, in February of 1966. Between 1966 and 1968 additional seismic recording networks were installed in the area, by the USGS and the Colorado School of Mines (Poollen & Hoover, 1969, Hsieh & Bredehoeft, 1981). Over 100 earthquakes have been felt at the surface, the largest having a magnitude of 5.3. Despite the cessation of fluid injection in 1966, resulting in a rapid reduction of pressure near the well, the pressure front continued to advance to greater distances from the well.

Rangely, Colorado, was the site of a detailed experiment by the USGS on the relationship between fluid pressure, principle earth stresses and the creation of earthquakes (Raleigh *et. al.*., 1976). Water has been injected into the reservoir

rock (the Weber sandstone) for secondary recovery of oil since 1957. An array of seismographs had recorded small earthquakes from the vicinity of the field since its installation in 1962. In 1967 a small array was installed and recorded 40 earthquakes in a 10 day period. Earthquakes above M_L=0.5 were studied, the largest recorded was M_L=3.1. The earthquakes occurred within the oilfield in two areas where fluid pressures due to water flooding was high. Further work installed 14 short period vertical seismometers and it was found that the earthquakes were located on a small fault in the Weber sandstone.

The first known application of a seismic technique to map a hydraulic fracture was by the Health Physics Division of the Oak Ridge National Laboratory for the subsurface disposal of radioactive waste. They wanted to create a horizontal fracture in a thick shale formation found at a depth of 150 to 300 metres (McClain, 1969). Initially they planned to use drilling to locate a sheet of radioactively tagged grout to define the extent of the fracture. Later, due in part to the expense of drilling, they decided to use short period geophones mounted on the surface to record the seismicity (McClain, 1971). Many seismic events were recorded but only 11 events were unequivocally related to the injection. Results of the fracture mapping test located these emissions in a horizontal plane and they concluded that the fractures had initiated and propagated horizontally or radially in a plane perpendicular to the wellbore axis.

The HDR concept, described earlier, originated at the Los Alamos National Laboratory in 1970. Following a desk study, a site was chosen and an exploratory borehole (GT-1) was drilled in 1972 into part of the Valdes Caldera, New Mexico. It reached a depth of 785 m and penetrated 143 m into the Precambrian granite. The bottom hole temperature was 100.4°C. A second exploratory well (GT-2) was drilled at Fenton Hill, about 2.5 km south of GT-1, in 1972. It reached a depth of 2929 m and had a bottom hole temperature of 197°C. Following hydrofracture and permeability tests, a second well (EE-1) was directionally drilled at Fenton Hill, in 1975, to a depth of 3064 m where a temperature of 205°C was recorded. It was planned not to intersect the fracture system of GT-2. Another hydraulic fracture from EE-1 successfully joined the two wells allowing initial tests to be carried out (Geothermal News and Views, 1982).

Los Alamos National Laboratory have monitored microearthquakes associated with two massive injections of water, 635 m^3 over 6 hours and 771 m^3 over 5 hours, into the granite via EE-1 (Albright & Pearson, 1980, Pearson, 1981, Albright & Pearson, 1982). The untreated water was injected a depth of 2930 m into an existing fracture that connected wells EE-1 and GT-2. During both injections they used a three component geophone tool with 10 Hz geophones locked in the shut-in well at a depth of 2695 m, it recorded during and after each injection episode. During the first injection the event rate increased shortly after the injection of 32 m^3 of water, reaching a fairly constant level. The second injection was relatively aseismic until 506 m^3 of water had been injected, after which the event rate increased rapidly to a higher constant level. They measured seismic events with local magnitudes of between -2 and -6, impulsive onsets and clear compressional and shear wave phases. The large S to P wave amplitude ratio

(11) of the signals was an indication of a shear failure source mechanism, probably on pre-existing planes of weakness in the rock, rather than tensile failures associated with the hydraulic fracture extension (tensile events tend to generate P and S phases with roughly equal amplitudes).

Source parameters were estimated from the seismic spectra of the signals. The sources had a diameter of approximately 3.5 m, reducing steadily throughout the experiment to 2 m, a seismic moment of $6*10^{13}$ dyne-cm increasing to $15*10^{13}$ dyne-cm, with a stress drop of 0.5 bars increasing to 1.8 bars. Pearson *et. al.*. (1983) found that seismic velocities measured during cross-well seismic surveys decreased during operation of the HDR geothermal system. They found that the relative P and S wave velocities decreased to a value very close to predicted values for rocks containing a high density of fluid saturated fractures.

Applications of acoustic emission in other types of geological structures have also taken place and in particular we note micro–acoustic studies of a LNG reservoir in Rock Salt (Meister, 1980, Durr & Meister, 1984), gas storage in sandstone in Coalville, Central Utah (Lingle & Francis, 1980) and monitoring of the New Haven gas storage facility, as reported by Hardy (1980), Hardy and Mowrey (1984). In all cases acoustic emission signals were detected and analysed.

A particularly large seismic event of magnitude = 5.1 was detected on February 3 1995 from the Trona mining district of Southwestern Wyoming. This was widely felt and recorded internationally. It is believed that this was caused by a major collapse of the Solvay Trona Mine (Pechmann *et. al.* 1995). A subsequent large event of M_L=4.0 was reported on October 26 1995 from the Cumberland-Benham area of Kentucky and was also thought to be due to a mine collapse (USGS QED Report).

Appendix 3

Microseismic Location techniques

A3 LOCATION OF MICROSEISMIC EVENTS

Many methods can be used for locating microseismic events (eg Riefenberg , Lienert 1996) but two specific methods have been used in this project: SIMPLEX optimisation and BACK-AZIMUTH PROPAGATION and these are discussed at length here.

A 3.1 Hypocentral Location Using the Simplex Method:

Consider a seismic network with known locations overlying a half-space with a constant P-wave velocity, V_p . For a given event with a hypocentral location (x, y, z) and origin time t_0, we can calculate the travel time to the ith station, $T_i(x,y,z)$. The residual time differences between the observed travel-times, t_i and predicted travel times for an arbitrarily chosen *guess* at x,y,z will be

$$\delta t_i = t_i - t_0 - (T_i(x,y,z) - T_0(x,y,z)) \qquad (1)$$

Where t_1 and $T_1(x,y,z)$ are the observed and predicted times of arrival at the station which detects the arrival first. We can then form an error function S to be minimised

$$S = \Sigma_i \delta t_i^2 \qquad (2)$$

This known as the L_2 norm (i.e least squares best-fit). This function is then minimised using the downhill simplex method in multidimensions. A simplex is a geometrical figure consisting in three-dimensions of a tetrahedron enclosing a volume of the space to be searched (in N-dimensions we envisage a N+1 dimensional polyhedron). From an initial starting position the algorithm moves the simplex to points of lower S by a series of moves which fall into four types (Press *et. al.* 1988).

a. A reflection away from the high point
b. A reflection and expansion away from the high point
c. A contraction in one dimension from the high point
d. A contraction in all dimensions towards the low point

The routine decides which of these *amoeboid* strategies is best at any step. Cacech1 and Caceheris(1985) explains the stategy in some detail. In our algorithm the velocity can be included as a parameter to be determined by the optimisation giving a four-dimensional problem and a five vertex simplex. However in practice it was found that it was generally better to fix the value of the velocity from known shots and borehole information than to let it vary. Gendzwill and Prugger (1989) give a description of their experience with a similar simplex based

algorithm with the incorporation of a layered earth which does not affect the simplex optimisation but does increase the calculation times for the predicted travel times. Riefenberg (1989) gives an example of the Simplex method with constant velocity which gives excellent results. The structural complexity of the Asfordby area precludes the use of any simple layered structure, and a simple uniform half space was used with a velocity of 3.2 kms^{-1}. However, we appreciate that the incorporation of an anisotropic velocity function or ray-tracing into the travel time calculations would be helpful in improving hypocentral locations. MATLAB function ***fmins*** was used to perform the simplex optimisation.

A 3.2 Back-Azimuth Propagation :Seismic Event Location Using Polarisation Analysis

We begin by expressing body waves as the propagation of a scalar field $u(t)$ with polarisation $\mathbf{p}$ through a 3-D media. The wave $u(t)$ and the noise $\mathbf{n}(t) = [n_1(t), n_2(t), n_3(t)]^T$ are recorded at a three-component seismic station as $\mathbf{s}(t) = [s_1(t), s_2(t), s_3(t)]^T$. T is the transpose and indices 1 to 3 correspond to Cartesian coordinates oriented in the vertical, east and north directions, respectively. Thus

$$\mathbf{s}(t) = u(t)\mathbf{p} + \mathbf{n}(t) \tag{3}$$

Similar to the polarisation analysis of Flinn (1965) and Vidale (1986), we assume that the wave package $u(t)$ and the noise $\mathbf{n}(t)$ are uncorrelated and that the noise $\mathbf{n}(t)$ has an expectation of zero. With these assumptions the covariance matrix of the signal averaged over a time window ΔT can be expressed as

$$\mathbf{S}(t) = U(t)\mathbf{p}\mathbf{p}^{*} + \mathbf{N}(t) \tag{4}$$

where

$$\mathbf{S}(t) = E\{\mathbf{s}(t)\mathbf{s}^{*}(t)\}, \quad U(t) = E\{u(t)u(t)\}, \quad \text{and} \quad \mathbf{N}(t) = E\{\mathbf{n}(t)\mathbf{n}^{*}(t)\} \tag{5}$$

Since U is proportional to the energy associated to the wave type embedded in the signal, the polarisation state of the wave can be determined by finding $\mathbf{p}$ that maximizes the energy of the desired wave type, constrained by $\mathbf{p}^T\mathbf{p} = 1$. In this case, $\mathbf{p}$ must satisfy the linear equation

$$(\mathbf{S} - \mathbf{N})\,\hat{\mathbf{p}} = \hat{\lambda}\,\hat{\mathbf{p}} \tag{6}$$

But because of the lack of information about the noise $\mathbf{N}$, only the eigenvalues (λ) and eigenvectors ($\mathbf{p}$) of $\mathbf{S}$ can be calculated and are expected to be "close" to $\hat{\lambda}$ and $\hat{\mathbf{p}}$, respectively.

The problem of determining the polarisation can be described as follows. The eigenvectors and eigenvectors of an ellipsoid describing the presumed wave are the difference of two ellipsoids: one measured from the recorded signal and the other due to the noise. Without knowing *a priori* the ellipsoid of the noise, it is not possible to determine the polarisation of the wave embedded in the signal. In general, the eigenvectors of the noise's ellipsoid are not parallel to the signal's ellipsoid, so that the resultant ellipsoid's eigenvectors form a nonlinear combination. Only when the two eigenvectors are parallel is it possible to determine the polarisation of the wave embedded in the signal. One case where the noise would not affect the polarisation of the wave is when the noise is isotropic, because then its ellipsoid is a sphere, in which case one can always choose the eigenvectors parallel to the signal's eigenvectors.

Following Vidale (1986), we convert $\mathbf{s}(t)$ into the analytical signal

$$\tilde{\mathbf{s}}(t) = \mathbf{s}(t) + i\mathcal{H}[\mathbf{s}(t)] \tag{7}$$

where $\mathcal{H}$ represents the Hilbert transform, then

$$\tilde{\mathbf{s}}(t) = \mathbf{p}\tilde{u}(t) + \tilde{\mathbf{n}}(t) \tag{8}$$

The covariance matrix $\mathbf{S} = E\{\tilde{\mathbf{s}}(t)\,\tilde{\mathbf{s}}^{\dagger}(t)\} = U\mathbf{p}\mathbf{p}^{\dagger} + \mathbf{N}$, where $U = E\{\tilde{\mathbf{u}}(t)\tilde{\mathbf{u}}(t)\}$, and $\mathbf{N} = E\{\tilde{\mathbf{n}}(t)\tilde{\mathbf{n}}^{\dagger}(t)\}$, is by definition now Hermitian; therefore, its eigenvalues are real. Furthermore, the imaginary part of $\mathbf{S}$ contains information of only the noise, because both $\mathbf{p}$ and U are real. Hence, only the real part of the covariance matrix has to be considered.

Each of the three eigenvalues (λ_i) is proportional to the energy associated with waves having the polarisation of its corresponding eigenvector. The degree of linear polarisation can be defined as (Samson and Olson, 1980)

$$P^{1} = \frac{(\lambda_1-\lambda_2)^2+(\lambda_1-\lambda_3)^2+(\lambda_2-\lambda_3)^2}{2(\lambda_1+\lambda_2+\lambda_3)^2} \tag{9}$$

which has the value of 1 when the signal is linearly polarised and which decreases to 0 when it is unpolarised.

The direction to the event is obtained from the eigenvectors and the distance to the event (R) is obtained from the time difference between the arrival of two phases using:

$$R = (t_2 - t_1).\left(\frac{V_1.V_2}{V_1-V_2}\right) \tag{10}$$

where: t_1 = arrival time of the first phase
t_2 = arrival time of the second phase
V_1 = velocity of the first phase
V_2 = velocity of the second phase

The phases normally used are the P-wave and the S-wave, but for in-seam waves the Airy phase can be used instead of the S wave.

A 3.3 Borehole Data Analysis Program

The data analysis software was written using MATLAB. MATLAB is a technical computing environment for high-performance numeric computation and visualization. MATLAB integrates numerical analysis, matrix computation, signal processing, and graphics in an easy-to-use environment. The name MATLAB stands for matrix laboratory and is produced by The MathWorks, Inc.

The program has a graphical user interface and is easy to use and can be easily customised for any configuration of sensors.

The program is started by typing **dataanal** at the MATLAB prompt. The following window is then seen. Just click on the 'Continue' button to continue.

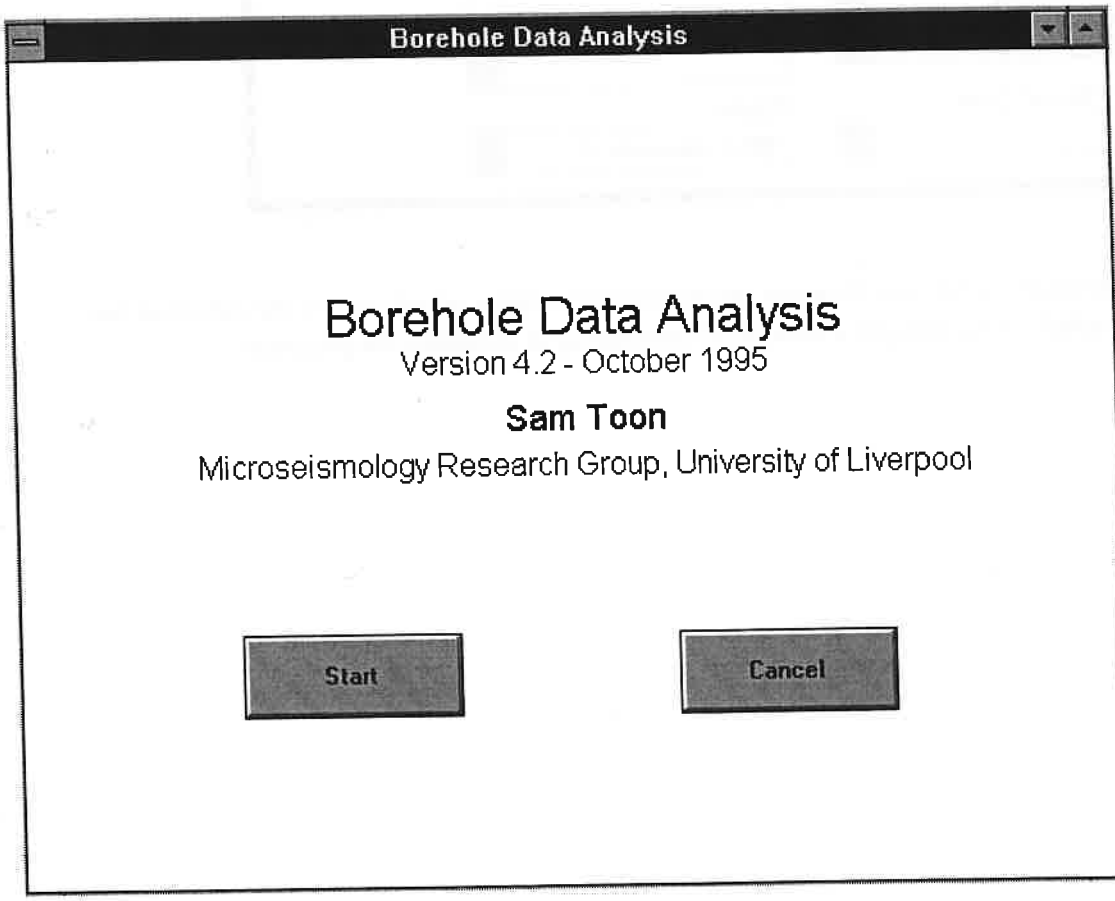

The following dialog box then prompts you to choose a data file to load. The data file must be a VIB or FIB file. A VIB file is the output from the FLASH2 program which converts the raw binary data from a flash card to ascii format. A FIB file is a VIB file that has been filtered to remove 50 Hz noise.

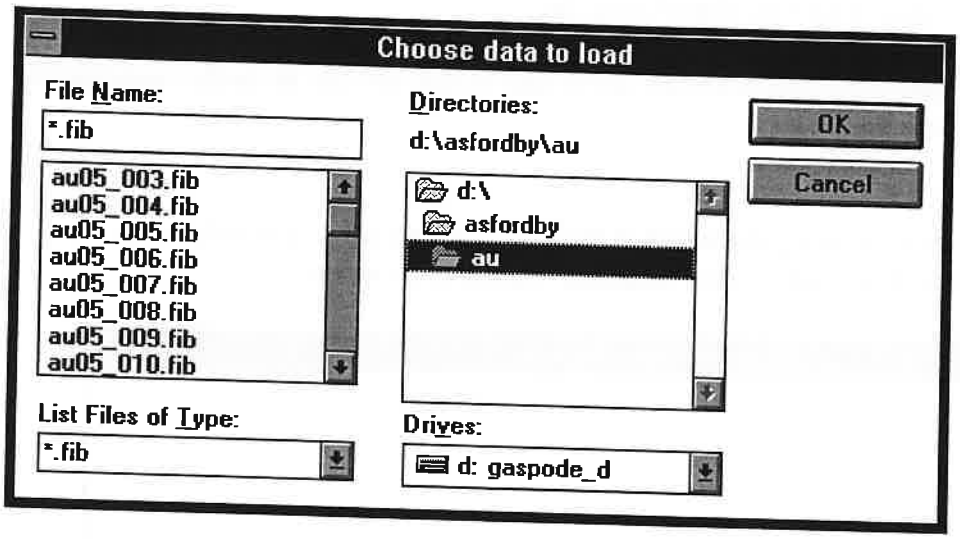

After choosing a file you then see the following window which shows the data that has been loaded. You also get a choose of continuing or stopping the program.

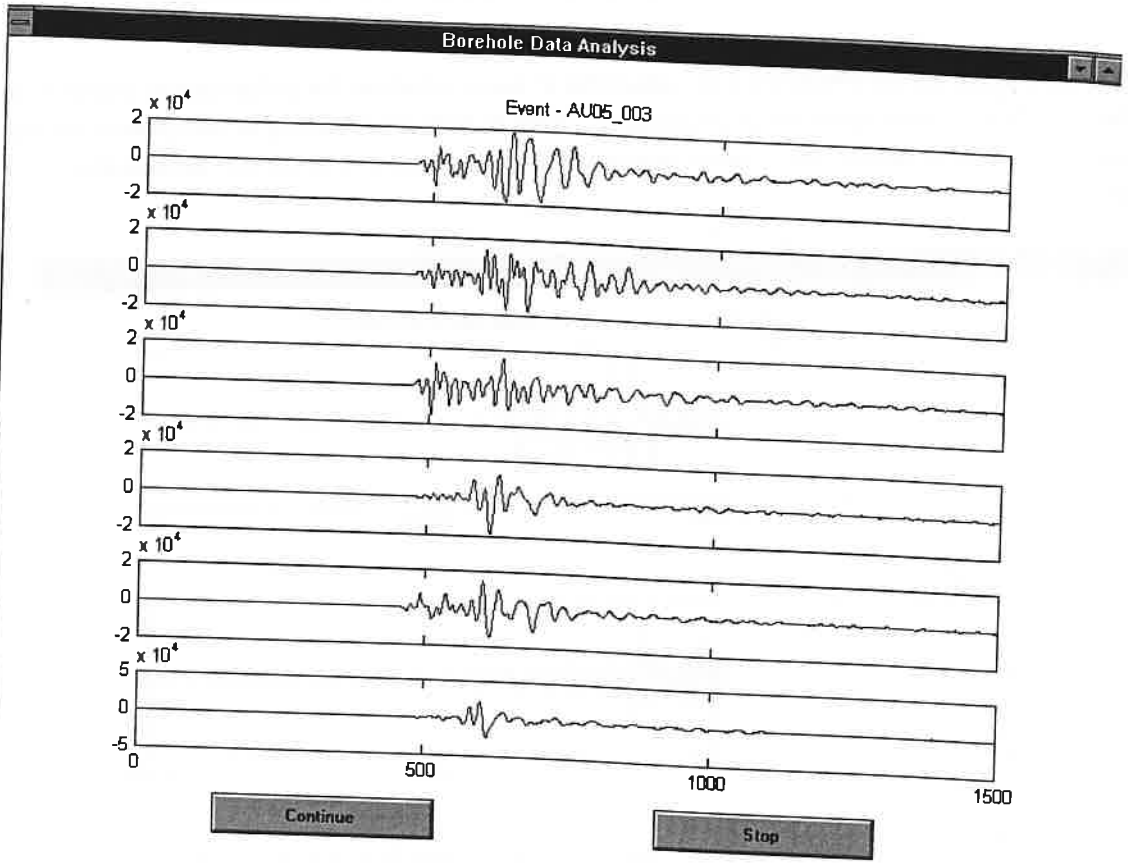
Borehole Data Analysis
Event - AU05_003
x 10^4
2
0
-2
x 10^4
2
0
-2
x 10^4
2
0
-2
x 10^4
2
0
-2
x 10^4
2
0
-2
x 10^4
5
0
-5
0
500
1000
1500
Continue
Stop

The next stage of the program is to select the P-wave window for polarisation analysis for the first three component set of geophones. This is done by clicking at two points on the waveform which define the P-wave window that you want to use for the polarisation analysis.

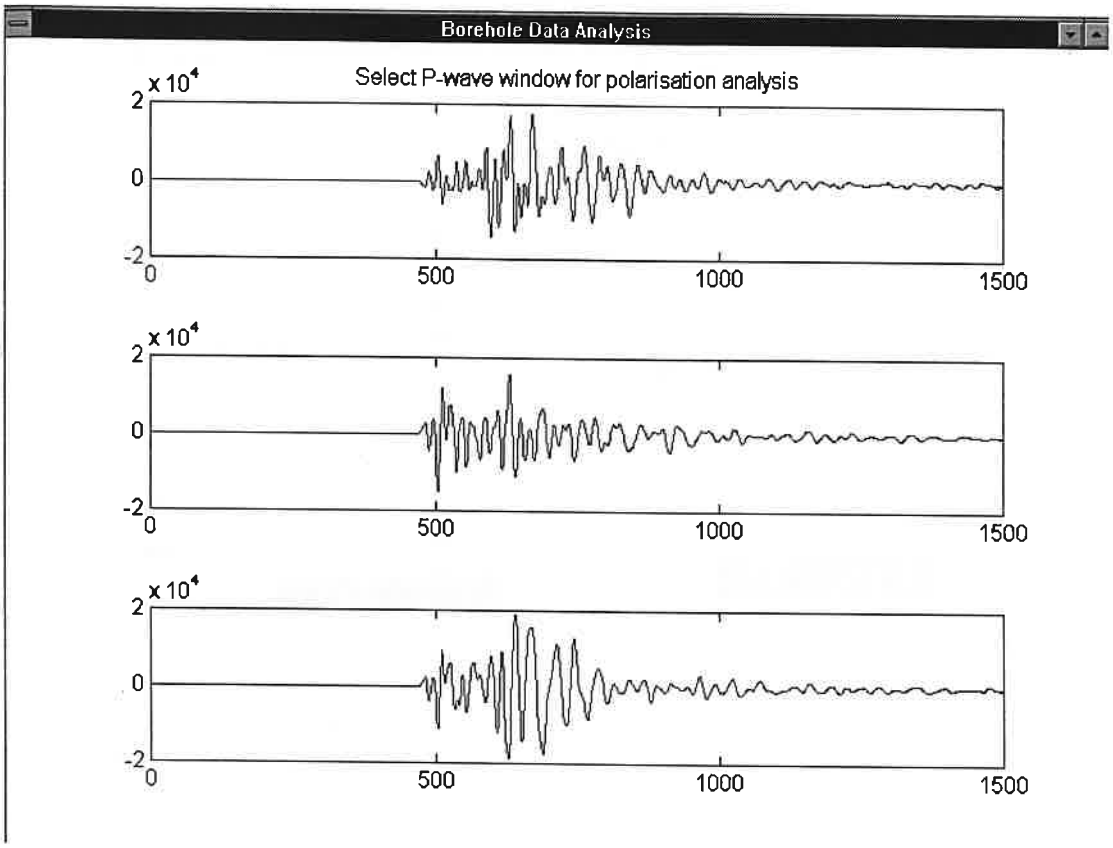

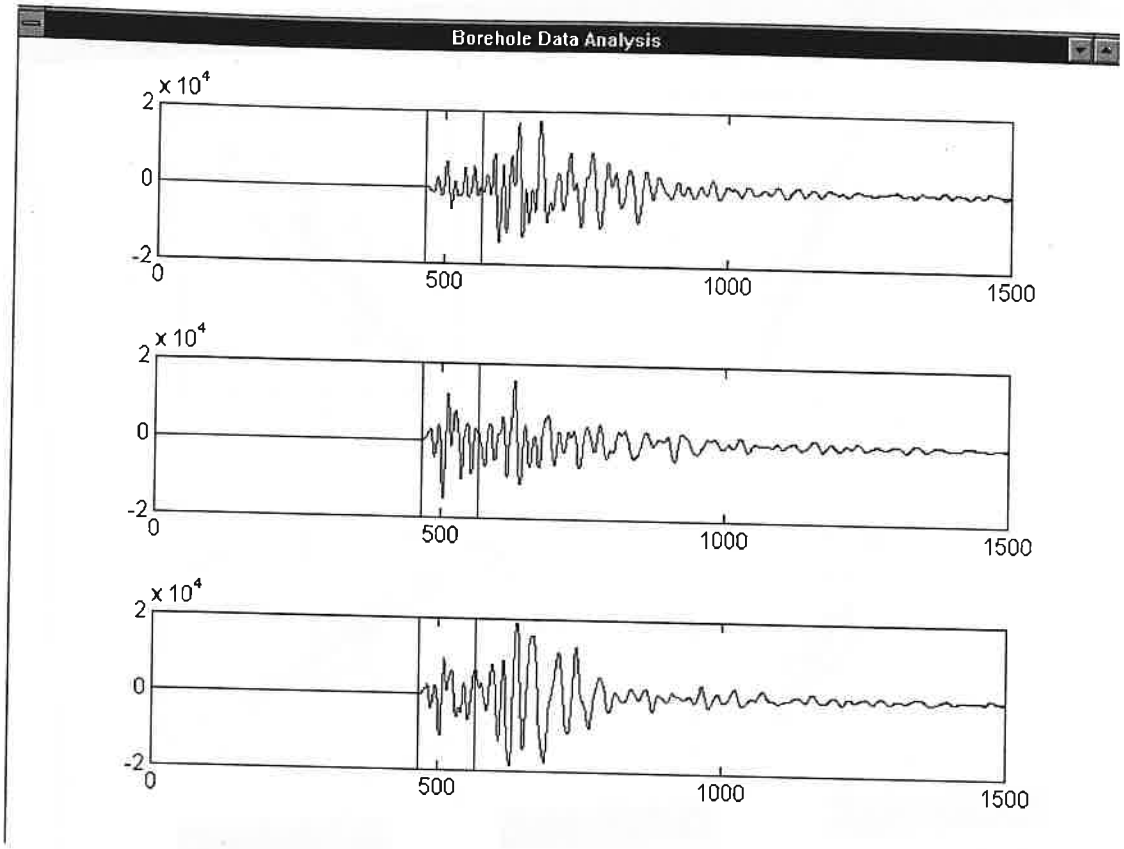

After selecting the P-wave window you are then shown the Hodograms for the selected window and given a chance to re-pick the window, continue to program or stop.

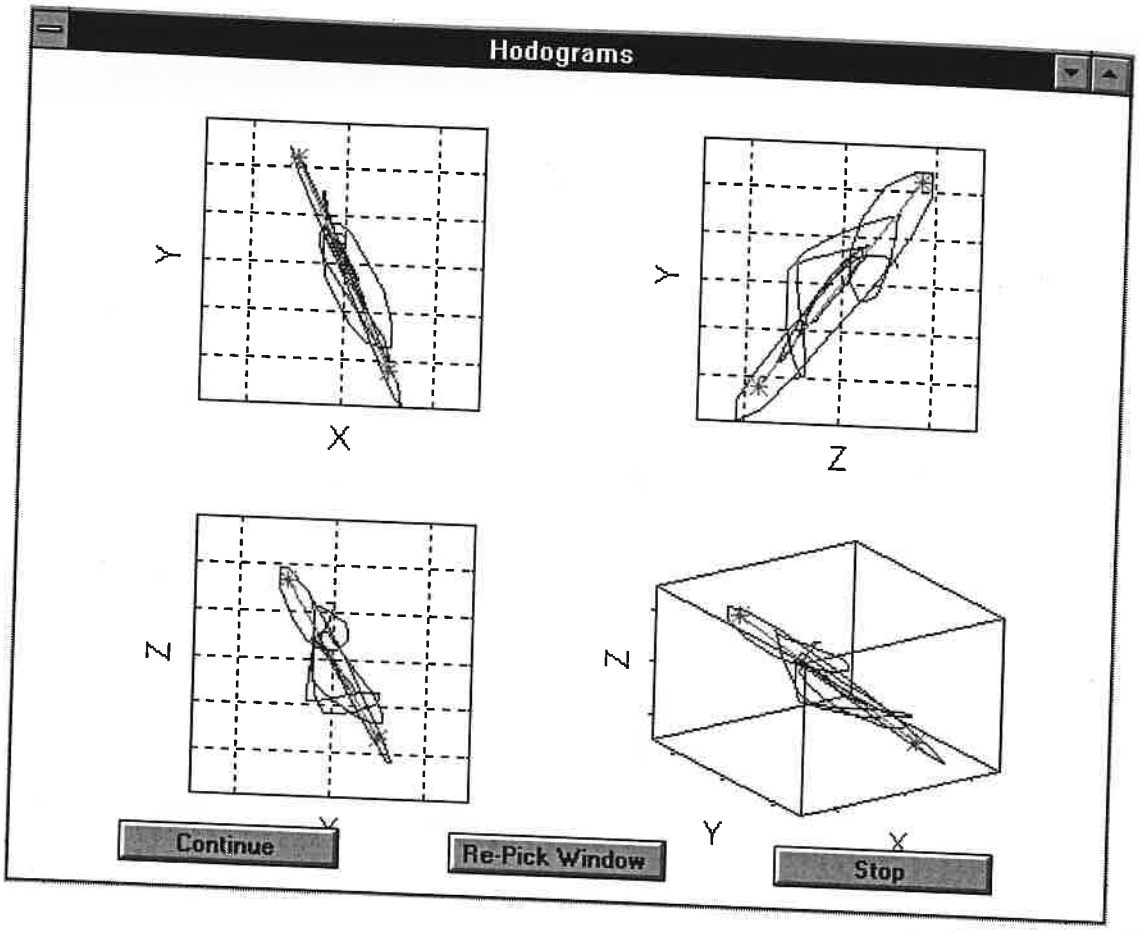
Hodograms
Y
X
Y
Z
Z
Y
Z
Y
X
Continue
Re-Pick Window
Stop

The next step is then to pick the P- and S-wave arrivals which will give us the distance to the event. The window show the original data and the waveforms rotated into principal components which should make it easier to pick the P- and S-wave onsets.

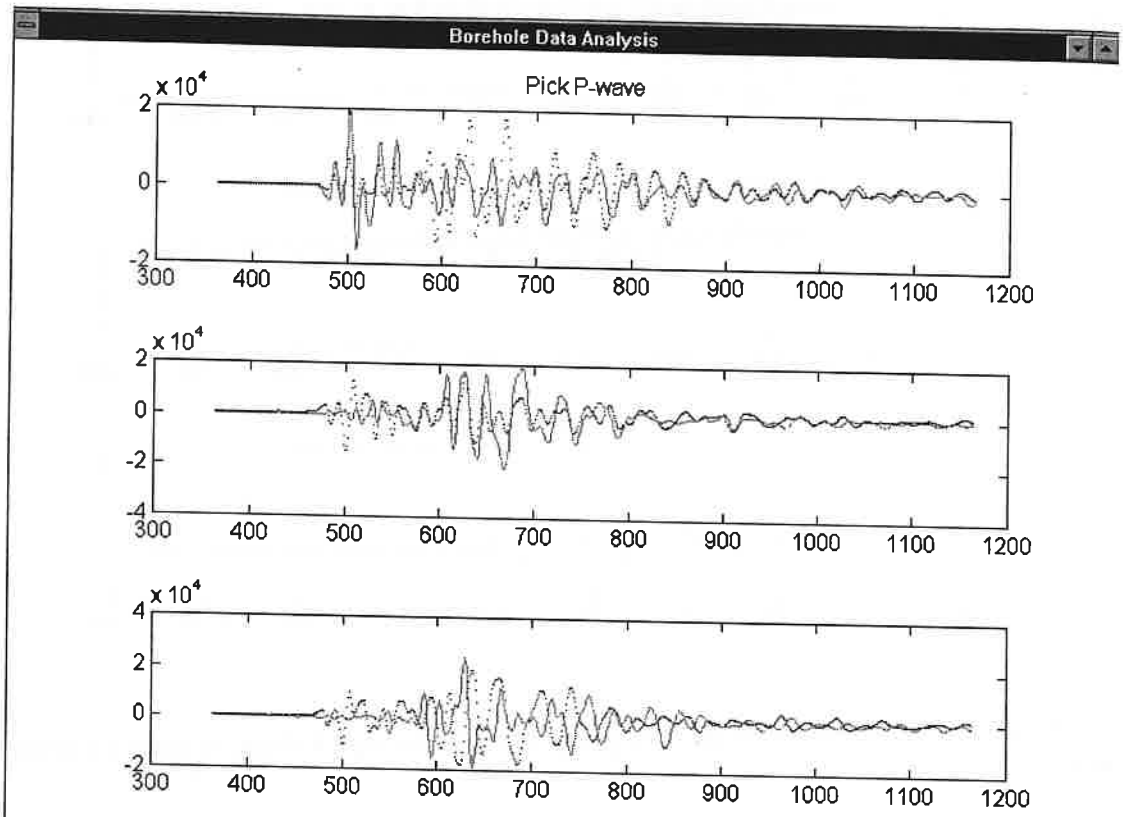

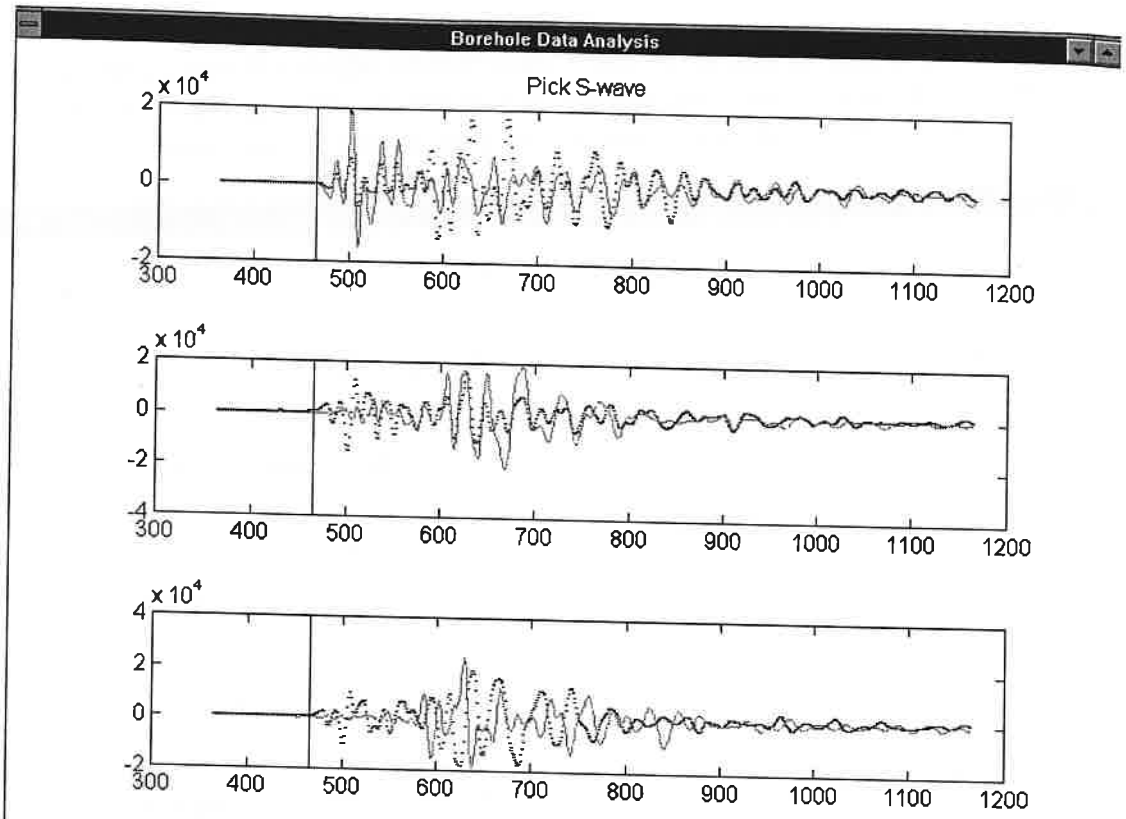

After picking the arrivals you are then given a chance to repick them, to carry on or to stop.

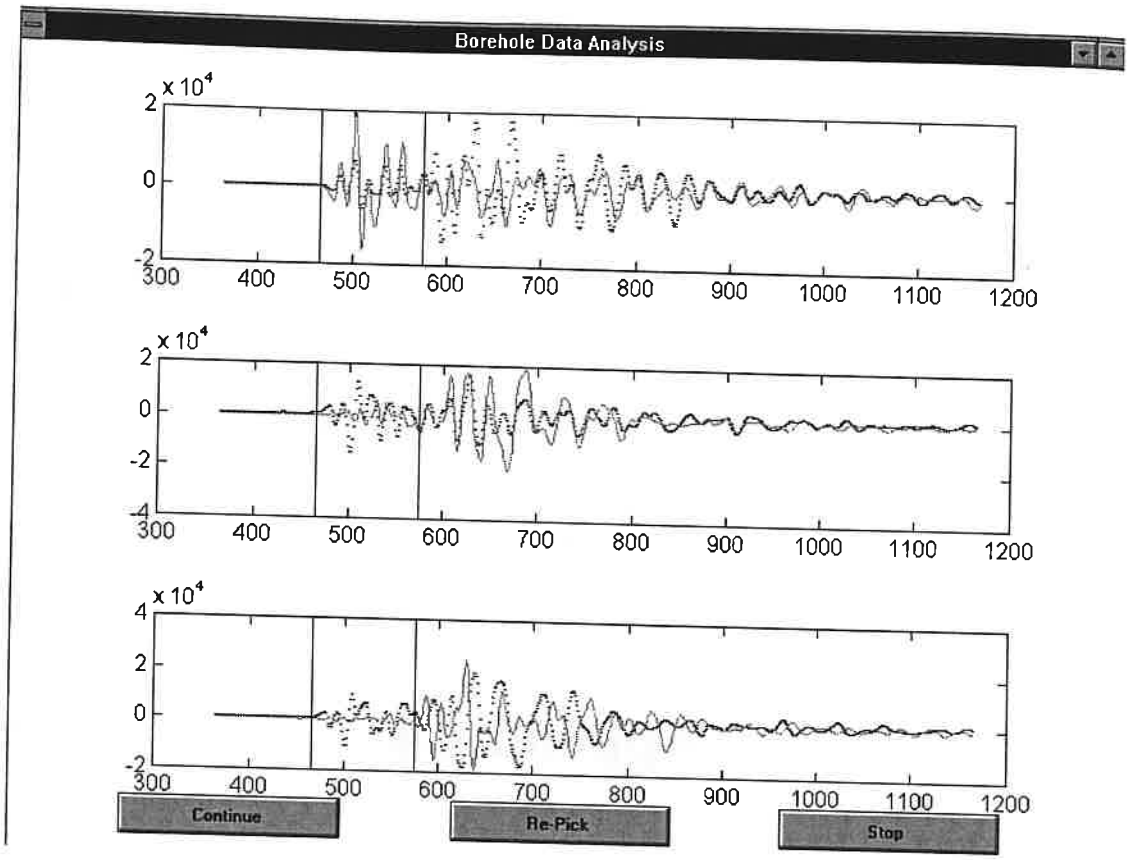

The next step is to repeat picking the P-wave window and the P- and S- wave arrivals for the second set of geophones. You are then shown the results of the program and asked if you want to save them to file.

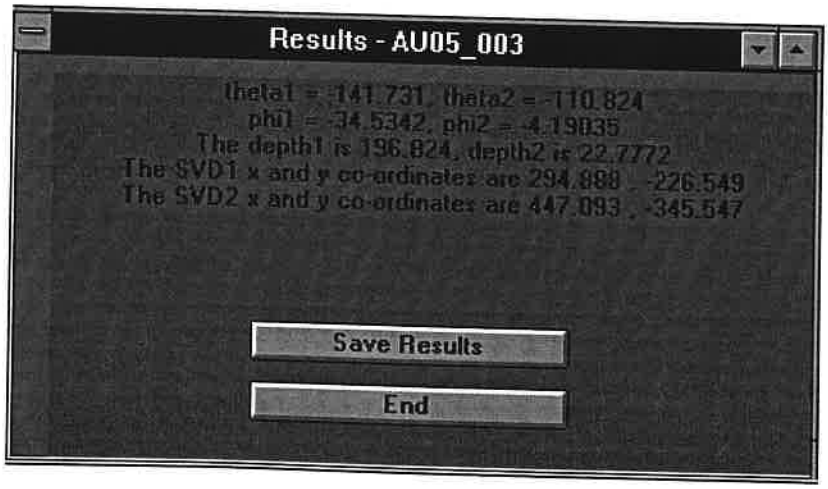

Appendix 4

Source Crack Kinematics and Seismic Source Determination

A4 SOURCE CRACK KINEMATICS

In order to determine the nature of the failure process which is occurring during a microseismic event we must determine the orientation of the fracture surface in space and the motion on that crack: ie the **source crack kinematics**. Source crack kinematics can be wholly defined by two vectors : one defining the crack motion (B), and another defining the normal to the crack surface (N). Vector, B, will show whether the source is a shear or tensile type fracture, and N specifies the crack orientation. The crack kinematics of the source control the source moment tensor. If the moment tensor can be found from the event data, then the crack kinematics of the source may also be found.

A4.1 Using Green's functions to find crack kinematics for a given event

The amplitudes of the P- and S-waves recorded at a sonde are controlled by the source moment tensor and the appropriate Green's functions. Thus, to find the source moment tensor from the event data, the Green's functions must first be known. The simplest Green's function is for a full isotropic homogeneous space, and it is these which I have used. This means the Green's functions used describe the variation of the amplitudes of the P- and S-waves with source-sonde direction (essentially they describe the P- and S-wave radiation patterns) and source-sonde displacement (they also describe geometrical spreading). To calculate the displacements due to a moment tensor source, the spatial derivatives of the Green's functions are used. Assuming that the source-sonde displacement is much greater than the wavelength of the P- and S-waves, only the far-field parts of the spatial derivatives of the Green's functions need to be used. The amplitudes of the Green's functions are given by :

$$|G_{ki,j}| = \frac{1}{4\pi\rho\alpha^3}\gamma_k\gamma_i\gamma_j\frac{1}{R} - \frac{1}{4\pi\rho\beta^3}(\gamma_k\gamma_i - \delta_{ki})\gamma_j\frac{1}{R} \qquad \textbf{(11)}$$

where

α = P-wave velocity,
β = S-wave velocity,
ρ = density,
R = source-sonde displacement, and
γ = [source location-sonde location]/R (i.e. vector of direction cosines).

The first part of the left hand side of equation 1 is the amplitude of the P-wave part of the far-field spatial derivative of the Green's function, and the second part is that for the S-wave.

The amplitudes of the P- and S-waves recorded at the sonde for a given moment tensor source are given by (summing over indices) :

$$u_{k_p} = Km_{ij}G_{ki,j_p}$$
$$u_{k_s} = Km_{ij}G_{ki,j_s} \qquad \textbf{(12)}$$

where K = a constant,

u = displacement in direction specified by indices, and
m = source moment tensor.

The value of the constant K (dependent on crack opening and crack radius) cannot be found from the available data, so the moment tensors, and crack kinematics vectors which are found are normalised. This is adequate since it is the directions of crack motion and the crack orientation which are of interest.

A4.2 S/P ratio error simplex minimisation using event data recorded at one sonde

The program **datloc2.m** calculates the amplitudes of the far-field spatial derivatives of the Green's functions for a given source-sonde system. **datloc2.m** also allows the user to pick the amplitudes of the P- and S-wave first arrivals for each component of the specified sonde. The source location was also loaded from the **dataanal.m** results file. The amplitudes of the Green's functions, of the P- and S-waves for each component, and the source and sonde locations are next used by the program **fit2.m**.

This program firstly takes 100 random crack kinematics systems, and compares the polarities of the resultant P- and S-wave first motion amplitudes which would be recorded at the sonde with the polarities of the P- and S-wave first motion amplitudes measured from the event data. Next, the crack kinematics system which gives the same polarities (and has the most similar S/P first motion amplitudes ratio to the event data) is used as the starting point for a simplex minimisation of a particular error function. The error function is defined as the sum of the differences between the ratio of the first motion S-wave amplitudes and P-wave amplitudes for each component of the event data, and those of the calculated data. The error is defined as a percentage of the sum of the ratios for all components of the event data. The S/P ratios are used because it was found that they are very sensitive to the crack kinematics.

The major problem with this minimisation method is that the error function has many discontinuities and local minima, making it virtually impossible to find the global minimum. To remedy this problem, a method had to be found to choose a starting point for the minimisation which is close to the global minimum. This would require a full moment tensor inversion, i.e. calculate the moment tensor directly from the event data, so that an approximation of the crack kinematics system could be found from an eigenvalue decomposition of the moment tensor.

A4.3 Moment tensor inversion

To calculate the source moment tensor from the event data, the system of six linear equations describing the P- and S-wave first motion amplitudes as a function of moment tensor elements and Green's functions amplitudes must be solved. The system must have six equations because the moment tensor, being symmetric, has six independent elements. The equations are solved by multiplying a 6x1 vector containing six measurements of the P- and S-wave first motion amplitudes by the inverse of a 6x6 matrix containing the appropriate Green's functions amplitudes to give a 6x1 vector containing the elements of the source moment tensor.

The P- and S-wave first motion amplitudes from each of the three components of a sonde give six pieces of information, which would appear to be enough to carry out the moment tensor inversion. However, the 6x6 matrix containing the Green's functions is very nearly singular, meaning that the inverse is inaccurate. A similar problem is found using event data recorded on two sondes.

With the 6x1 first motion amplitudes vector containing the P- and S-wave first motion amplitudes recorded on either the x- or y-component at three sondes, the appropriate Green's function amplitude matrix can be inverted accurately, and the moment tensor can be calculated. Thus, event data recorded at three sondes can be used to calculate the source moment tensor. This is what the program **mti.m** does.

A4.4 Moment tensor inversion using synthetic waveforms

To test **mti.m**, synthetic waveforms were generated for a crack kinematics system with the following properties :

$\underline{B} = [1\ 0\ 0]$ $\underline{N} = [0\ 0\ 1]$

for the **au11_018.res** event location, and the Cants Thorn 1 upper sonde. Using these synthetic waveforms as the event data used in **mti.m**, the moment tensor was

calculated for both the x- and y-component data, and was found to be correct, to more than four decimal places. The same situation was found for the following crack kinematics system :

$$\underline{B} = [-2\ -1\ 3]\underline{N} = [2\ 1\ 0] \text{ (unnormalised)}$$

which has a more complicated source moment tensor than the previous case.

A4.5 Eigenvalue decomposition of the moment tensor to estimate crack kinematics

An approximation to $\underline{B}$ and $\underline{N}$ can be made by performing an eigenvalue decomposition of the source moment tensor. Whether the source is a shear or tensile crack can be found by calculating :

X = (intermediate eigenvalue/maximum eigenvalue)
- (minimum eigenvalue/maximum eigenvalue)

X has values between 0 and 1, with the case X=1 applying to a pure shear crack, and X=0 applying to a pure tensile crack. If X~0 or X~1 then $\underline{B}$ and $\underline{N}$ can be approximated by :

$2\underline{B}$ = (eigenvector for maximum eigenvalue)
+ (eigenvector for minimum eigenvalue)

$2\underline{N}$ = (eigenvector for maximum eigenvalue)
- (eigenvector for minimum eigenvalue)

A4.6 Moment tensor inversion and eigenvalue decomposition for an actual event recorded on three sondes

The datasets au08_001, al08_002, and bl08_001 are from the same event. Using **mti.m**, a moment tensor was found using the x-components. An eigenvalue decomposition was carried out, and the two vectors defining the crack kinematics system were estimated. These were used as a starting point for a simplex minimisation of the S/P first motion amplitudes ratio error for the dataset **au08_001.fib**. The results of the minimisation were :

$\underline{B}$ = [-0.1476 0.0946 0.9845]
$\underline{N}$ = [0.1368 0.9795 0.1477]

where B is the normalised vector of crack motion. The ratio error for the above system was less than 0.0001%. Thus, the event au08_001 is near vertical movement on a crack roughly perpendicular to the y-direction.

A4.7 Constrained source mechanisms

To find the six components of a seismic moment tensor, six pieces of data have to be used. This requires the event to be recorded on at least three sondes. Most events are only recorded on one sonde, or two adjacent sondes, and there are only two pieces of data, the P- and S-wave amplitudes. Thus the source mechanism cannot be found for the majority of the recorded events.
However, by making certain assumptions which constrain four of the six moment tensor elements, it is possible to find the two unconstrained elements from the event data. This is done by solving simultaneous equations in terms of the P- and S-wave amplitudes, and the relevant parts of the Green's function for a homogeneous full space, to find the moment tensor elements.
There are three things which must be considered when deciding on the assumptions to be made. These are :

(a) Which two moment tensor elements give the most relevant information?
(b) Are the assumptions made geophysically probable?
(c) Do the two moment tensor elements relate simply to the crack geometry of the source mechanism?

By assuming that the source mechanism is a vertically downwards shear failure, the two moment tensor components which can be calculated are proportional to the x- and y-components of the crack normal. This means that the azimuth of the vertical crack plane can be found.
The program fplane.m does this for the x- and y-components of the event data, and then takes the average of the crack normals found for each component. The average is taken because this was found to give the best results for synthetic source mechanisms with a non-vertical crack plane and a mixture of shear and tensile failure. The z-component of the event data is not used because of problems caused by the linear dependence of the Green's function elements.
The results show strong correlations of crack azimuth with event locations. Changes in azimuth between events with similar Eastings and Northings is often observed to correlate with changes in depths of events, suggesting that source mechanisms may depend on geology.

Errors arise from the actual source mechanism not being a vertical shear failure, and also in some locations the Green's function has more influence on the calculated moment tensor elements than the P- and S-wave amplitudes.

References

Albright J. N. and Pearson C. F., 1980. Location of hydraulic fractures using microseismic techniques. SPE 9509.

Albright J. N. and Pearson C. F., 1982. Acoustic emissions as a tool for hydraulic fracture location: Experience at the Fenton Hill hot dry rock site. Society Petroleum Engineers Journal. 523-530 (August 1982).

Allen, R.V. (1978) Earthquake recognition and timing from single traces. Bull Seismol. Soc. Am., 68, 1521-1532.

Baria R., Green A. S. P. and Jones R. H., 1987. Anomalous seismic event observed at the CSM HDR project. Submitted to Annales Geophysicae, 28th July 1987.

Baria, R., Hearn, K. and Batchelor, A. S., 1989. The monitoring of the induced seismicity during the hydraulic of the potential hot dry rock geothermal reservoir. In: Proceedings of the Fourth Conference Acoustic Emission/Microseismic Activity in Geological Structures and Materials, Hardy (ed), 1985, Trans Tech Publications, pp. 327-352.

Batchelor A. S., Baria R. and Hearn K., 1983a. Microseismic detection for Camborne Geothermal Project. In Rockbursts: Prediction and control. Institute of Mining and Metallurgy. 147-160.

Batchelor A. S., Baria R. and Hearn K., 1983b. Monitoring the effects of hydraulic stimulation by microseismic event location: A case study. SPE 12109.

Bieniawski, Z.T., 1987. Strata Control in mineral engineering, (AA Balkema, Rotterdam).

Blake, W., 1984a. Evaluation of some rockburst precursor phenomena. In: Proceedings of the Third Conference Acoustic Emission/Microseismic Activity in Geological Structures and Materials, 1981, Hardy and Leighton (eds), Trans Tech Publications, pp. 239-250.

Blake, W. F., and Leighton, F., 1970. Recent developments and applications of the microseismic method in deep mines, Proceedings 11 Symp on Rock Mechanics, (Berkeley 1969), AIME New York, pp. 429-443.

Bourbonnais, J., 1984. A research application of multi-channel microseismic monitoring to rockbursting at the East Malarctic Mine in Northwerstern Quebec. In: Proceedings of the Third Conference Acoustic Emission/Microseismic Activity in Geological Structures and Materials, 1981, Hardy and Leighton (eds), Trans Tech Publications, pp. 252-268.

Brown, K. M. and McDonald, P., 1984. A microseismic study of an outburst-prone coal seam. In: Proceedings of the Third Conference Acoustic Emission/Microseismic Activity

in Geological Structures and Materials, 1981, Hardy and Leighton (eds), Trans Tech Publications, pp. 479-497.

Browitt, C. W. A., (1979), Seismograph Networks of the Institute of Geological Sciences, U.K., Physics of the Earth and Planetary Interiors, 18, 127-134.

Cacechi, M. S., and Cacheris, W.P, (1984), Fitting curves to data (the Simplex algorithm is the answer), Byte, 9, no 5, 340-362.

Calder, P. N., Archibald, J. F., Madsen, D., and Bullock, K., (in press). High Frequency Precursor Analysis Prior to a Rockburst. Second International Symposium of Rockbursts and Seismicity in Mines, Minneapolis, 1988.

Choi, D.S. and McCain D.L., 1982, Design of Longwall Systems, Trans. SME-AIME, 268

Cook, N.G.W., (1963) the seismic location of rockbursts. In: Fairhurst, C. (Ed.), *Rock Mechanics: Proceedings of the Fifth Symposium on Rock Mechanics*. Pergammon Press: New York, 493-516

Davison, C., (1905), Earthquakes in Mining Districts, Geological Magazine, 2, 219-223.

Davison, C., (1919), The Stafford Earthquakes of January 1914-15, 1916, and the relationship between twin earthquakes, of the Midland Counties, Geological magazine, 6, 302-312.

Dechellette, O., Josien, J. P., Revalor, R. and Jonis, R., 1984. Seismo-acoustic Monitoring in an Operational Longwall Face with a high rate of advance, In: Rockbursts and Seismicity in Mines, S.A.I.M.M., 6, Gay and Wainwright (eds), pp. 83-87.

Deflandre, J.P., Laurent, J., Michon, D. and Blondin, E., (1995) Microseismic surveying and repeated VSPs for monitoring an underground gas storage reservoir using permanent geophones. First Break. 13(4), 129-138

Dollar, A.T.J., (1951). Catalogue of Scottish Earthquakes, 1916-1949, Transactions of the Geological Society of Glasgow, 21, (2), 283-361.

Durr, K. and Meister, D., 1984. Evaluation of pillar deformation and stability in a salt mine utilising acoustic emission mine survey and rock deformation data. In: Proceedings of the Third Conference Acoustic Emission/Microseismic Activity in Geological Structures and Materials, 1981, Hardy and Leighton (eds), Trans Tech Publications, pp. 283-302.

Evans D. M., 1966. The Denver area earthquakes and the Rocky Mountain Arsenal disposal well. Mountain Geologist, 3(1), 23-36.

Fairhurst, C. (Ed.), (1990) *Rockbursts and Seismicity in Mines: Proceedings of the 2nd International Symposium on Rockbursts and Seismicity in Mines*. A.A. Balkema: Rotterdam, pp. 439

Feignier B., & Young, R.P. 1992. Moment tensor inversion of induced microseismic events: evidence of non-shear failures in the -4 < M < -2 moment magnitude range. Geophysical Research Letters 19, 1503-1506.

Flinn, E.A., 1965, Signal Analysis using rectilinearity and direction of particle motion. Proc. IEEE, 53, 1874-1876

Follington, I.L., (1988) *Geotechnical Influences upon Longwall Mining*. Ph.D.Thesis: University of Wales

Gay, N.C. & Wainwright, E.H. (Ed.), (1984) *Rockbursts and Seismicity in Mines: Proceedings of the 1st International Symposium on Rockbursts and Seismicity in Mines*. SAIMM: Johannesburg, pp. 363

Gendzwill, D. J., and Prugger, A. F., 1989. Algorithms for Micro-Earthquake Locations. In: Proceedings of the Second Conference Acoustic Emission/Microseismic Activity in Geological Structures and Materials, 1978, Hardy and Leighton (eds), Trans Tech Publications, pp. 601-615.

Geothermal news and views, 1982. Los Alamos Hot dry rock development program. Geothermics, 11(3), 201-214.

Gibbons, M. G., 1980. Low frequency microseisms in relation to Mine roof stability. In: Proceedings of the Second Conference Acoustic Emission/Microseismic Activity in Geological Structures and Materials, 1978, Hardy and Leighton (eds), Trans Tech Publications, pp. 245-258.

Gibowicz, S. J., 1984. The Mechanism of large mining tremors in Poland. In: 'Rockbursts and Seismicity in Mines', Gay and Wainwright (Eds), S.A.I.M.M., 6, pp. 17-28.

Gibowicz, S.J., (1985) Seismic moment and seismic energy of mining tremors in the Lubin copper basin in Poland. *Acta Geophys. Pol.*, **33**, 243-257

Gibowicz, S.J. & Cichowicz, A., (1986) Source parameters and focal mechanism of mining tremors in the Nowa Ruda coal mine in Poland. *Acta Geophys. Pol.*, **34**, 215-232

Godson, R. A., Bridges, M. C., and McKavanagh, B. M., 1980. A 32-Channel Rock noise source location system. In: Proceedings of the Second Conference on Acoustic Emission/Microseismic Activity in Geological Structures and Materials, 1978, Hardy and Leighton (eds), Trans Tech Publications, pp. 117-161.

Grezl, K. J., Leung, L., and Ahmed, M., 1980. Microseismic monitoring for gas outbursts at Leichardt colliery. In: The occurrence, prediction and control of outbursts in coal mines. Symp. Southern Queensland Branch of the Australasian Inst. of Mining and Metallurgy, Brisbane, Australia, 1980. Parkville, Australia, AIMM, pp. 15-158.

Hardy, H.R., (1977) Emergence of acoustic emission/microseismic activity as a tool in geomechanics. In: Hardy, H.R. & Leighton, F.W. (Ed.), *Proceedings of the First Conference on Acoustic Emission/Microseismic Activity in Geological Structures and Materials*. Trans Tech Publications: Clausthal, 13-31

Hardy, H. R. Jr., 1980. Stability monitoring monitoring of and underground gas storage reservoir, In: Proceedings of the Second Conference Acoustic Emission/Microseismic Activity in Geological Structures and Materials, 1978, Hardy and Leighton (eds), Trans Tech Publications, pp. 331-358.

Hardy H. R. Jr. and Leighton F. W., (Editors), Proceedings of the First Conference on Acoustic Emission/ Microseismic Activity in Geological Structures and Materials - The Pennsylvania State University, June 9-11, 1975; Series on Rock and Soil Mechanics, 2, 1977, Trans Tech Publications.

Hardy H. R. Jr. and Leighton F. W., (Editors), Proceedings of the Second Conference on Acoustic Emission/ Microseismic Activity in Geological Structures and Materials - The Pennsylvania State University, November 13- 15, 1978; Series on Rock and Soil Mechanics, 5, 1980, Trans Tech Publications.

Hardy H. R. Jr. and Leighton F. W., (Editors), Proceedings of the Third Conference on Acoustic Emission/ Microseismic Activity in Geological Structures and Materials - The Pennsylvania State University, October 5-7, 1981; Series on Rock and Soil Mechanics, 8, 1984, Trans Tech Publications.

Hardy, H. R. Jr., and Mowrey, G. L., 1976. Study of microseismic activity associated with a longwall coal mine operation using a near surface array. Proceedings First Inter. Symp. Induced Seismicity, Jour. Eng. Geol., 10, pp. 263-281.

Hardy, H. R. Jr., and Mowrey, G. L., 1984. Analysis of Microseismic Data from a Natural Gas Storage Reservoir. In: Proceedings of the Third Conference Acoustic Emission/Microseismic Activity in Geological Structures and Materials, 1981, Hardy and Leighton (eds), Trans Tech Publications, 365-392.

Hatherly, P., Luo, X., Dixon, R., McKavanagh, B., Barry, M., Jecny, Z. and Bugden, C., 1995. Roof and Goaf monitoring for strata control in longwall mining. CSIRO Report no: 189F. pp. 75.

Hedley, D.G.F., (1990) Peak particle velocity for rockbursts in some Ontario mines. In: Fairhurst, C. (Ed.), *Rockbursts and Seismicity in Mines: Proceedings of the 2nd International Symposium on Rockbursts and Seismicity in Mines*. A.A. Balkema: Rotterdam, 345-348

Hedley, D. G. F., Bharti, S., West, D. and Blake, W., 1989. Fault-slip rockbursts at the Falconbridge Mine. In: Proceedings of the Fourth Conference Acoustic Emission/Microseismic Activity in Geological Structures and Materials, 1985, Hardy (ed), Trans Tech Publications, pp. 159-170.

Hodgson, E. A., 1958. Dominion Observatory Rockburst Research 1938-1945, Dept. of Mines and Technical Surveys, Canada, Dominion Observatories, p 20.

Holub, K., 1985. Study of Microseismic Activity Associated with Mining. Proceedings of the 3rd International Symposium on The Analysis of Seismicity and Seismic Risk, Liblice Castle, Czechoslovakia, 1985, pp. 160-164.

Holub, K., Korinek, J., Kalenda, P., Slavik, J., and Schreiber, P., 1987. Recent developments and applications of microseismic methods in conditions of the rockburst hazard in the Ostrava-Karvina Coal Basin, Czechoslovakia, 22 Int. Conference Safety in Mine Research, Beijing, China, Dai Guoquang (ed), pp. 259-274.

Hsieh P. A. and Bredehoeft J. D., 1981. A reservoir analysis of the Denver Earthquakes: a case of induced seismicity. Journal of Geophysical Research, 86(B2), 903-920. 491-509

Hughes, J. E. T., 1973. Outbursts of coal and gas of the anthracite area of S. Wales. MSc thesis, University of Wales, Cardiff.

Isaacs, A.K., and Follington, I., L., (1988), Geotechnical influences upon Longwall Mining, in Engineering Geology of Underground Movements, Geol. Soc. Engineering Geology Special Publication, 5, 234-242.

Isobe, T., 1974. Measurements of seismic waves causd by underground ectraction of coal seams, Proceedings of the 3rd ISRM Congress, Denver, Vol II, Part B, pp. 1278-1282.

Isobe, T., Mori, N., and Fukushima, A., 1976. Further investigation on the problems of underground Rock destruction by using seismic method, Proceedings of the 4th ISRM, Sydney, pp. 50-54.

Isobe, T., Mori, N., Ishijima, Y., and Fukushima, A., 1976. Measuremnts and analysis of ground tremors caused by working coal seams, 6th International Conference on Strata Control, Canada, Paper 10.

Isobe, T., Mori, N., Sato, K., Goto, T., 1979. Development and application of computer system for monitoring seismicity induced by underground coal mining. In: Application of computers abd operations research in the mineral industry, O'Neill (ed.), AIME, New York, pp. 513-527.

Isobe, T., Mori, N., Sato, K., Goto, T., 1980. Measurement and analysis of seismic events in deep level coal mines. In: The occurrence, prediction and control of outbursts in coal mines. Symp. Southern Queensland Branch of the Australasian Inst. of Mining and Metallurgy, Brisbane, Australia, Sep. 1980. Parkville, Australia, AIMM, pp. 127-138.

Isobe, T., Sato, K., Mori, N., and Goto T., 1984. Microseismic Activity Induced by Hydraulic Mining of Steeply inclined Coal Seams. In: Proceedings of the Third Conference Acoustic Emission/Microseismic Activity in Geological Structures and Materials, 1981, Hardy and Leighton (eds), Trans Tech Publications, pp. 403-424.

ISS International, (1993) *The Integrated Seismic System: ISS*. ISS International Ltd: Welkom, pp. 4

Kaneko, K., Sugawara, K., and Obara, Y., (in press). Rock Stress and Microseismicity in Coal Burst District. Second International Symposium of Rockbursts and Seismicity in Mines, Minneapolis, 1988.

Konecny, P., (1989) Mining induced seismicity (rock bursts) in the Ostrava-Karviná Coal Basin. *Beitr. Geophys.*, **98**, 525-547

Kusznir, N. J., Al-Saigh, N. H., and Ashwin, D. P., 1984. Induced seismicity generated by long-wall mining in the North Staffordshire coal-field, U.K. In: 'Rockbursts and Seismicity in Mines', Gay and Wainwright (Eds), S.A.I.M.M., 6, pp. 153-160.

Kusznir, N. J., Farmer, I. W., Ashwin, D. P., Bradley, L. G., and Al-Saigh, N. H., 1980. Observations and mechanics of seismicity associated with coal mining in North Staffordshire, England. In: Proceedings of 2lst U.S. Symp. on rock mechanics, University of Rolla, Missouri, 27 May 1980, pp. 632-640.

Langstaff, J. T., 1977. Hecla's rockburst monitoring system, Mining Congress Journal, pp. 45-51.

Leighton, F., 1984a. Microseismic activity associated with outbursts in coal mines. In: Proceedings Third Conference on AE/MS activity in Geol. Structures and Materials, 1981, Hardy and Leighton (eds), Trans Tech Publications, pp. 467-477.

Leighton, F. J., 1984b. Microseismic Monitoring and warning of Rockbursts. In: 'Rockbursts and Seismicity in Mines', Gay and Wainwright (eds), S.A.I.M.M., 6, pp. 287-296.

Leighton, F. J. and Blake, W., 1970. Rock noise source location techniques, USBM R.I. 7432, 14pp.

Leighton, F. and Steblay, B. J., 1975. Coal mine bounce and roof fall research. Proceedings First Conference Underground Mining (Louisville 1975), 11, pp. 104-119.

Li, D., 1989. Application of AE techniques to prediction of mining structure failures. In: Proceedings of the Fourth Conference Acoustic Emission/Microseismic Activity in Geological Structures and Materials, 1985, Hardy (ed), Trans Tech Publications, pp. 181-187.

Lienert, B.R. and Havskov, J., 1996, A computer program for locating earthquakes both locally and globally. Seismological Research Letters, 66(5), 26-36.

Lingle, R. and Francis, G. G., 1980. Acoustic emission monitoring at Coalville, Utah. In: Proceedings of the Second Conference Acoustic Emission/Microseismic Activity in Geological Structures and Materials, 1978, Hardy and Leighton (eds), Trans Tech Publications, pp. 359-373.

McClain W. C., 1969. Disposal of radioactive wastes by hydraulic fracturing: Part V. Site evaluations. Nuclear Engineering and Design, 9, 315-326.

McClain W. C., 1971. Seismic mapping of hydraulic fractures. Oak Ridge National Laboratory, ORNL-TM-3502 (August 1971) 32 pp.

McKavanagh, B. M., Enever, J. R., 1980. Developing a microseismic outburst warning system. In: Proceedings of the Second Conference on Acoustic Emission/Microseismic Activity in Geologic Structures and Materials, 1978, Hardy and Leighton (eds), Trans Tech Publications, pp. 211-225.

Meister, D., 1980. Microacoustic studies in rock salt. In: Proceedings of the Second Conference Acoustic Emission/Microseismic Activity in Geological Structures and Materials, 1978, Hardy and Leighton (eds), Trans Tech Publications, pp. 259-275.
Nakajima, I., Watanabe, Y. & Fukai, T., (1984) Acoustic emission uring advance boring associated with the prevention of coal and gas outbursts. In: Hardy, H.R. & Leighton, F.W. (Ed.), *Proceedings of the Third Conference on Acoustic Emission/Microseismic Activity in Geological Structures and Materials*. Trans Tech Publications: Clausthal, 529-548

Mendecki, A.J., (1993) Keynote Address: Real time quantitative seismology in mines. In: Young, R.P. (Ed.), *Rockbursts and Seismicity in Mines: Proceedings of the 3rd International Symposium on Rockbursts and Seismicity in Mines*. A.A. Balkema: Rotterdam, 287-295

Minney, D.S. & Naismith, W.A., (1993) Quantitative analysis of seismic activity associated with the extraction of a remnant pillar in a moderately deep level gold mine. In: Young, R.P. (Ed.), *Rockbursts and Seismicity in Mines: Proceedings of the 3rd International Symposium on Rockbursts and Seismicity in Mines*. A.A. Balkema: Rotterdam, 95-100

Neilson, G., Musson., R. M. W., and Burton, P W., (1984), Macroseismic reports on the historical British earthquakes, V., Midlands, British Geological Survey, Global Seismology Report No. 228(b), Edinburgh.

Neumann, M., and Makuch, A. P., 1989. Analysis of Microseismic Activity Prior to Pillar Rockburst in Campell Red Lake Mine F-2 Zone. In: Proceedings of the Fourth Conference on Acoustic Emission/Microseismic Activity in Geological Structures and Materials, 1985, Hardy (ed) Trans Tech Publications, pp. 225-240.

Niitsuma, H., Takanohashi, M., Chubachi, N. and Yokohama, H., 1989. Downhole AE measuremnt of a geothermal reservoir and its application to reservoir control. In: Proceedings of the Fourth Conference Acoustic Emission/Microseismic Activity in Geological Structures and Materials, 1985, Hardy (ed), Trans Tech Publications, pp. 475-489.

Obert, L., (1977) The microseismic method: discovery and early history. In: Hardy, H.R. & Leighton, F.W. (Ed.), *Proceedings of the First Conference on Acoustic Emission/Microseismic Activity in Geological Structures and Materials*. Trans Tech Publications: Clausthal, 11-12

Oliver, P., and McDonald, P., 1989. The microseismic monitoring system at Creighton Mine, Inco Ltd. In: Proceedings of the Fourth Conference Acoustic Emission/Microseismic Activity in Geological Structures and Materials, 1985, Hardy (ed), Trans Tech Publications, pp. 241-248.

Pakalnis, V., 1984. Strengths and limitations of Microseismic monitoring for rockburst control in Ontario Mines. In: Proceedings of the Third Conference Acoustic Emission/Microseismic Activity in Geological Structures and Materials, 1981, Hardy and Leighton (eds), Trans Tech Publications, pp. 549-558.

Pattrick, K.W., Kelly, A.M. and Spottiswoode, S.M., 1990. A Portable Seismic System for Rockburst Applications. International Deep Mining Conference: Technical Challenges in Deep Level Mining. Johannesburg, SAIMM. pp.1133-1146.

Pearson C. F., 1981. The relationship between microseismicity and high pore pressure during hydraulic stimulation experiments in low permeability granitic rocks. Journal of Geophysical Research. 86(B9), 7855-7864.

Pechmann, J.C., Walter, W.C., Nava, S.J. and Arabasz, W.J., 1995, The February 3, 1995, M_L 5.1 Seismic Event in the Trona Mining District of Southwestern Wyoming . Seismological Research Letters, 66(3), 25-34.

Peng, S.S. and Chiang, H.S., 1984, Longwall Mining, Wiley, New York

Pine R. J. and Batchelor A. S., 1984. Downward migration of shearing in jointed rock during hydraulic injections. Int. J. Rock Mech. Min. Sci. & Geomech Abstr. 21, 249-263.

Plouffe, M., Cajka, M. G., Wetmiller, R. J., and Andrew, M. D., (in press). The Sudbury Local Telemetered Seismograph Network. Second International Symposium of Rockbursts and Seismicity in Mines, Minneapolis, 1988.

Poolen H. K. van and Hoover D. B., 1969. Waste disposal and earthquakes at the Rocky Mountain Arsenal - Derby, Colorado. SPE 2558.

Prugger, A.F. & Gendzwill, D.J., (1990) Results of microseismic monitoring of Cory mine, 1981-1984. In: Fairhurst, C. (Ed.), *Rockbursts and Seismicity in Mines: Proceedings of the 2nd International Symposium on Rockbursts and Seismicity in Mines*. A.A. Balkema: Rotterdam, 215-219

Prugger, A.F. & Gendzwill, D.J., (1993) Fracture mechanism of microseisms in Saskatchewan poatash mines. In: Young, R.P. (Ed.), *Rockbursts and Seismicity in Mines: Proceedings of the 3rd International Symposium on Rockbursts and Seismicity in Mines*. A.A. Balkema: Rotterdam, 239-244

Raleigh C. B., Healy J. H. and Bredehoeft J. D., 1976. An experiment in earthquake control at Rangely, Colorado. Science, 191, 1230-1236.

Reches , Z. and Lockner, D. A., (1993), Nucleation and growth of faults in brittle rock, J. Geophysical Research, 99, 18159-18173.

Redmayne, D. W. (1988), Mining Induced Seismicity in UK Coalfields identified on the BGS National Seismograph Network, in Engineering Geology of Underground Movements, Engineering Geology Special Publication, 5, Geological Society, London, 405-413.

Redmayne, D.W., Richards, J.A. and Wild, P.W., (1996) Seismic monitoring of mining-induced earthquakes during the closing stages of production at Bilston Glen colliery, Midlothian, 1987-1990. British Geological Survey - Technical Report WL/96/14. Edinburgh.

Revolar, R., Dechellette, O. and Verstraete, M., 1986. Detection of coal-bump risk using seismo-acoustic Monitoring at the probence Collieries. Min. Sci. Tech, 4, pp. 11-23.

Revolar, R., Josien, J. P., Besson, J. L., and Magron, A., (1990). Seismic and Seismo-acoustic Experiments Applied to the Prediction of Rockbursts in French Coal Mines. Second International Symposium of Rockbursts and Seismicity in Mines, Minneapolis, 1988.

Riefenberg, J. S., (1989). A simplex-Method-Based Algorithm for determining the source location of Microseismic Events, U. S. Bureau of Mines, RI 9287, 12pp.

Rigby, N. and Bolt, P. B., 1989. Development and application of an underground microseismic monitoring system for outburst prone coalmines, The Mining Engineer. November 1989, pp. 197-203.

Rigby, N. and Wardle, J., 1984. Microseismic monitoring and outburst prediction, Proceedings 15th Ann. Inst Coal Mine Health, safety and Research, Blacksburg, Virginia.

Samson, J.C. and Olson, J.V., 1980, Some comments on the description of polarization states of waves. Geophys. J. R. Astr. Soc., 61, 115-129.

Sarda J.-P., 1984. Well-linking by hydraulic fracturing: problem of hydraulic fracture orientation. Bulletin de la Societe Geologique de France, (7), XXVI, no. 5, 827-831.

Sato, K., and Fujii, Y., 1987. Seismicity associated with a large scale outburst. Fred Leighton Memorial Workshop on Mining Induced Seismicity, Montreal, 1987, pp. 277-286.

Sato, K., and Fujii, Y., 1988. Induced Seismicity Associated with Longwall Coal Mining. International Journal Rock Mechanics Mining Sciences and Geomechanical Abstracts, vol. 25 no. 5, pp. 253-262.

Sato, K., Fujii, Y., Ishijima, Y., Kinoshita, S., 1989. Microseismic activity induced by Longwall Coal Mining. In: Proceedings of the Fourth Conference Acoustic Emission/Microseismic Activity in Geological Structures and Materials 1985, Hardy (ed), Trans Tech Publications. pp. 249-263.

Sato M., Matsumoto N., Niitsuma H. and Nakatsuka K. 1988. Shear-wave splitting analysis of acoustic emission in geothermal field sub-surface crack evaluation. Abstract of a paper given at the Camborne School of Mines Borehole Seismics Conference, September 5th to 7th, 1988.

Semadeni, T. J., Rochon, P., and Niewiadowski, J., (in press)b. Waveform Analysis of Mine-Induced Seismic Events Recorded at Rio Algom's Quirke Mine. Second International Symposium of Rockbursts and Seismicity in Mines, Minneaoplis, 1988.

Spottiswoode, S.M., (1987) Perspectives on seismic and rockburst research in the South African gold mining industry: 1983 to 1987. In: Young, R.P (Ed.), *Proceedings of the Fred Leighton Memorial Workshop on Mining Induced Seismicity (Preprints).* 129-140

Stewart, R.D. & Spottiswoode, S.M., (1993) A technique for determining the seismic risk in deep-level mining. In: Young, R.P. (Ed.), *Rockbursts and Seismicity in Mines: Proceedings of the 3rd International Symposium on Rockbursts and Seismicity in Mines.* A.A. Balkema: Rotterdam, 123-128

Styles, P. and Emsley, S. J. 1987a. Integrated microseismic monitoring and early warning system for outbursts of coal and firedamp, NCB/ECSC Research Contract YCE 28/17619:, Final Report.

Styles, P., Jowitt, T., and Browning E., 1987b. Surface Microseismic Monitoring for the prediction of Outbursts, 22 Int. Conference Safety in Mine Research, Beijing, China, Dai Guoquang (ed), pp. 767-780.

Styles, P., Emsley, S. J., and McInairnie, E. A., 1991. Microseismic prediction and control of coal outbursts in Cynheidre Colliery, In: Proceedings of the Fifth Conference Acoustic Emission/Microseismic Activity in Geological Structures and Materials , Hardy (ed), Trans Tech Publications, Clausthal, Germany, pp. 249-263.

Subbarumu, K. R., Rao, B. S. S., Krishnamurthy, R., and Srinivsan, C., 1989. Seismic investigations monitoring of rockbursts in the Kolar Goldfields. In: Proceedings of the Fourth Conference Acoustic Emission/Microseismic Activity in Geological Structures and Materials, Hardy (ed), Trans Tech Publications, pp. 265-274.

Talebi, S. & Young, R.P., (1990) Characterising microseismicity associated with stope development. In: Fairhurst, C. (Ed.), *Rockbursts and Seismicity in Mines: Proceedings of the 2nd International Symposium on Rockbursts and Seismicity in Mines.* A.A. Balkema: Rotterdam, 189-194

Talebi S., Cornet F. H. and Martel L., 1989. Seismo-acoustic activity generated by fluid injections in a granitic rock mass. In: Proceedings of the Fourth Conference Acoustic Emission/Microseismic Activity in Geological Structures and Materials, Hardy (ed), Trans Tech Publications, Clausthal, Germany pp. 491-509.

Toon, S.M. (1990) The location of faults in coal seams using microseismic activity. B.Sc. Dissertation (Unpublished), University of Liverpool

Toon, S.M., Styles, P. and Jackson, P. 1992. Microseismic imaging of Fractures Around Longwall Coal Faces Using Downhole Three Component Geophones. *XVIIth General Assembly, European Geophysical Society, Edinburgh, 6-10 April 1992.* Abstract.

Toon, S.M. and Styles, P., (1993) Microseismic event location around longwall coal face using borehole in-seam seismology. In : Young, R.P. (Ed.), *Rockbursts and Seismicity in Mines: Proceedings of the 3rd International Symposium on Rockbursts and Seismicity in Mines.* A.A. Balkema: Rotterdam, pp. 441-444.

Vance, J. B. and Mottahead, P., 1989. AE/MS applications to Potash Mining Problems. In: Proceedings of the Fourth Conference Acoustic Emission/Microseismic Activity in Geological Structures and Materials, 1985, Hardy (ed), Trans Tech Publications, pp. 275-286.

Vidale, J.E., 1986, Complex polarization analysis of particle motion. Bull. Seism. Soc. Am., 76, 1393-1405

Westbrook, G. K., Kusznir, N. J., Browitt, C. W. A., and Holdsworth, B. K., 1980. Seismicity induced by coal mining in Stoke-on-Trent (UK), Engineering Geology, 16, pp. 225-241.

Whitworth, K. , North, M.D., Onions, K. R., 1994, Investigation into the effects of lithology on the magnitude and ratio of in-situ stress in Coal Measures, Commission of the European Communities, Agreement Number 7220-A-F/854, DG XVII-D2.

Will, M., 1980. Seismoacoustic activity and mining operations. In: Proceedings Second Conference on Acoustic Emission/Microseismic Activity in Geological Structures and Materials, 1978, Hardy and Leighton (eds), pp. 191-209.

Will, M. & Rakers, E. 1990. Induced seismoacoustic events in burst prone areas of West German coal mines. Gerlands Beitr. Geophysik 99, 54-78.

Wong, I. G., 1984. Mining induced seismicity in the Colorado, western United States and its implications for the siting of an underground high-level waste repository. In: 'Rockbursts and Seismicity in Mines', Gay and Wainwright (Eds), S.A.I.M.M., 6, pp. 147-152.

Wong, I. G., 1985. Mining induced earthquakes in the Book Cliffs and Eastern Wasatch Plateau, Utah, U.S.A. International Journal of Rock Mechanics and Mining Sciences and Geomechanical Abstracts; vol. 22, no. 4, pp. 263-270.

Wong, I. G., Humphrey, J. R. and Silva, W., 1989. Microseismicity and subsidence associated with a potash solution mine, South-Eastern Utah. In: Proceedings of the Fourth Conference Acoustic Emission/Microseismic Activity in Geological Structures and Materials, 1985, Hardy (ed), Trans Tech Publications, pp. 287-306.

Wong, I. G., and McGarr, A., (in press). Implosional Failure in Mining-Induced Seismicity: A Critical Review. Second International Symposium of Rockbursts and Seismicity in Mines, Minneapolis, 1988.

Young, R.P. (Ed.), (1993) *Rockbursts and Seismicity in Mines: Proceedings of the 3rd International Symposium on Rockbursts and Seismicity in Mines*. A.A. Balkema: Rotterdam, pp. 449

Young, R.P. & Maxwell, S.C. 1992. Seismic characterisation of a highly stressed rock mass using tomographic imaging and induced seismicity. Journal of Geophysical Research 97, 12361-12373.

Zhang, W., Ma. F., Tu, X., Nakajima, I., Ujihira, M. and Ohga, K., 1987. The relationship between acoustic emission and gas emission due to coal mining operations. In: Proceedings 22nd Int. Conference Safety in Mines Research, Beijing, China, Dai Guoquan (Ed), pp. 135-146.